NEXT GENERATION PLANETARY GEODESY

Study Report prepared for the W. M. Keck Institute for Space Studies (KISS)

Team Leads: Michael Sori (Purdue University), James Tuttle Keane (Jet Propulsion Laboratory, California Institute of Technology), Anton Ermakov (University of California, Berkeley)

Director: Prof. Tom Prince
Executive Director: Michele Judd
Editing and Formatting: Meg Rosenburg
Cover Image: Chuck Carter/Keck Institute for Space Studies (KISS)

Keck Institute for Space Studies,
California Institute of Technology

Team Leads

Michael Sori
Purdue University

James Tuttle Keane
Jet Propulsion Laboratory
California Institute of Technology

Anton Ermakov
University of California, Berkeley

Workshop 1: June 7–11, 2021
Participants

Alexander Berne
California Institute of Technology

Carver Bierson
Arizona State University

Bruce Bills
Jet Propulsion Laboratory
California Institute of Technology

Carmen Boening
Jet Propulsion Laboratory
California Institute of Technology

Ali Bramson
Purdue University

Simone D'Amico
Stanford University

C. Adeene Denton
Purdue University

Anton Ermakov
University of California, Berkeley

Alex Evans
Brown University

Doug Hemingway
Maxar Technologies

Sonia Hernandez
Jet Propulsion Laboratory
California Institute of Technology

Kristina Hogstrom
Jet Propulsion Laboratory
California Institute of Technology

Kristel Izquierdo
Purdue University

Peter James
Baylor University

Brandon Johnson
Purdue University

James Tuttle Keane
Jet Propulsion Laboratory
California Institute of Technology

Harriet Lau
University of California, Berkeley

Thomas Navarro
McGill University

Francis Nimmo
University of California, Santa Cruz

Joseph O'Rourke
Arizona State University

Luju Ojha
Rutgers University

Ho Jung Paik
University of Maryland

Ryan Park
Jet Propulsion Laboratory
California Institute of Technology

Mark Simons
California Institute of Technology

David E. Smith
Massachusetts Institute of Technology

Sue Smrekar
Jet Propulsion Laboratory
California Institute of Technology

Krista Soderlund
University of Texas

Michael Sori
Purdue University

Gregor Steinbrügge
Stanford University

Sonia Tikoo
Stanford University

Nick Wagner
Baylor University

Renee Weber
Marshall Space Flight Center,
NASA

Maria Zuber
Massachusetts Institute of Technology

Workshop 2: November 8–11, 2021
Participants

Alex Austin
Jet Propulsion Laboratory
California Institute of Technology

Jonathan Bapst
Jet Propulsion Laboratory
California Institute of Technology

Alexander Berne
California Institute of Technology

Carver Bierson
Arizona State University

Bruce Bills
Jet Propulsion Laboratory
California Institute of Technology

Ali Bramson
Purdue University

Simone D'Amico
Stanford University

C. Adeene Denton
Purdue University

Anton Ermakov
University of California, Berkeley

Alex Evans
Brown University

Doug Hemingway
Maxar Technologies

Kristel Izquierdo
Purdue University

Peter James
Baylor University

Melinda Kahre
Ames Research Center,
NASA

James Tuttle Keane
Jet Propulsion Laboratory
California Institute of Technology

Thomas Navarro
McGill University

Marc Neveu
University of Maryland College Park
Goddard Space Flight Center, NASA

Joseph O'Rourke
Arizona State University

Luju Ojha
Rutgers University

Ho Jung Paik
University of Maryland

Ryan Park
Jet Propulsion Laboratory
California Institute of Technology

Paul Rosen
Jet Propulsion Laboratory
California Institute of Technology

Mark Simons
California Institute of Technology

David E. Smith
Massachusetts Institute of Technology

Krista Soderlund
University of Texas

Michael Sori
Purdue University

Gregor Steinbrügge
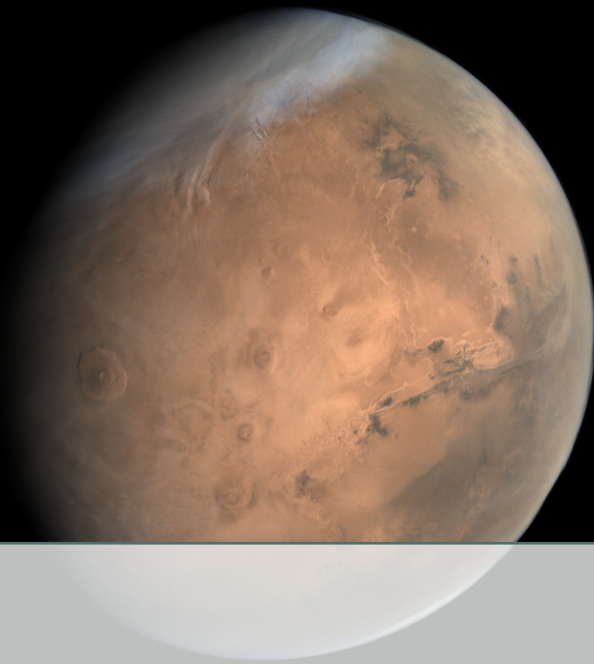Stanford University

Sonia Tikoo
Stanford University

Steve Vance
Jet Propulsion Laboratory
California Institute of Technology

Nick Wagner
Baylor University

Renee Weber
Marshall Space Flight Center,
NASA
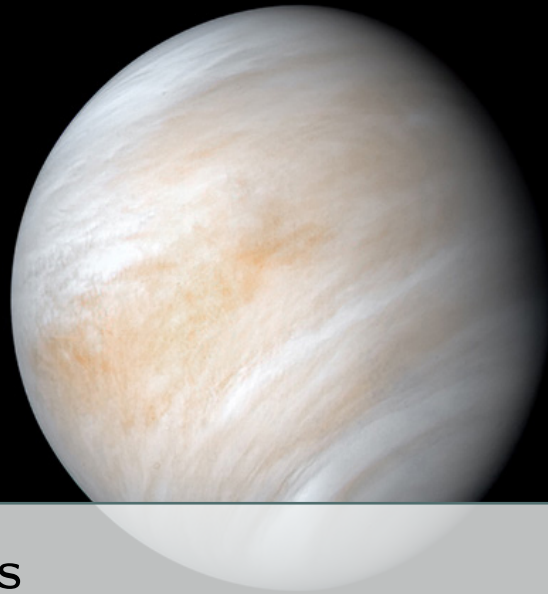
Howard Zebker
Stanford University

Contents

List of Figures

Executive Summary

Geodesy has the capability to address some of the highest-priority questions in planetary science. Despite their utility, geodetic measurements have been limited at other planets and moons, and have not received the same focus as they have at the Earth and the Moon. This issue motivated our Keck Institute for Space Studies (KISS) study program. We reviewed the state-of-the-art methods for next-generation geodesy, and identified science questions that could be advanced by future geodetic investigations at Mars, Venus, and Ocean Worlds. Essential geodetic investigations at Venus would be conducted by NASA's VERITAS mission, and we recommend that mission be flown as planned as soon as possible. By the conclusion of our study, we determined that Mars, Europa, and Enceladus were the solar system destinations where currently unplanned next-generation geodesy investigations would lead to the most transformative advances in the near future. For these worlds, we identified a set of priority science themes:

> *Priority Science Themes for Mars:*
> Terrestrial planet geodynamics and climate change.

> *Priority Science Themes for Europa and Enceladus:*
> Ocean World interior structure, mass and energy budget, and habitability.

We identified four mission concepts that would provide compelling tests of key science hypotheses related to these priority science themes. These mission concepts are, in no particular order:

1. *Mars Gravity Mapper with InSAR*: an orbital mission at Mars that collects gravity data using spacecraft-to-spacecraft tracking and collects surface deformation measurements using InSAR,

2. *Mars Geophysical Helicopter*: a mobile aerial platform at the Martian surface with geophysics-focused instrumentation including a gravimeter and magnetometer,

3. *Enceladus Geophysical Orbiter*: a geophysical orbiter at Enceladus that collects gravity, topography, and deformation measurements, and

4. *Europa Geophysical Orbiter*: an orbiter at Europa with a gravity gradiometer and magnetometer.

We conclude that the geodesy community should continue to be established as an important subfield within planetary science, including through topical meetings, conference sessions, and mission concept studies.
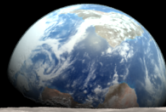
1. Introduction

Geodesy—the study of a world's shape, gravity field, orientation, and the time-variability of these properties—is one of the most powerful ways to investigate the formation, evolution, structure, and geological processes of bodies in the solar system. The power of geodesy has been best demonstrated in the Earth–Moon system with carefully tracked grounded assets and with high-precision orbital measurements of gravity and topography from spacecraft missions like the Gravity Recovery and Climate Experiment (GRACE), GRACE Follow-On (GRACE-FO), the Gravity Field and Steady-State Ocean Circulation Explorer (GOCE), the Lunar Reconnaissance Orbiter (LRO), and the Gravity Recovery and Interior Laboratory (GRAIL). At Earth, numerous missions have measured deformation using Interferometric Synthetic Aperture Radar (InSAR). In the Earth–Moon system, these measurements have transformed geodesy from a geophysical tool into one that unlocks substantial advances in climate change, geology, geochemistry, hydrology, surface processes, and atmospheric science.

Geodesy has been used to address a great number of high-priority science questions in the Earth–Moon system (Figure 1.1). The GRACE mission (Tapley et al., 2004) and GRACE-FO mission (Kornfeld et al., 2019) have been used to monitor climate change in real time, including measurement of hydrological cycles, mass loss of ice sheets, and sea level change (Tapley et al., 2019). Geodetic receivers on the ground have been used to measure surface deformation and constrain the viscosity structure of the Earth's interior (e.g., Khan et al., 2008; Lau et al., 2017). Terrestrial InSAR measurements have been used to probe active deformation related to a variety of processes—from slip on faults, to propagation of magma in volcanic systems, evolution of groundwater aquifers, the dynamics of glaciers and ice shelfs, and more (see Simons and Rosen, 2015 for a review). On the Moon, high-precision topography data from LRO's laser altimeter (Smith et al., 2017) and gravity data from
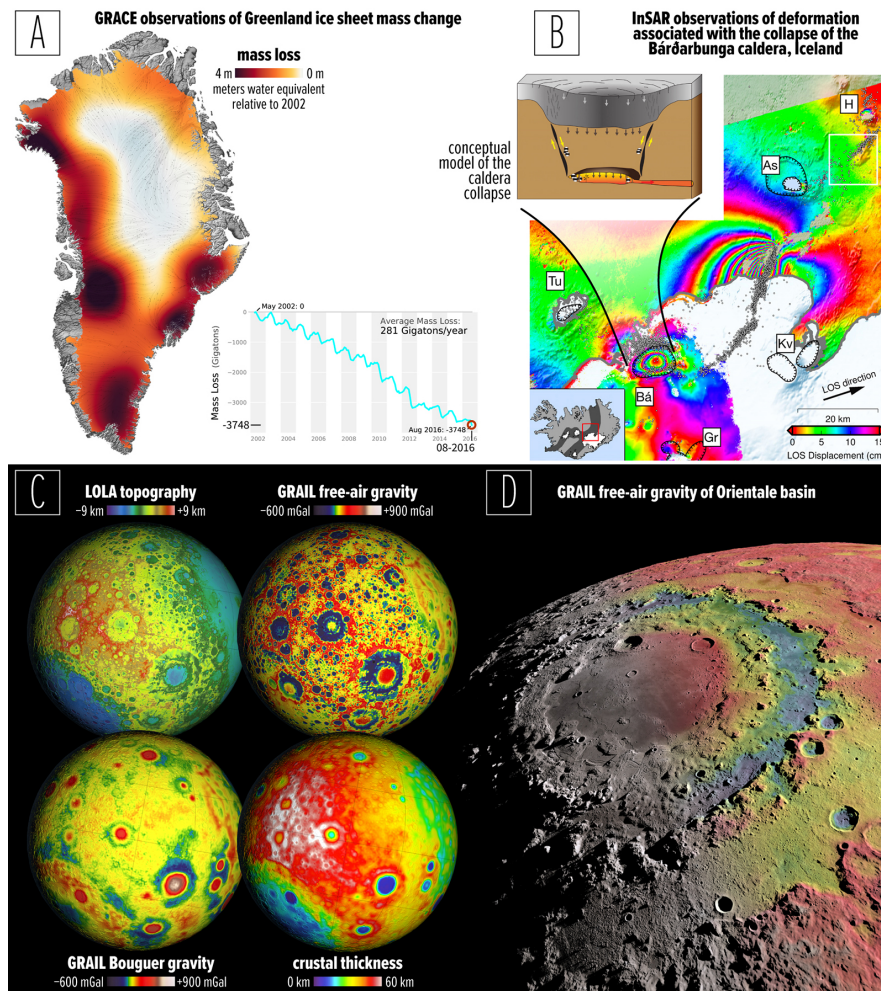
Figure 1.1: Examples of transformative science results enabled by geodesy investigations at the Earth and Moon. (A) Mass loss from the Greenland ice sheet, as measured by the Gravity Recovery and Climate Experiment (GRACE) mission from 2002 to 2016. Red/orange regions are where there has been substantial ice loss, whereas white regions have little/no ice loss. Average ice flow lines are indicated in gray, and measured from satellite radar interferometry. Image credit: Tapley et al., 2019, NASA. (B) InSAR measurements of the line-of-sight (LOS) component of ground motion (colored fringes, wrapped in 15-cm increments) of northwestern Vatnajökull, Iceland over a period of time in Fall 2014. The collapse of the Bàrðarbunga caldera (inset cartoon) can be inferred from bullseye pattern. Earthquakes are identified with white dots, and can be linked to the caldera collapse and the active dike to the northeast. Image credit: Riel et al. 2015. (C) LOLA- and GRAIL-derived global maps of various geophysical parameters for the Moon, including topography (top left), free-air gravity anomaly (top right), Bouguer gravity anomaly (bottom left), and modeled crustal thickness (bottom right). Image credit: Smith et al., 2017; Zuber et al., 2013b, 2016, NASA's Scientific Visualization Studio. (D) Synthetic view of the Orientale impact basin, showing shaded relief (gray), colored by GRAIL free-air gravity anomaly (colors). Image credit: NASA's Scientific Visualization Studio.

GRAIL (Zuber et al., 2013a,b) have, for example, been used to characterize the lunar crust in great detail (Wieczorek et al., 2013), constrain impact bombardment in the inner solar system (Neumann et al., 2015), and elucidate basin formation (Johnson et al., 2016) and the associated creation of crustal porosity (Soderblom et al., 2015). Careful geodetic tracking of landed retroreflectors on the Moon measures the changing distance between the Earth and Moon over time and provides tests of general relativity (Williams et al., 2006).

While geodesy at the Earth and the Moon has flourished, geodesy at other worlds has lagged behind. This gap is well demonstrated by comparing the state of knowledge for the gravity and topography of the Earth and Moon to other planetary bodies. The precision and resolution to which we know gravity and topography of Earth and the Moon is far superior, often by orders of magnitudes, compared to other planets and moons (Figure 2.2). However, this measurement gap does not reflect a gap in the potential scientific value of geodesy at different worlds.

Geodetic measurements beyond the Earth–Moon system have great power to address central questions in planetary science and astrobiology. This is well demonstrated in the recently released Planetary Science and Astrobiology Decadal Survey, "Origins, Worlds, and Life: A Decadal Strategy for Planetary Science and Astrobiology 2023–2032" (OWL for short). OWL is organized around 12 priority science questions—each with dozens of sub-questions and strategic research items (364 in total). An easy way to see how prevalent geodetic methods are in the Decadal Survey is to look at how frequently geodetic measurements (e.g., gravity, topography, deformation, etc.) are called out as priority strategic research. Table 1.1 shows this synthesis, and Appendix 2 lists the full set of relevant Strategic Research items. In short, geodetic methods are pervasive throughout OWL.

The prevalence of geodetic measurements in many Priority Science Questions within OWL is not surprising. For example, gravity and topography are powerhouses for investigating solid body interiors and surfaces (Q5) and circumplanetary systems (Q8). Some examples include:

- "Investigate the properties of subsurface water or magma oceans and melt reservoirs within Europa, Io, Titan, Enceladus, Triton and the Uranian Moons via electromagnetic sounding (active/passive) or induction, or geodetic measurements from orbiting or landed spacecraft." (OWL Q5.1)

- "Investigate the potential for active volcanism and deformation, and where and how crustal recycling is happening on Venus with synthetic aperture radar infrared, ultraviolet, or repeat-pass interferometry measurements of the Venusian surface and atmosphere." (OWL Q5.6)

- "Determine if/how tides have shaped the crustal structure, tectonics, and (cryo)volcanism of the large/mid-sized Saturnian (e.g., Enceladus, Titan) and Galilean (Io, Europa,

Ganymede, Callisto) satellites by characterizing the three-dimensional structure of their crusts through topography, gravity, ice-penetrating radar, and other geophysical methods." (OWL Q8.2)

However, it is important to note that geodesy is also relevant and implied in many other Priority Science Questions that may be surprising—including in the Life and Habitability theme. Some examples include:

- "Understand interior structures, tidal dissipation dynamics, and surface-interior exchange for icy shells of ocean worlds via measurement by spacecraft, theory, and modeling to determine the magnitudes and timescales of heating and persistence of liquid water." (OWL Q10.1)

- "Establish whether liquid water is present on Mars today in the subsurface by geochemical measurements of ices and recent hydrous minerals and geophysical measurements to probe the upper crust." (OWL Q10.3)

- "Prepare for characterizing life in the subsurface of ocean worlds by determining the heterogeneity of thicknesses of ice shells via planetary mission data as well as validating and deploying emerging technologies for life characterization, and maturing technology for accessing the subsurface for exploration, by work in the field and in the laboratory." (OWL Q11.4)

A full listing of relevant Strategic Research Items are included in Appendix 2.

We conducted a Keck Institute for Space Studies (KISS) study program titled "Next-Generation Planetary Geodesy" to identify the transformative science that would be enabled by geodetic measurements beyond the Earth–Moon system and the technologies and mission architectures that would be needed to achieve that science. We held two KISS workshops in 2021 to achieve this goal. In the first workshop, held virtually in June 2021, we identified the highest-priority questions in planetary science that could be obtained by new geodetic and complementary measurements at Mars, Venus, and Ocean Worlds. The choice of these targets was motivated by a combination of scientific and practical factors. In the second workshop, held in person at the Keck Institute on the campus of the California Institute of Technology in November 2021, we determined the needed technology developments and most compelling mission concepts and architectures to obtain these measurements.

This document reports the results of the KISS study program. The report is organized as follows: Part I (Sections 2–5) is focused on Science, and describes the most compelling planetary science that could be achieved by new geodetic data at worlds beyond the Earth–Moon system. Ocean Worlds (with a particular emphasis on Europa and Enceladus) are discussed in Section 2, Mars is discussed in Section 3, Venus is discussed in Section 4, and

Themes	A) Origins			B) Worlds and Processes					C) Life and Habitability			Cross-Cutting Linkage
Priority Science Questions:	Q1 Evolution of the protoplanetary disk	Q2 Accretion in the outer solar system	Q3 Origin of Earth and inner solar system bodies	Q4 Impacts and dynamics	Q5 Solid body interiors and surfaces	Q6 Solid body atmospheres, exospheres, magnetospheres, and climate evolution	Q7 Giant planet structure and evolution	Q8 Circumplanetary systems	Q9 Insights from terrestrial life	Q10 Dynamic habitability	Q11 Search for life elsewhere	Q12 Exoplanets
Prevalence of Geodesy:	8%	36%	11%	3%	43%	7%	18%	45%	0%	13%	5%	0%

Table 1.1: The prevalence of geodesy in the Planetary Science and Astrobiology Decadal Survey, "Origins, Worlds, and Life: A Decadal Strategy for Planetary Science and Astrobiology 2023–2032." Colors indicate the frequency of geodetic methods (e.g., gravity, topography, etc.) being identified in Strategic Research items for each Priority Science Question. Dark pink indicates geodetic methods are mentioned in >40% of strategic research items; medium pink indicates >10%; light pink indicates >0%; off-white indicates 0%. This analysis includes all geodetic measurements, and does not distinguish between target bodies (for example, this includes geodetic measurements for small bodies and gas giants, despite them not being the focus of this report).

other worlds (including ice giants, other planetary satellites, etc.) are discussed Section 5. Part II (Sections 6–7) is focused on Technology and Implementation. In Section 6, we identify current and future spacecraft instrumentation and technologies needed to achieve the scientific advances described in Sections 2–5. These technologies include both classically defined geodetic instrumentation and other geophysical methodology that has especially synergistic capabilities with geodesy (e.g., electromagnetic sounding, seismology, thermal measurements, etc.). In Section 7, we make recommendations for four spacecraft mission concepts that could be flown in the coming decade and provide the most compelling pathways to achieve the advances in planetary science we identified. In Section 8, we describe other future directions for planetary geodesy and make concluding remarks.
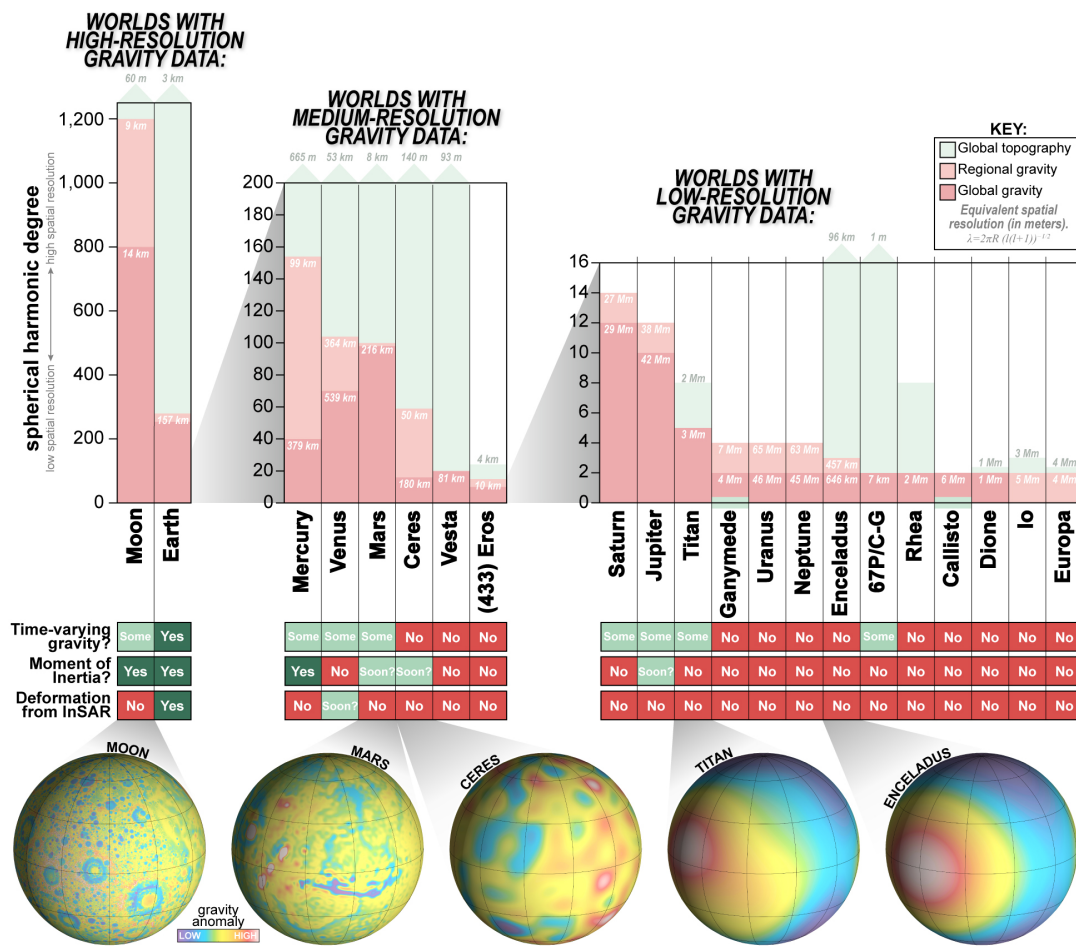
Figure 1.2: Comparison of the spatial resolutions to which the topography and gravity fields of Solar System objects from orbital remote sensing spacecraft are known. Image credit: James Tuttle Keane.

Part I

Science
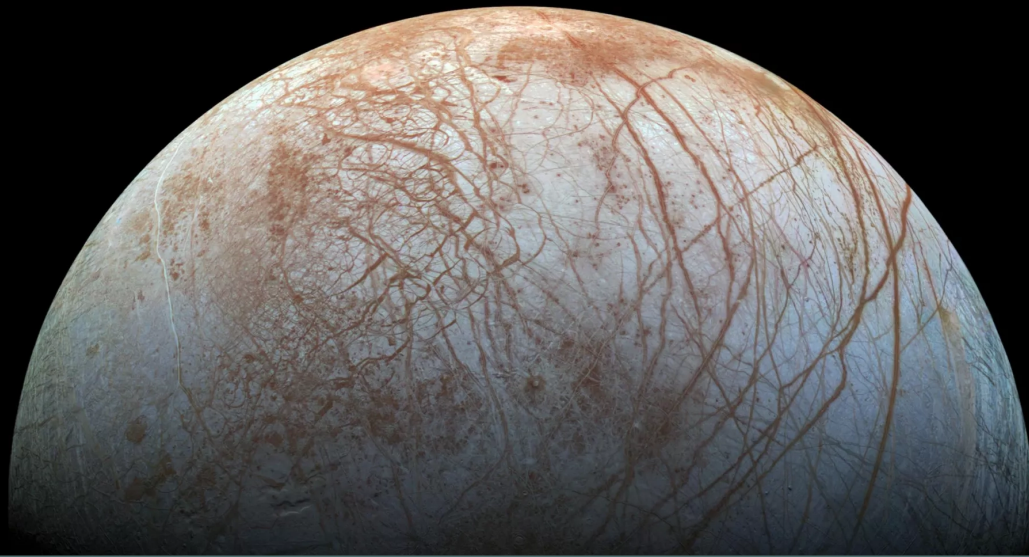
2. Ocean Worlds

2.1 Introduction

Ocean Worlds—bodies with a subsurface liquid water ocean beneath an ice shell—have recently emerged as one of the most fascinating and important classes of planetary bodies in the solar system (e.g., Nimmo and Pappalardo, 2016). Their internal liquid water oceans raise the intriguing possibility of habitable environments in the outer solar system and their high level of complexity and geologic activity make them invaluable for studying active geologic processes. For those Ocean Worlds that orbit giant planets (e.g., Europa, Enceladus), the moons offer the chance to learn about the coupled thermal and orbital evolution in giant planet systems. Missions like Galileo, Cassini, and Juno have given us tantalizing glimpses of Ocean Worlds in the Jupiter and Saturn systems, but outstanding fundamental questions remain. For example, how are these relatively small bodies, which should cool rapidly, able to sustain such extraordinary levels of geologic activity and keep their internal liquid water oceans from freezing? For the larger moons, radiogenic heating from the rocky interior may be important, but for the smaller moons such as Enceladus, tidal interaction with their massive parent bodies must play a significant role. Yet, Mimas is closer to Saturn and has a more eccentric orbit but no signs of geological activity, cautioning against simple models of thermal and geological evolution.

We are only just beginning to understand the complex interactions between planets and satellites. Many questions about the coupled thermal and orbital evolution of these worlds remain open. Importantly, we are still far from understanding how and where energy is dissipated within the interiors of these bodies, and how tidal dissipation affects other complex, interrelated aspects of an Ocean World—including the internal temperature structure, ice

shell and ocean dynamics, surface deformation, surface heat flow, fluid interactions with the deeper rocky interior, and the nature and behavior of ocean-to-surface pathways including the active cryovolcanic eruptions observed at Enceladus (e.g., Porco et al., 2006). Our ability to investigate these processes is limited by the lack of geodetic measurements collected to date for Ocean Worlds.

Understanding the interior structure and transport of mass and energy through time is an essential part of assessing the potential habitability of Ocean Worlds (e.g., Vance et al., 2018). Figure 2.1 shows a schematic illustration of these processes. Characterizing the nature and mechanics of any ocean-to-surface pathways is important both for determining how and where to search for signs of life and for assessing the degree to which any erupted materials may be representative of internal reservoirs. Characterizing the energy budgets, mass and energy transport, internal structure and dynamics, tidal interactions, and active deformation processes is key to fundamental understanding of the evolution and behavior of the giant planet systems and of the solar system in general.
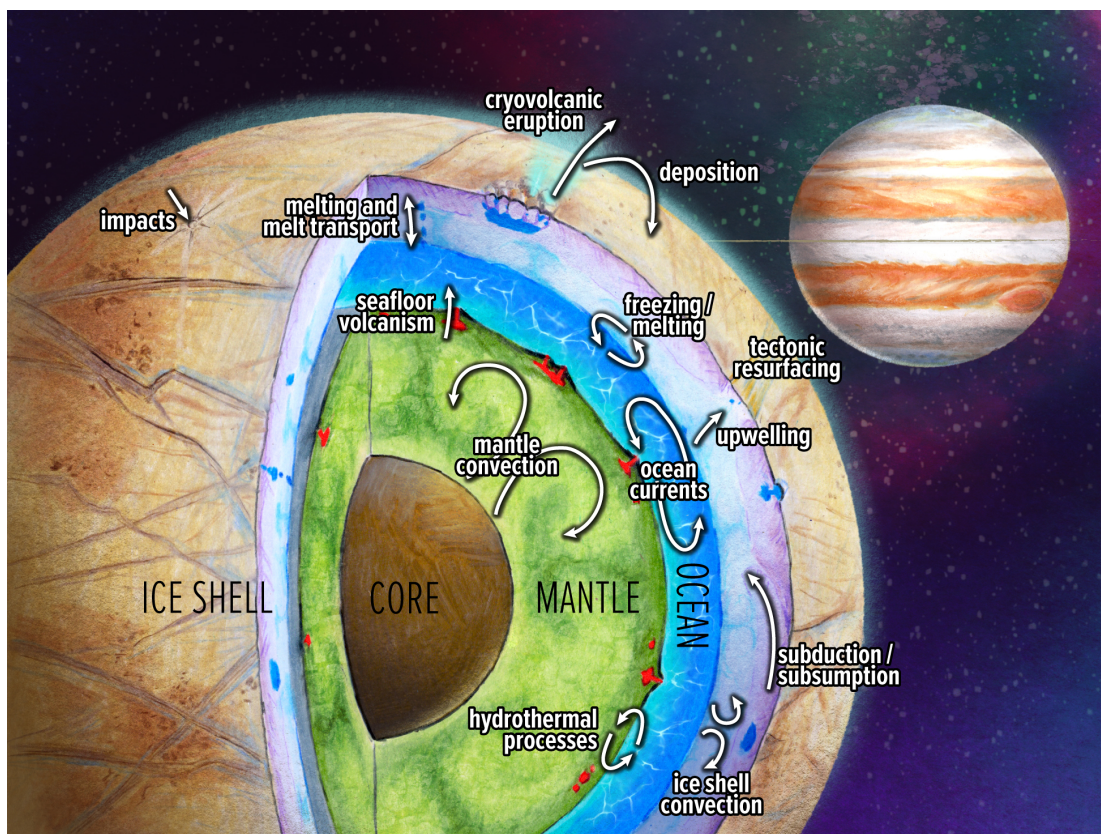
Figure 2.1: Schematic illustration of the interior structure, and the transport of mass and energy through an ocean world (showing Europa as an example case). Image credit: James Tuttle Keane and Aaron Rodriquez.

While the Galileo and Cassini missions helped us to more fully recognize the rich complexity and importance of Ocean Worlds, their encounters with these bodies were limited to a handful of flybys at best. Geodetic measurements to date have been consequently sparse, and global-scale interior structure models are correspondingly coarse. In some cases, there have barely been enough complementary observations to yield basic interior structure models (e.g., Europa: Anderson et al., 1998), but in all cases, there are large uncertainties that make it impossible to resolve many of the open questions. Moreover, with very limited exceptions, there have been insufficient revisits of these bodies to observe changes through time, whether secular or tidally modulated. Future geodetic measurements that can improve upon current spatial and temporal coverage have the potential to transform understanding of the physical state, evolution, and ongoing activity of Ocean Worlds, and the potentially habitable environments in their interiors.

Our growing appreciation for the complexity and dynamics of icy Ocean Worlds, and the puzzles they present, coincides with recent advances in geodetic techniques applied to Earth and the Moon (e.g., Kornfeld et al., 2019; Zuber et al., 2013b). The timing is ideal to determine the science questions we could address and the puzzles we could begin to solve if geodetic knowledge of Ocean Worlds is elevated to a level approaching what has recently been achieved for Earth and the Moon. Three driving science questions in understanding Ocean Worlds that can be addressed with geodetic observations and related techniques are:

1. What are the interior structures and tectonic evolutions of Ocean Worlds?

2. What are the sources, sinks, and transport mechanisms of mass and energy within an Ocean World?

3. Where are the habitable environments within an Ocean World, and how long do they survive?

Below, we describe the importance of these questions, the current state of knowledge in their answers, and how future geodetic and related data at Ocean Worlds would provide fundamental leaps in addressing them.

2.2   Ocean Worlds Driving Science Question 1: What are the interior structures and tectonic evolutions of Ocean Worlds?

The interior structures of Ocean Worlds provide the basic context necessary for addressing many of these bodies' fundamental questions. The basic structure is a differentiated icy world, with any silicates and metals concentrated toward the center, surrounded by an envelope of mainly H_2O, including an outer ice shell, an underlying subsurface liquid water ocean and, in some cases, high-pressure phases of ice (Figure 2.2).

Figure 2.2: Models for the interiors of Europa (left) and Enceladus (right) informed by geodetic datasets. The two worlds are not shown to the same scale (Europa is much larger than Enceladus), although the interior layers for each body are shown to scale. In both of these models, a relatively thin ice shell overlies an ocean, which surrounds a large rocky interior. For Europa, a metallic core is also present. Image credit: Doug Hemingway.

The icy surfaces of Ocean Worlds can be characterized by visible and spectroscopic analyses, but understanding of their interiors relies on other instrumentation, including geodetic observations of shape, gravity, and rotational dynamics. The most basic piece of information is the mass, which constrains bulk density and permits estimates of the silicate mass fraction. Measurements of the spherical harmonic degree/order 2 shape and gravitational field sometimes permit inferences about the moment of inertia, which can be related to the radial density structure (e.g., Anderson et al., 1998; Hemingway et al., 2018; Iess et al., 2014; Schubert et al., 2009). In some cases, these measurements can yield an estimate of the total thickness of the water envelope (e.g., Gomez Casajus et al., 2021), but large uncertainties often remain, especially regarding the deeper interior. These ambiguities may be resolved with measurements of the shape and gravity field across a range of length scales and timescales, particularly when combined with measurements of rotational dynamics (e.g., libration, precession, nutation) and other complementary observations (e.g., magnetic induction, ice-penetrating radar). Shape and gravity data also allow measurement of an Ocean World's non-hydrostaticity, which can reveal the stresses that can be supported in the interior and how topography is supported (e.g., Akiba et al., 2022). Below, we discuss the structure and evolution of the three major components of an Ocean World interior—the solid ice shell, the liquid water ocean, and the silicate interior—and the ways in which geodetic data can elucidate outstanding scientific questions related to these components.

2.2.1 Ice shell structure and tectonics

The ice shell structure and thickness, its internal dynamics, and its tectonic evolution are all fundamentally related. Ice shell thickness is controlled by the body's energy budget and the balance between internal heating (tides, radiogenic heating, etc.) and cooling to space. A very thin ice shell reflects rapid heat loss, implying that any internal liquid water ocean would freeze rapidly unless internal heating is sufficiently high. Heat loss may be slower if the ice shell is thicker, but thicker ice shells may also undergo convection (e.g., Tobie, 2003), transporting heat more efficiently than a conductive shell of similar thickness. Therefore, ice shell dynamics is critical in controlling thickness. Lateral variability in the ice shell thickness may offer clues to these dynamics (e.g., Nimmo and Bills, 2010). Thickness variations are difficult to maintain in an active, convecting ice shell unless there are also very large lateral variations in heating, either within the ice shell or applied at its base. If no heating is taking place within the ice shell, then lateral shell thickness variations should be small if the ocean redistributes heat efficiently, especially if the ice shell is convecting. However, ocean dynamics can concentrate heat in certain regions such that variations in the shell thickness can also reflect ocean dynamics. An oceanographic "ice pump" mechanism can further reduce basal ice topography where thick ice melts and reaccretes below thinner ice as a result of pressure-induced differences in the melting temperature (Lewis and Perkin, 1986; Soderlund et al., 2014). The ice shell structure also provides clues about how and where energy is being dissipated within the interior of the body (Hemingway and Mittal, 2019).

For an Ocean World that orbits a giant planet, like Europa or Enceladus, tidal effects on the ice shell can provide an opportunity to effectively constrain ice shell thickness. The response to tides is generally amplified if the ice shell is decoupled from the deeper interior by a global ocean. For example, the large amplitude of Titan's tidal deformations—quantified by the tidal potential Love number, k_2 (Iess et al., 2012)—strongly implies a decoupled ice shell and therefore a global subsurface ocean. Similarly, the large amplitude of the forced physical librations observed at Enceladus (Thomas et al., 2016) suggests a decoupled ice shell. The amplitude of the tidal response is a function of shell thickness and rigidity, and can therefore be used to constrain those quantities (e.g., Moore and Schubert, 2003). Similarly, the physical libration amplitude is a function of shell thickness. For a rigid and relatively thick (compared to the body radius) ice shell, the amplitude of the physical libration is a strong inverse function of the shell thickness—as is the case for Enceladus. For a thin shell (compared to the body radius), the tidal deformation and librational motion is coupled. As the thinner shell deforms due to tides, its amplitude of physical libration becomes a weaker function of the shell thickness. Thus, for a thin shell, such as Europa's, libration is only weakly sensitive to the shell thickness (Van Hoolst et al., 2013). Obliquity measurements can also provide evidence for a decoupling ocean. This approach can be challenging in practice because obliquity values are often small, but obliquity measurements have been used to

support the presence of an ocean on Titan (Baland et al., 2014). Together, measurements of tidal deformation and rotational dynamics can provide constraints on shell thickness.

Lateral variability in the ice shell's thickness can be inferred from the relationship between gravity and topography (e.g., Akiba et al., 2022) or from ice penetrating radar mapping of the ice–ocean interface (Blankenship et al., 2009). The relationship between gravity and topography (quantified by the "admittance") reveals how topography is supported. For example, if long wavelength topographic variations are accompanied by only weak variations in the gravitational field, topography is likely compensated isostatically. Depending on the specific nature of the compensation, lateral variations in shell thickness, composition, or porosity can be inferred from the observed topography (Besserer et al., 2013; Hemingway and Mittal, 2019). Because of the wavelength dependence of the viscoelastic response of the ice shell and compensation mechanism, it is especially valuable to obtain gravity and topography measurements across a range of length scales (or equivalently, spherical harmonic degrees). If the gravity and topography can be constrained to sufficiently high spherical harmonic degrees, it is possible to estimate the mean shell thickness based on the wavelength at which the topography transitions from compensated to uncompensated. Where topography is compensated, lateral shell thickness variations can be inferred (Akiba et al., 2022).

Ocean-to-surface pathways are an important component of ice shell structure that are related to lateral variability in ice shell thickness (Figures 2.3 and 2.4). Important questions include (Degruyter and Manga, 2011; Hemingway et al., 2020; Ingersoll and Nakajima, 2016; Kite and Rubin, 2016; Manga and Michaut, 2017; Nakajima and Ingersoll, 2016; Spencer et al., 2018):

- How does tectonic activity create open fissures in the ice shell?

- How can these conduits between the ocean and the surface be maintained over geologic time?

- What controls the geometry of these conduits?

- How do these pathways determine mass and energy transport through the ice shell?

- How does the presence of tectonic cracks affect ice shell deformation on local and regional scales?

- What is the relationship between fractures and intrusions of water in the form of dikes or sills?

- How do ice shell fractures result in cryovolcanic eruptions?

Real-time measurements of topographic deformation in the vicinity of these conduits using geodetic observations would be particularly valuable. The amplitude and phase of tidally controlled deformation varies depending on whether the conduits penetrate the ice shell entirely through to the ocean (Běhounkovà et al., 2017; Souček et al., 2016). Because ice shell deformation should be sensitive to shell thickness (Beuthe, 2018), jointly interpreting active deformation measurements with ice shell thickness constraints would be especially enlightening.

Observations of the current state of the ice shell may reveal present-day tectonic deformation processes and constrain their history (Kattenhorn and Hurford, 2009; Patterson et al., 2018). Time-variable measurements of gravity or topography could reveal the magnitude and character of any ongoing deformation, helping to better determine the nature and history of ice shell dynamics. These measurements would be a powerful supplement to high-resolution optical images that identify potentially important active or extinct tectonic features, especially if the gravity and topography measurements could be made at length scales comparable to the features of interest (e.g., troughs, ridges).

2.2.2   Ocean structure

The dimensions and dynamics of the ocean are important for a number of questions related to mass transport, energy transport, and habitability. Ocean thickness is difficult to directly measure from static gravity data because of the similarity in density between solid ice and liquid water. However, ocean thickness can be inferred by jointly measuring the hydrosphere thickness and estimating the ice shell thickness (Section 2.2.1).

Measurements of magnetic induction are particularly valuable for determining the existence of oceans and their thickness for worlds that are exposed to time-varying magnetic fields (e.g., Kivelson et al., 2000). For example, because Jupiter's magnetic field is tilted ~$10°$ from its spin axis, all of its satellites experience a time-varying magnetic field as Jupiter rotates on its ~10-hour spin period. This is a useful measurement because the magnitude of the induced magnetic field is not degenerate with other types of geophysical observations. The inductive response depends on the ocean conductivity, which depends on the salinity, depth to the ocean (i.e., ice shell thickness), and ocean thickness. Although the inductive response at a single frequency does not provide a unique answer for the ocean, the resulting ambiguities can be resolved by measuring the magnetic induction signal at a range of different frequencies (Khurana et al., 2009; Vance et al., 2021).

Lateral variations in shell thickness may correspond to variations of the ice–ocean interface and reveal ocean properties. The "topography" along this interface relates to any ongoing freezing or melting taking place at the top of the ocean, which in turn could affect regional variations in ocean salinity due to ponding of fresh water where ice is melting or salt rejection where ocean water is freezing onto the base of the ice shell (Čadek et al., 2019; Hemingway
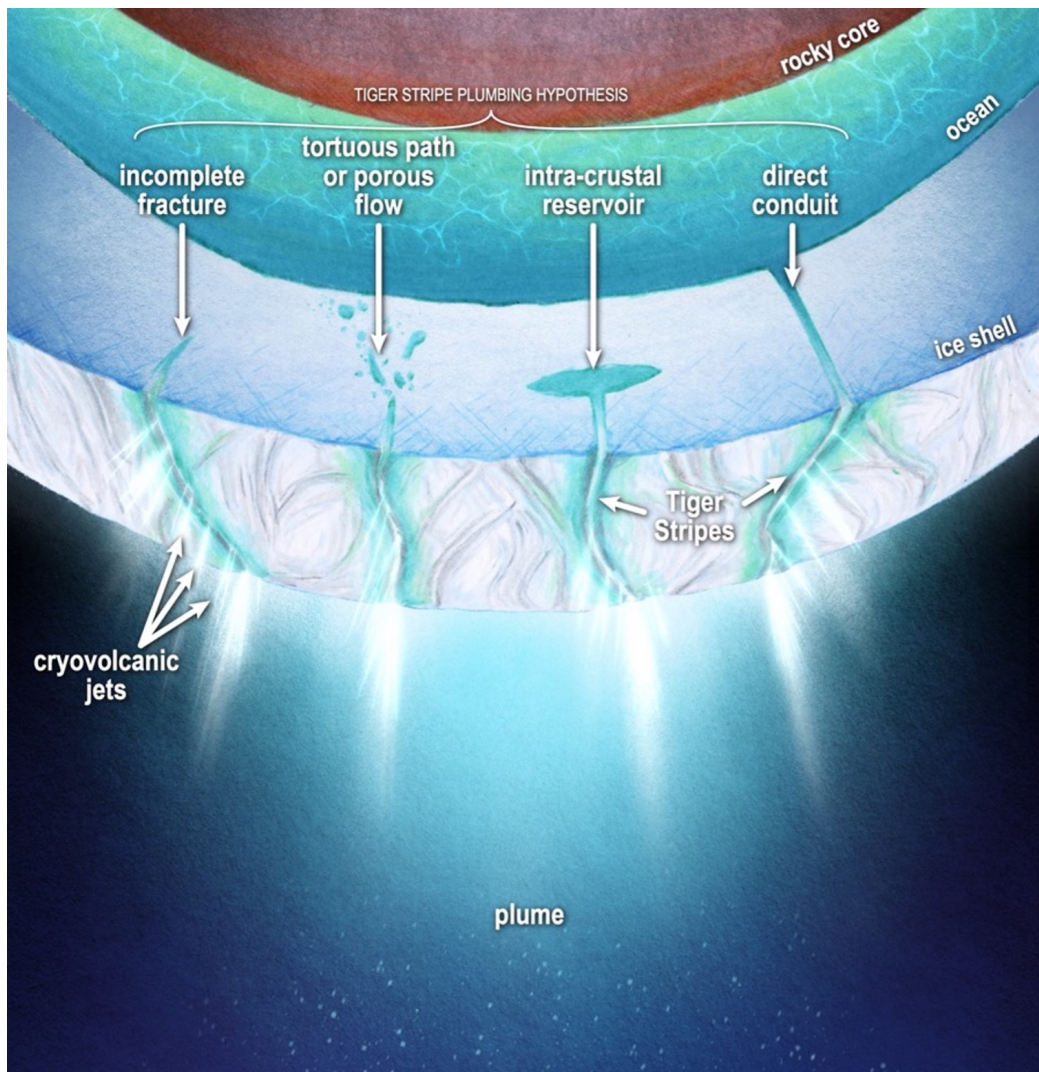
Figure 2.3: Illustration of various models for how Enceladus' ocean may make it to the surface at the Tiger Stripes. Enceladus' Tiger Stripes are the conduits by which water is ejected into space, yet we do not understand how they form, evolve, or the nature of their plumbing. Do they directly tap the ocean, some intra-crustal reservoir, or something else? Image credit: James Tuttle Keane and Aaron Rodriquez.

and Mittal, 2019; Kvorka et al., 2018; Lobo et al., 2021). In this way, the dynamics of the ice–ocean interface can drive salinity gradients that may control ocean circulation, and ice shell thickness gradients may control the pattern of oceanic heat flux into the ice shell (e.g., Kang et al., 2022). Gravity waves in a stratified ocean can produce detectable time-variable gravity signals, revealing compositional gradients within the ocean.

Patterns of ocean circulation determine how mass and energy are transported across and throughout the ocean. In particular, how ocean circulation develops under different conditions determines whether heat transfer through the ocean is stronger at the equator or at the poles (e.g., Amit et al., 2020; Kvorka and Čadek, 2022; Soderlund, 2019; Zeng and Jansen, 2021). Ocean dynamics, particularly the formation of resonant waves, also determines the degree to which tidal energy can be dissipated within the ocean itself (e.g.,Chen et al., 2014; Hay and Matsuyama, 2019; Lemasquerier et al., 2017; Rovira-Navarro et al., 2019; Tyler, 2011). Measurements to constrain ocean dynamics are an area of active research, and geodesy (Čadek
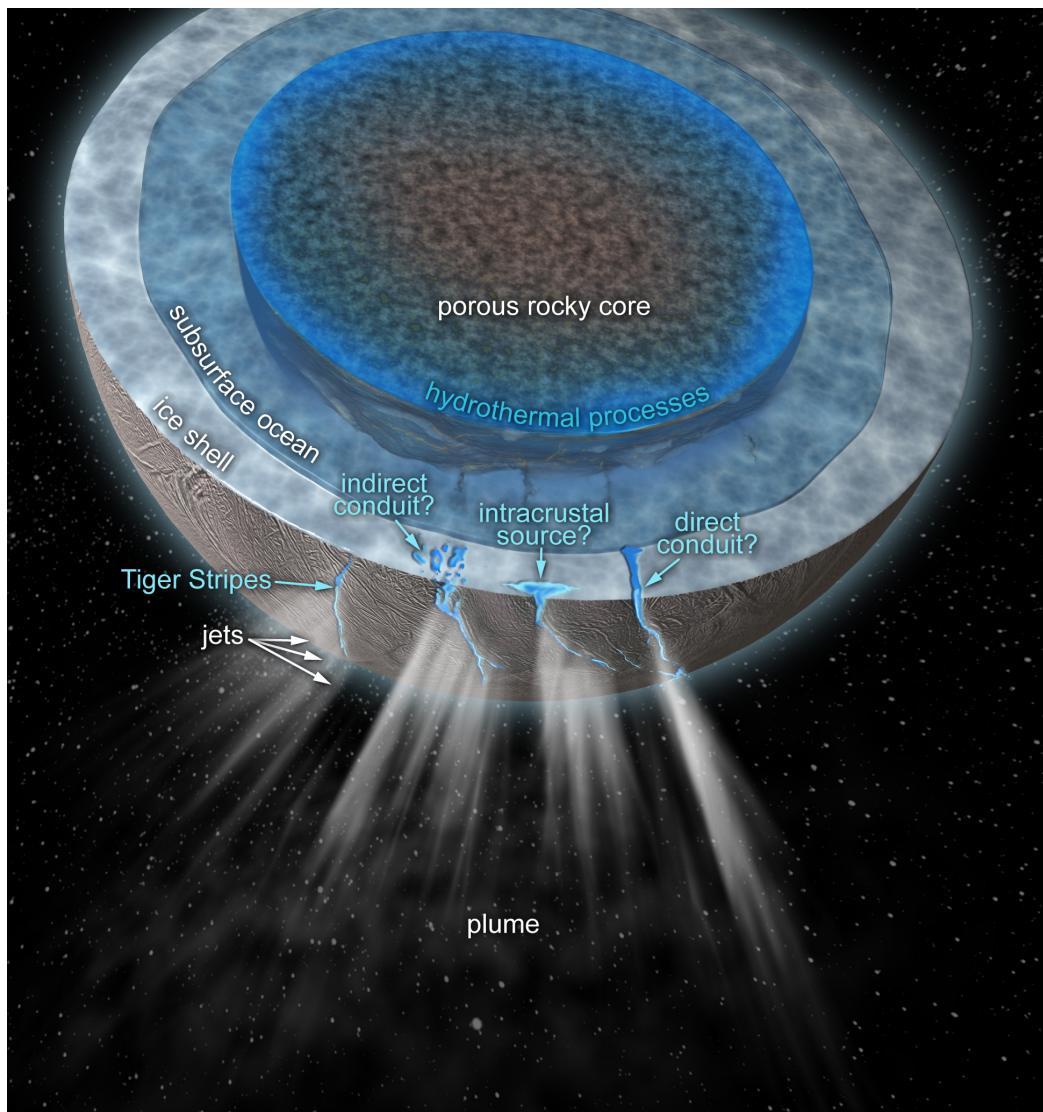
Figure 2.4: Illustration of the interior structure of Enceladus, and the various processes and pathways by which water circulates through, and ultimately out of, the Enceladus. Image credit: Charles Carter, James Tuttle Keane, Keck Institute for Space Studies.

et al., 2019; Kvorka et al., 2018), magnetic induction (Vance et al., 2021), and seismology (Panning et al., 2018) show particular promise.

The nature of the seafloor is important for understanding the potential for chemical exchanges between the ocean and the silicate portion of the interior. The temperature and pressure conditions at the seafloor provide important context for such processes and can be estimated from knowledge of the overlying ice shell and ocean (i.e., their thicknesses and densities). Any ongoing geological activity (e.g., tectonics, hydrothermal processes) at the seafloor would be difficult to detect from the exterior of the body, but inferences can be made from the likely conditions and the presence of any topographic anomalies, which are potentially detectable from geodetic observations such as gravity and topography. Such signals arising from seafloor topography (Dombard and Sessa, 2019; Koh et al., 2022) may be obscured by gravity and topography anomalies originating in the ice shell, but there may be opportunities to separate the contributions given an ice shell decoupled from the deeper interior. Radar sounding may be able to infer and map the topography of the ocean-ice interface, the gravitational effect of which can subsequently be corrected for, thus allowing gravitational probing of the seafloor topography. Also, monitoring the orientation of the shell in combination with time-variable gravity measurements at a variety of tidal phases may permit determination of the shape of the rocky interior.

For Ocean Worlds the size of Europa and smaller, the ocean water is likely in direct contact with the silicates beneath. For larger worlds (e.g., Ganymede), the base of the ocean may instead be in contact with high pressure water ice phases (Journaux et al., 2020), potentially hindering interactions between the liquid ocean and the rocky interior (Kalousová and Sotin, 2018, 2020).

2.2.3 Rocky interior structure

The interior structure of the deep, rocky interior is critical to understand Ocean Worlds, but is more difficult to analyze compared to the ice shell by nature of its depth. Knowledge of the bulk density of the deep interior helps constrain its composition, porosity, and mechanical properties. The composition is directly relevant to understanding the body's formation history and the magnitude of radiogenic heating taking place within the interior. The mechanical and elastic properties of the deep interior are important in controlling how tidal energy is dissipated within the body. For example, the tidal response of an Ocean World may be very different depending on whether the rocky part of the interior is consolidated and largely intact, highly fractured, or a loose rubble pile (Roberts, 2015). The porosity and permeability of the rocky interior are important for understanding interactions with the overlying ocean, including the possibility of hydrothermal processes where fluids flow through the tidally heated rocky interior (Choblet et al., 2017), or heating due to tidally controlled flushing of fluids through

the porous rock (Randolph-Flagg et al., 2020; Rovira-Navarro et al., 2022). Orbital gravity and landed seismology represent ways to constrain the rocky interior structure.

2.3 Ocean Worlds Driving Science Question 2: What are the sources, sinks, and transport mechanisms of mass and energy within an Ocean World?

2.3.1 Global energy budget

Understanding the global energy budget of an Ocean World is fundamentally linked to its interior structure. There are two potentially important heat sources: radiogenic heating and tidal heating. The relative importance of these sources depends on the composition, structure, and orbit of a given world. The magnitude of radiogenic heating is often estimated by assuming the silicate interior has chondritic abundances of radiogenic elements (Castillo-Rogez and Lunine, 2010; Malamud and Prialnik, 2016; Neveu et al., 2017).

Tidal heating—heat generated from periodic deformation due to tidal forces—is an important heat source for many of the Ocean Worlds that are moons of a giant planet. The total dissipation rate of eccentricity-tide induced heating in the solid layers of a planetary body, in the approximation of low eccentricity, is given by:

$$\dot{E} = \frac{21}{2}\frac{k_2}{Q}\frac{n^5 R^5}{G}e^2 \tag{2.1}$$

where E describes total energy dissipation rate, k_2 the degree-2 gravitational potential love number, Q the tidal quality factor, n the mean motion, e the body's eccentricity, and R is the radius of the moon. In this equation only k_2 and Q depend on the internal structure of the satellite, and are generally the least certain terms. Because of this uncertainty, it is common to treat them as a grouped parameter (k_2/Q) which encapsulates the uncertainty in internal structure. Dissipation can also be caused by a moon's obliquity. This heat is often less significant compared to dissipation from eccentricity tides in solid body dissipation (Chen et al., 2014; Hay and Matsuyama, 2017), but can be important in ocean heating.

We estimate the approximate relative importance of radiogenic heat and tidal heat for a variety of icy moons in Figure 2.5. To provide a plausible range for tidal heating, we show two values of k_2/Q (1/100 and 1/1,000) and vary each satellite's eccentricity between its current eccentricity and 0.01 (roughly the eccentricity of Europa). The heat from radioactive decay is calculated by assuming a carbonaceous chondrite abundance of radiogenic elements in the silicate interior (Bierson et al., 2018). The mass of that interior is calculated using each moon's bulk density, assuming a silicate density of 3,500 kg/m^3 and that the moon is a mixture of silicates and ice. The "ocean limit" line is the point below which an ocean would be refreezing if it exists (derived in the following section). A heat production above this limit is necessary but not sufficient to sustain an ocean.
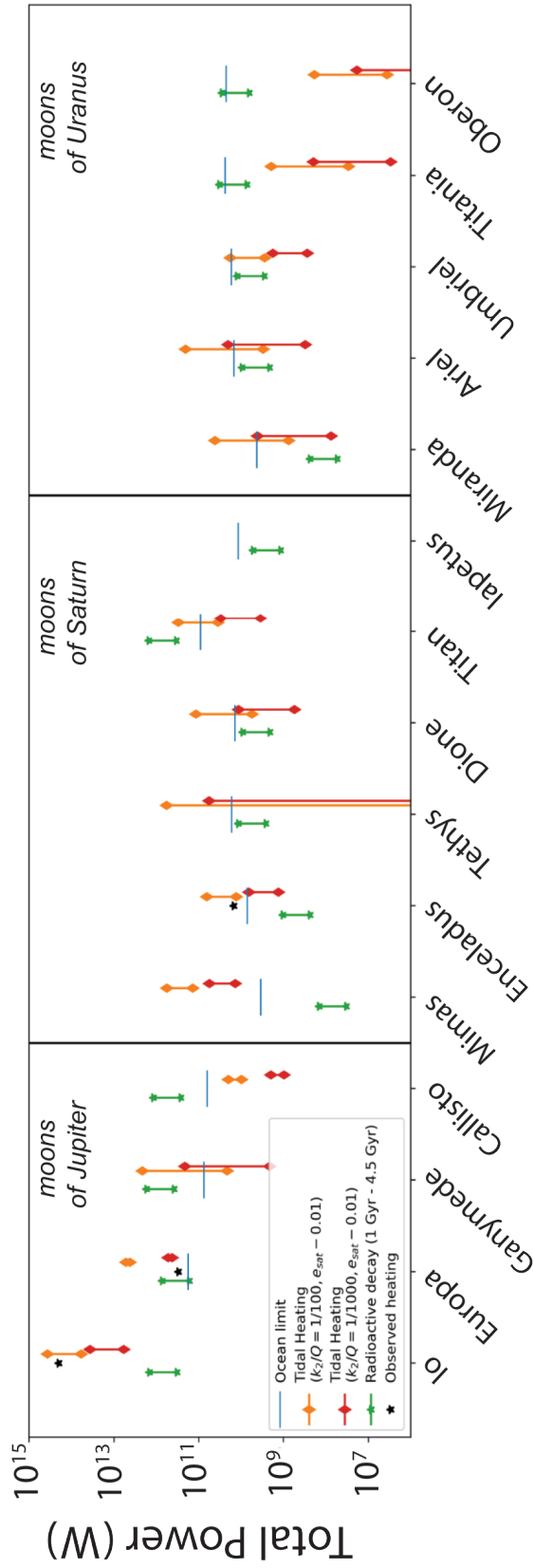
Figure 2.5: Estimate of the total power from radiogenic heating and tidal heating on some moons of the outer planets. The "ocean limit" is the heat production below which an ocean cannot be sustained assuming a conductive ice shell. Estimated power from observations is shown for Io (Rathbun et al., 2004), Europa (Ruiz, 2005), and Enceladus (Howett et al., 2011b). For each moon, the eccentricity is varied from current eccentricity up to 0.01 to account for the possibility of past eccentric orbits. For all moons except Io, the current eccentricity is the lower end of the tidal heating bars for a given k_2/Q.

Figure 2.5 emphasizes that, across the giant planet systems, there are worlds where tidal heating dominates (Io, Enceladus), worlds where radiogenic heating dominates (Callisto, Iapetus, Titania, Oberon), and worlds for which the two heat sources may be comparable or were comparable in the past. One outlier on this plot is Mimas, which is expected to have high tidal heating due to its high eccentricity ($e = 0.02$), but does not show signs of extensive geological activity. This is a well-known (but not well understood) problem demonstrating that uncertainties in k_2/Q may be large, with a true value much lower than shown in this plot (Meyer and Wisdom, 2007; Squyres et al., 1983).

Figure 2.5 represents an estimate of the relative importance of heat sources based on current knowledge, but is largely based on assumptions and parameters with high uncertainty. Geodetic observations are central in addressing this issue and in estimating accurate values for both types of heat sources. In particular, the uncertainty in k_2/Q is very high. Future geodetic measurements could dramatically improve knowledge of this parameter, and therefore the global heat budget of Ocean Worlds, by providing measurements of the tidal potential phase lag from spacecraft radiometric tracking or long-term astrometric monitoring that directly constrains k_2/Q (e.g., Lainey et al., 2009).

2.3.2 Where is tidal dissipation occurring?

The total amount of tidal dissipation in an Ocean World is described by Equation 2.1, but this equation does not describe the spatial distribution of that dissipation. Tidal dissipation is not uniformly distributed throughout an Ocean World (Figure 2.6). Where that heat is dissipated (both radially and laterally) controls the effects of tidal heating, including on surface geology and subsurface habitability.

The spatial distribution of tidal heating depends on the rheology of the internal layers. Tidal dissipation is maximized when the period of the tidal forcing is comparable to the time over which stress can be dissipated, known as the Maxwell time (Findley et al., 1976). The Maxwell time τ_{m} is given by

$$\tau_{\mathrm{m}} = \eta/G \tag{2.2}$$

where η is the viscosity, and G the shear modulus. The orbital period of Ocean Worlds is typically on the order of several days, which is comparable to the Maxwell time of ice near its melting point near the ice–ocean boundary. Therefore, the ice shell is often assumed to be the likely region where most of the dissipation is occurring (Sotin et al., 2009).

For most Ocean Worlds, tidal dissipation within the ocean is thought to be small compared to dissipation in the ice shell (Chen et al., 2014). Dissipation in the ocean depends on the highly uncertain basal ocean friction and ocean thickness (Hay and Matsuyama, 2017). Only for moons with low eccentricity and high obliquity is ocean dissipation expected to be an

important component of the global energy budget (Hay and Matsuyama, 2019; Matsuyama et al., 2018).
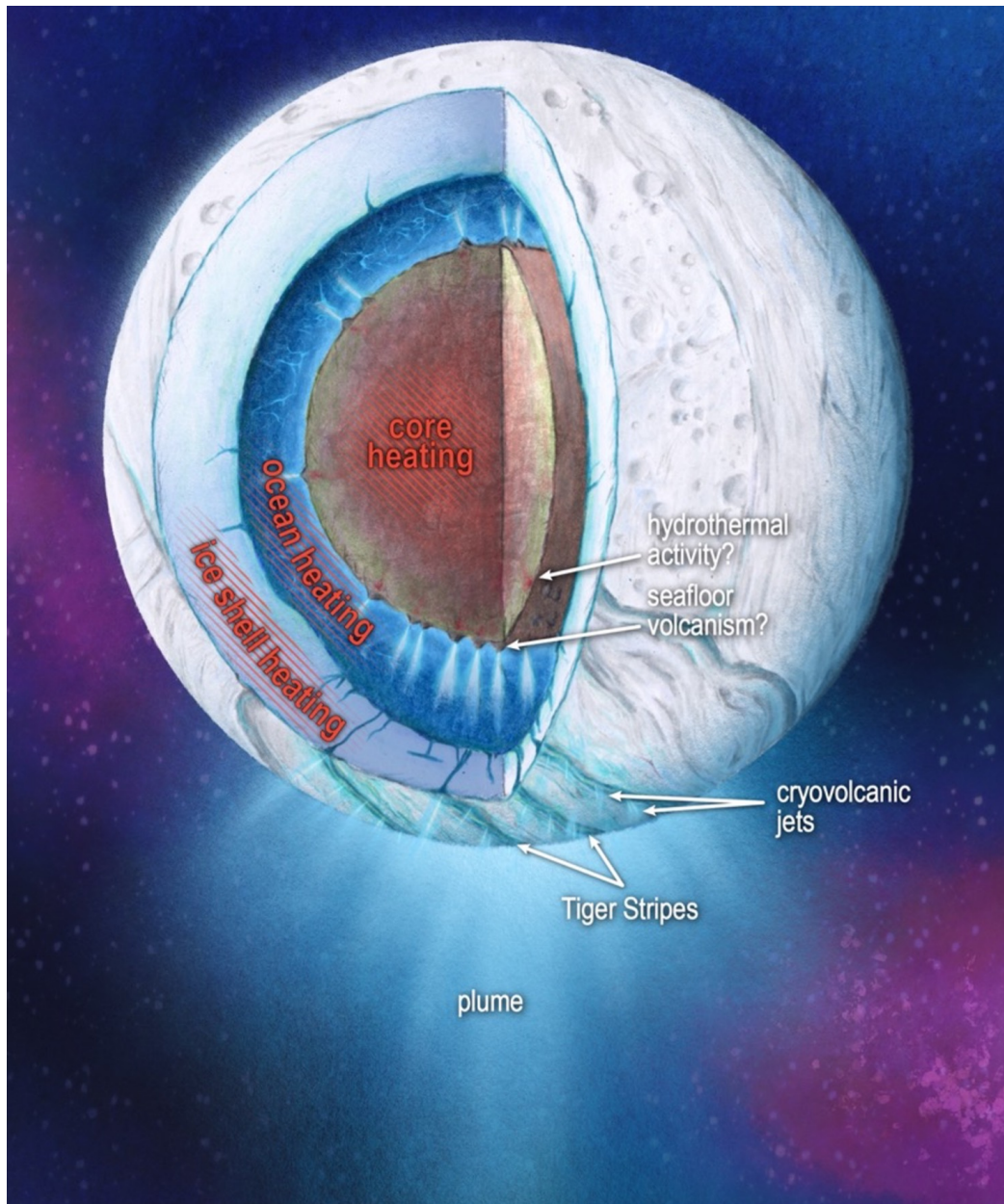
Figure 2.6: Illustration of possible locations of heating within an ocean world (showing Enceladus as an example). The overall energy budget of ocean worlds is poorly constrained. Image credit: James Tuttle Keane and Aaron Rodriquez.

It is generally considered unlikely that substantial tidal dissipation occurs within the silicate interior because of the high viscosity of silicates (Sotin et al., 2009). These previous estimates have been performed using a Maxwell rheology model. However, experimental data has

shown that this Maxwell model consistently underpredicts the amount of dissipation in high viscosity materials (Jackson et al., 2014; McCarthy and Cooper, 2016). Recent work on Io has considered other rheological models (Bierson and Nimmo, 2016; Renaud and Henning, 2018). It may be the case that the interior of icy worlds would be more dissipative than previously thought when these other rheological models are considered.

Additional complexities may exist in some Ocean Worlds, such as Enceladus. Gravity data has suggested that Enceladus has a very low-density core (McKinnon, 2013) that may represent a highly porous interior. Fluids from the ocean may be flushing through this interior pore space, arguably supported by observations of nano-silicate particles (Hsu et al., 2015). In this case, additional energy could be dissipated by the fluid flow through this porous core (Roberts, 2015; Rovira-Navarro et al., 2022), although the magnitude and impact of such dissipation is currently uncertain (Choblet et al., 2017; Liao et al., 2020; Rovira-Navarro et al., 2022). Additionally, tidally induced shear heating at the south polar tiger stripe faults may dissipate significant energy (Nimmo et al., 2007; Roberts and Nimmo, 2008; Souček et al., 2019). In this way, tidal heating can be locally concentrated along heterogeneities in the ice shell. Using geodetic observations to measure local deformation would allow for detailed investigations into these effects and the laterally variable spatial distribution of tidal heating (Souček et al., 2019). Similarly, deviations from spherical symmetry may break degeneracy in Love numbers (e.g., Zhong et al., 2012). For a spherically asymmetric structure, Love numbers of different order but the same degree would be different. Therefore, estimating Love numbers independently would allow for probing of asymmetries in an Ocean World.

Tidal dissipation is not necessarily laterally uniform even if the ice shell is laterally homogenous. Under most conditions, heat patterns are symmetric around the equator but vary with latitude and are often concentrated in polar regions (Beuthe, 2013). This enhanced polar heating can help explain why Enceladus' active eruptions are concentrated at a pole, but not why there is a north–south asymmetry (Beuthe, 2019).

2.3.3 Ice shell mass and energy transport

In the ice shell, a central question about energy transport is whether heat is transferred primarily by convection or conduction. The shell thickness of a purely conductive ice shell can be calculated using ice's temperature-dependent thermal conductivity and Fourier's law (e.g., Carnahan et al., 2021). The minimum energy required to produce or sustain a water ocean can be computed using Fourier's law, by assuming a certain ocean temperature, and considering the maximum ice shell thickness allowed by the bulk density. Convection transports heat more efficiently than conduction and leads to thicker ice shells. The presence or absence of convection is controlled by the dimensionless Rayleigh number Ra of the ice shell:

$$Ra = \frac{\rho g \alpha \left(T_{\mathrm{b}} - T_{\mathrm{s}}\right) d^3}{\kappa \eta_{\mathrm{b}}} \tag{2.3}$$

where ρ is the ice shell density, d is the ice shell thickness, g is the gravitational acceleration, α is the thermal expansivity, κ is the thermal diffusivity, T_b and T_s are the basal and surface temperatures respectively, and η_b is the viscosity at the base of the ice shell. For convection to occur, this Rayleigh number must exceed the critical Rayleigh number Ra_c that can be approximated by (Solomatov, 1995):

$$Ra_c = 20.9 \left(\gamma \left[T_b - T_s \right] \right)^4 \tag{2.4}$$

where γ is an exponential constant that describes how viscosity decreases with increasing temperature.

On Enceladus, geodetic measurements have found the ice shell to be between 19–26 km thick on average and as locally thin as 3–5 km thick (e.g., Hemingway and Mittal, 2019), all implying conduction as the likely dominant heat transport mechanism. Advection of liquid water through the tiger stripes is likely a secondary but important contribution to heat loss at Enceladus' south pole (Howett et al., 2011a; Spencer and Nimmo, 2013). On Europa, the state of the ice shell is less certain. Some studies have argued that ice shell thicknesses greater than ~15 km likely imply convection (Moore and Schubert, 2003; Nimmo and Pappalardo, 2016), but this estimate depends strongly on viscosity and associated parameters that affect viscosity like ice grain size (Goldsby and Kohlstedt, 2001). Within this uncertainty both conductive and convective ice shells are plausible (Hussmann et al., 2002).

Mass transport through the ice shell can occur in several ways. Ice shell convection involves mass movement by definition and can occur under certain conditions as described in the previous paragraph. Subsumption (a process somewhat analogous to subduction of tectonic plates on Earth) has been proposed to occur in Europa's ice shell (Collins et al., 2022; Kattenhorn and Prockter, 2014), but is uncertain and is only feasible under certain compositions and porosities of the shell (Johnson et al., 2017). Cryovolcanic processes can transport material through the ice shell on an Ocean World, possibly including all the way from the ocean to the surface. Cryovolcanism has been observed on Enceladus in the form of the south polar plumes, but the existence of active plumes is debated on Europa. Effusive cryovolcanic constructs have been proposed to exist on Europa (e.g., Quick et al., 2017), but remain uncertain.

Geodetic measurements can elucidate energy and mass transport through the ice shell. Because ice shell thickness is closely tied to the dominant heat transport mechanism (with purely conductive shells being thinner than convective shells), the static and time-variable gravity and topography analyses that constrain shell thickness (see Section 2.2.1) also constrain energy transport. Subsumption, if it is occurring on Europa today, may have rates of order centimeters per year (Kattenhorn and Prockter, 2014). InSAR measurements could conceivably measure such deformation from flyby or orbit. Alternatively, a landed geodetic station in the region of proposed subduction capable of making measurements at this sensitivity could be used

to test the subduction hypothesis. High resolution topography data would support the geomorphological interpretation of putative cryovolcanic features and allow for tests of their origin.

2.3.4 Ocean transport and dynamics

Ocean dynamics are an essential component of the ice–ocean exchange process as strong currents are expected, transporting heat and materials relatively quickly across them. Fluid motions within icy satellite oceans are driven by convection due to thermo-compositional density gradients, mechanical forcings (e.g., tides, libration, and orbital precession), and magnetic forcing due to electromagnetic pumping (Soderlund et al., 2020).

Heat flux from the seafloor combined with heat loss through the overlying ice shell is expected to drive thermal convection globally in the oceans. When the influence of rotation on convection is relatively strong, as may be expected for Enceladus, the oceans have multiple zonal jets, axial convective motions, and most efficient heat transfer at high latitudes (Soderlund, 2019). For a more moderate rotational influence, which has been hypothesized for Europa's ocean, three zonal jets form, Hadley-like circulation cells develop, and heat flux peaks near the equator (Soderlund et al., 2014). Weak rotational influence allows overturning cells with no preferred orientation.

Ocean composition and its thermodynamic properties may have a significant impact on global circulations due to the presence of a stable stratosphere if the thermal expansion coefficient is negative (e.g., Melosh et al., 2004; Zeng and Jansen, 2021 or if salinity gradients are maintained across the ocean. If the vertical thermal and compositional gradients oppose each other, double-diffusive convection may be expected (e.g., Bouffard et al., 2017) with a "staircase" configuration characterized by well-mixed layers separated by steps in salinity and temperature (e.g., Schmitt, 1994). Conversely, if both thermal and compositional gradients are unstable, the vigor of convection will increase. Melting and freezing along the ice–ocean interface will also lead to regions that are locally enhanced with fresher (i.e., stably stratified) and saltier (i.e. unstably stratified) water, respectively, that may drive additional circulations (e.g., Kang et al., 2022; Lobo et al., 2021; Zhu et al., 2017). If heterogeneous melting/freezing leads to large-scale topographic variations along the ice–ocean interface, the local melting temperature and properties of the ocean and ice shell would change, promoting mechanically driven flows in the ocean.

Icy moons that are tidally locked with eccentric orbits and rotational axes tilted with respect to their orbital axes have time-changing tidal bulges, librations, and precessions that can heat their interiors and drive ocean currents (e.g., Le Bars, 2015; Hay et al., 2020). Barotropic tides lead to periodic surface displacements that propagate towards the east and west, respectively, for eccentricity and obliquity tides (e.g., Tyler, 2008). When three-dimensional effects are included, internal gravity waves may also develop, which concentrate energy along internal

shear layers (e.g., Rovira-Navarro et al., 2019). Moreover, deviations from sphericity can induce elliptical instabilities and produce domain-filling turbulence (e.g., Lemasquerier et al., 2017).

Finally, in the Jovian and potentially ice giant satellites, the salty ocean water is electromagnetically pumped by temporal variations of the planet's magnetic field to drive a retrograde oceanic jet and weaker upwelling/downwelling motions at low latitudes (Gissinger and Petitdemange, 2019). Because the zonal jet is unidirectional, it may contribute to non-synchronous rotation of the ice shell. The associated Ohmic dissipation is smaller on average than both radiogenic and tidal heating, but it can be significant locally at high latitudes where it is concentrated in a thin layer beneath the ice–ocean interface.

Ocean dynamics have few observational constraints at present and additional modeling work is required to determine what geophysical observations and their fidelity are necessary to test these hypotheses. Using gravity and topography data to constrain ice shell thickness variations (Section 2.2.1) and the resulting inferences about oceanic heat fluxes would elucidate ocean dynamics (Čadek et al., 2019; Kvorka et al., 2018). More direct tests may be achievable through observations of dynamic topography associated with upwelling ocean flows impinging on the ice shell, detection of hypothesized non-synchronous rotation, magnetic induction due to motions of the electrically conducting salt water within the host planet's magnetic field (Vance et al., 2021), the seismic noise spectrum associated with radial ocean flows (Panning et al., 2018), or the gravity anomalies associated with zonal flows (analogous to detection of deep zonal winds in the interiors of giant planets [Kaspi et al., 2018]—although the magnitude of such anomalies would be extremely small).

2.3.5 Rocky interior mass and energy transport

The silicate interiors of Ocean Worlds represent an important source of radiogenic heat. This radiogenic heat is often thought to be dominant over tidal heating in the silicate interior (e.g., Sotin et al., 2009), although tidal heating may be significant depending on the rheology considered (Renaud and Henning, 2018). On a world like Enceladus with a porous silicate interior (Iess et al., 2014; Roberts, 2015), porosity may additionally allow heat transfer through fluid advection or turbulent dissipation through the permeable interior (Liao et al., 2020; Rovira-Navarro et al., 2022). Whatever the source of heat, characterizing the magnitude and distribution of heating from the silicate interior is important for understanding the chemistry present at the base of the ocean and its implications for habitability (see Section 2.4.2).

Gravity measurements can be used to estimate the amount of heat flux from the silicate interior. High heat fluxes out of the silicate interior would allow for effective compensation of seafloor topography, so measurements of higher order gravity terms (spherical harmonic degrees 10–50) could constrain this interior heat flux (Dombard and Sessa, 2019; Koh et al., 2022). At Europa, the large size of the silicate interior may imply that convection is the

dominant heat transfer mechanism within that interior, and seafloor volcanism could be present at the base of the ocean (Běhounkovà et al., 2021; Bland and Elder, 2022). It has been argued that the presence of volcanic edifices on the seafloor could be tested by analyzing the magnitude of gravity anomalies at length scales of hundreds of kilometers (Dombard and Sessa, 2019).

2.4 Ocean Worlds Driving Science Question 3: Where are the habitable environments within an Ocean World, and how long do they survive?

The search for life beyond Earth is one of the highest priority topics in planetary science. On an Ocean World, key locations to study include local brine pockets in the ice shell, the ocean itself, the interface between the ocean and the ice shell, and the interface between the ocean and the rocky interior (i.e., the seafloor; e.g., Schmidt, 2020). Habitability of these locations is tied to mass and energy fluxes (Section 2.3). The degree to which the ocean might host significant biomass will be determined by the presence of any features that can concentrate the exchange of nutrients (e.g., through stair-case diffusive mode double diffusive convection) and whether nutrients can be generated and delivered reliably. Therefore, mass fluxes from the seafloor are important to potentially habitable regions in the upper ocean and ice, and any organisms at the seafloor would benefit from fluxes from the ocean above. Note that if a global biogeochemical cycle exists in a given Ocean World, energy sources and sinks may change through time, for example as the seafloor cools and the ice thickens, and thus habitability may change. Geodesy has a unique role in contributing to understanding the habitability of Ocean Worlds (Figure 2.7). Here, we consider the habitability of regions in an Ocean World, with Europa as the main example.

2.4.1 Ice shell habitability

Fluid pockets within the ice shell may form due to the combination of tidal/dynamical flexure of the ice, the presence of impurities such as salts and enclathrated volatiles, and the potential for convective and cryovolcanic transport of subsurface ocean material. Convection may also transport surface oxidants downward through the ice to generate chemical disequilibria (a source of energy for life), with an efficiency that might be greater in regions where the ice is more vigorously convecting, or where oxidants are entrained from surface areas richer in radiolytically altered materials. Tidal flexing can force melting at grain boundaries (McCarthy and Cooper, 2016). Local melting within the ice shell has been invoked to varying degrees to explain chaotic terrains and double ridges observed on Europa (e.g., Culberg et al., 2022; Johnston and Montési, 2014; Kattenhorn and Prockter, 2014; Schmidt et al., 2011).

The accumulation of photolytically and radiolytically produced oxidants at the surface creates an opportunity for life if these accumulated materials are entrained into the underlying ice and make their way into the ocean. Along the way, oxygen-enriched melt pockets might also provide energy for microbes eating trapped silicate impurities. The viability of life in ice is an

INVESTIGATIONS ROADMAP TO OCEAN WORLDS

IDENTIFY OCEAN WORLDS → CHARACTERIZE OCEAN WORLDS → ASSESS HABITABILITY → SEARCH FOR LIFE

LEGEND:
- Solid Foundation
- Basic Foundation
- Little Foundation

OCEAN WORLDS	ENERGY SOURCES	OCEAN SIGNATURES	SOLVENTS	ROCK / OCEAN INTERFACES	ENERGY FOR LIFE	PHYSICOCHEMICAL CONDITIONS FOR LIFE	BIOMARKERS
Enceladus							
Europa							
Titan							
Ganymede							
Callisto							
Triton							
Ceres							
Pluto							
Other Saturnian & Uranian Satellites							

(Left axis labels: OCEAN WORLDS for Enceladus–Callisto; POSSIBLE OCEAN WORLDS for Triton–Other Saturnian & Uranian Satellites)

Example outstanding science questions on the Roadmap to Ocean worlds that require (or benefit from) geodetic measurements:

ENERGY SOURCES	OCEAN SIGNATURES	SOLVENTS	ROCK / OCEAN INTERFACES	ENERGY FOR LIFE	PHYSICOCHEMICAL CONDITIONS FOR LIFE	BIOMARKERS
• What is the current tidal dissipation rate? • What is the heat budget, and how does it vary globally? • What is the 3D distribution of tidal dissipation? • What is the 3D structure (thickness, density, mechanical properties, etc.) of the ice shell, ocean, and deeper interior (high pressure ice, rocky mantle, core, etc.)?	• Is there a subsurface ocean? • What is the thickness of the ocean, and how does it vary globally? • What is the density, temperature, salinity, and composition of the ocean? • Is the ocean stably stratified? • What is the circulation structure of the ocean?	• What is the density, temperature, salinity, and composition of the ocean? • Is the ocean stably stratified?	• What is the energy and mass exchange between the rocky interior and the ocean? • What is the physical state (shape, topography, composition, density, porosity, mechanical properties, etc.) of the rocky interior?	• What is the energy and mass exchange between the rocky interior and the ocean? • Is there seafloor volcanism and/or hydrothermal activity?	• What is the temperature of the ocean? • How old is the ocean? • What are the pH and eH of the ocean? • What is the water activity of the ice shell? • How do the aforementioned properties vary in 3D? • What is the ice shell recycling rate?	• What are the pathways by which ocean material gets to the surface (or plume), and how is it fractionated along the way? • Is ocean material accessible at the surface?

Figure 2.7: Comparison of the "NASA Roadmap to Ocean Worlds" (Hendrix et al., 2019) to the capabilities of Next-Generation Geodesy, as detailed in this report.

active field of research in Earth's cryosphere. This possible biomass may be small in volume but would be closer to the surface than the ocean, and therefore the most readily accessible reservoir (Wolfenbarger et al., 2022). This potential for biosignature detection in an ice shell drives the need to understand the detailed distribution of structural and compositional heterogeneities and associated transport processes within ice shells.

Geodetic observations can contribute to the understanding of ice shell habitability by showing the plausible locations of fluid pockets within the ice shell. High-resolution topography would facilitate the quantitative geomorphological interpretation of surface features hypothesized

to form as a result of local water in the ice (e.g., Culberg et al., 2022; Schmidt et al., 2011). Although the densities of solid ice and liquid water are close, a global gravity field with spherical harmonic degree and order of ~100 or better could allow for mapping of the ice–ocean interface (e.g., Dombard and Sessa, 2019). This resolution of gravity field will not be achieved by Europa Clipper, providing motivation for a follow-on mission.

2.4.2   Ocean and seafloor habitability

The liquid water ocean, including the upper interface between the ocean and ice shell, and the lower interface between the ocean and silicate interior (i.e., the seafloor) are excellent candidate locations for habitability studies. In Earth's oceans, global currents carry nutrients and entrained organisms over thousands of kilometers. The flux of nutrients into an extraterrestrial ocean is constrained by the extent of downwelling materials in the ice shell and upwelling of products of water–rock interactions at and below the seafloor. If downwellings feed into larger channels, analogous to rivers on Earth, then life in the ocean might focus around those outflows and follow the effluents along the flow channels. The complementary source of reductant materials from any hydrothermal activity at the seafloor may set up similar dynamics. Enhanced cryovolcanic activity near the poles, in both Europa (Běhounkovà et al., 2021) and Enceladus (Choblet et al., 2017) could render the redox state of these high latitude bands much different (more habitable due to greater gradients, and thus greater lack of chemical equilibrium) from the mid-latitude regions. Vertical and latitudinal gradients in heat and water salinity may lead to convective turbulence and produce banded zonal currents and overturning ocean circulations, which would be modulated by flows driven by libration, tides, precession, and electromagnetic pumping (Soderlund et al., 2020). Because of spatial gradients in nutrient fluxes from the ice shell and seafloor and the likelihood for heterogeneous ocean mixing, it is important to understand how materials are distributed and transported within the ocean (see Section 2.3.4).

The seafloor on Ocean Worlds like Europa or Enceladus, where the water ocean is in direct contact with the silicate interior (as opposed to worlds like Ganymede, where the ocean is instead in contact with a higher-pressure phase of ice), is a particularly important location for habitability studies. In seafloor hydrothermal systems, chemolithoautotrophic organisms could subsist independent of direct sources of oxygen. As on Earth, the fluxes of reduced materials such as hydrogen, methane, and iron sulfide may thus determine the energy available for life. In Europa, estimates of the depths to which fluids might percolate in ultramafic olivine have been made based on the mechanics of thermal fracturing caused by thermal expansion anisotropy between grains. Based on these estimates, fluids may circulate up to 25 km below the seafloor. Water–rock interactions—the hydroxylation of olivine into serpentine—pertain only to newly exposed anhydrous rock. In the published estimates, the fracture front progresses at a rate of less than microns per year (Vance et al., 2007). At Enceladus, this mechanism

has been interpreted to permit fracturing from the moon's formation, consistent with the high-porosity crust inferred from Cassini data (Glein et al., 2018).

Geodetic observations can support habitability investigations in the ocean and on the seafloor by providing essential geophysical context for these regions. Gravity inversions, especially when coupled with observations of magnetic induction and ice-penetrating radar, can constrain important quantities—such as the thickness of different layers, the salinity of the ocean, etc. As discussed in Section 2.3.5, analysis of gravity and topography can be used to constrain seafloor topography and heat flow out of the silicate interior, if these datasets are spatially resolved up to spherical harmonic degree and order ~50 (Dombard and Sessa, 2019) (Koh et al., 2022). Finally, due to spatial gradients in nutrient fluxes from the ice shell and seafloor, as well as the likelihood for heterogeneous ocean mixing, it is important to understand how materials are distributed and transported within the ocean, as described in Section 2.3.4.

2.5 Synthesis

Dedicated collection of geodetic data at Ocean Worlds would enable compelling science in understanding interior structure, the global energy budget and associated heat transport, mass transport, and habitability. Global gravity and topography observations have the power to unlock Ocean World science far beyond the detection or rejection of the existence of an ocean. Real-time observations of orbital and rotational dynamics (e.g., libration) are particularly important for understanding those Ocean Worlds that are also icy moons. The joint interpretation of geodetic datasets with measurements of magnetic induction is particularly compelling for certain Ocean Worlds, like Europa. The science questions identified, and the observables needed to address them, are shown in Table 2.1.

Science Questions	Physical Parameters	Example Measurements
What are the interior structures of Ocean Worlds? (Section 2.2)	Determine the moment of inertia	Gravity field (degree-2), global shape (degree-2), libration amplitude, obliquity
	Determine the ice shell thickness, including any lateral variability	Tidal deformation (e.g., k_2), libration amplitude, obliquity, gravity field (across a range of length scales), topography (across a range of length scales), electromagnetic sounding (ideally at multiple frequencies), surface deformation (e.g., InSAR), radar sounding, seismic signals
	Determine the ocean thickness	Gravity field (degree-2), global shape (degree-2), libration amplitude, obliquity, tidal deformation (e.g., k_2), electromagnetic sounding (ideally at multiple frequencies), seismic signals
	Constrain the ocean salinity	Electromagnetic sounding (ideally at multiple frequencies), seismic signals
	Measure any seafloor topography	Gravity field (across a range of length scales), topography (across a range of length scales), seismic signals
	Determine the density of rocky mantle (and core, if applicable)	Gravity field (degree-2), global shape (degree-2), libration amplitude, obliquity, seismic signals
What are the sources, sinks, and transport mechanisms of mass and energy within an Ocean World? (Section 2.3)	Determine the global energy balance	Tidal phase lag (e.g., complex k_2), heat flow (total and spatial distribution), astrometric observations (e.g., rate of change of orbit)
	Determine the thermal state of ice shell	Gravity field (across a range of length scales), topography (across a range of length scales), heat flow (total and spatial distribution)
	Constrain ocean dynamics	Time-variable gravity field, dynamic topography, electromagnetic sounding (ideally at multiple frequencies), seismic signals, heat flow (total and spatial distribution)
	Constrain any core/mantle dynamics	Tidal phase lag (e.g., complex k_2)
Where are the habitable environments within an Ocean World, and how long do they survive? (Section 2.4)	Assess habitable niches within the icy shell	Radar sounding, high-resolution gravity field (sufficient for detecting subsurface water reservoirs), high-resolution topography (sufficient for geomorphological studies)
	Determine the ocean composition	Electromagnetic sounding (ideally at multiple frequencies), gravity field (across a range of length scales), heat flow (total and spatial distribution)
	Quantify the vigor of water–rock interactions at the seafloor	Tidal phase lag (e.g., complex k_2), gravity field (across a range of length scale), topography (across a range of length scales)

Table 2.1: Summary of Ocean World science questions, physical parameters, and example measurements. Quantitative measurement requirements and candidate instrumentation for specific mission concepts are provided in tables in Section 7.

3. Mars

3.1 Introduction

Mars offers an excellent opportunity to learn about terrestrial planet evolution. It is known that the smaller size of Mars relative to Earth is a key factor in the distinct geological histories of the two planets (Zuber, 2001). However, critical questions remain in understanding how and why the interior, surface, climate, and habitability of the planets evolved differently. Geodetic observations like topography and gravity are key to addressing these issues.

Global topography data on Mars primarily come from the Mars Orbiter Laser Altimeter (MOLA, Smith et al., 2001a), an instrument that operated on board the Mars Global Surveyor (MGS) spacecraft. Topography data come from range measurements where the round-trip flight time from individual MOLA laser pulses traveling from the spacecraft to the Martian surface and back are converted into a surface elevation. Individual ranging measurements have a precision of tens of centimeters and are spaced 300 meters apart along a spacecraft track. These measurements (about 600 million individual measurements in total) provide a global geodetic grid to which other Martian datasets can be referenced. In some regions, temporal changes in MOLA measurements over the same region have been used to constrain time-variable topography (Smith et al., 2001b). The global MOLA topography can be locally supplemented in regions of interest by elevation data of higher spatial resolution sourced from stereo images from imaging instruments like the High-Resolution Imaging Science Experiment (HiRISE) camera (McEwen et al., 2007) aboard the Mars Reconnaissance Orbiter (MRO). Figure 3.1a shows Mars topography from MOLA.

Unlike at the Earth–Moon system, gravity data have not been collected at Mars with a dedicated mission. Rather, gravity data have been inferred using radio tracking from the

NASA Deep Space Network of Mars-orbiting spacecraft like MGS, MRO, and Mars Odyssey (e.g., Zuber et al., 2007a). These data have been used to construct models of the Martian gravity field, which can be combined with MOLA topography data to infer a map of Bouguer anomalies (e.g., Genova et al., 2016; Konopliv et al., 2011; Lemoine et al., 2001). These gravity fields are not as precise or highly resolved as could be achieved with a dedicated gravity mission, but do allow for some geophysical analyses (e.g., Wieczorek, 2008; Zuber et al., 2007b). Figure 3.1b shows the current knowledge of the Martian gravity field. In addition to gravity measurements from orbit, local gravity measurements have been acquired from the Curiosity rover using its on-board navigational accelerometers (Lewis et al., 2019).

One notable geodetic instrument on the surface of Mars is the Rotation and Interior Structure (RiSE) instrument on the InSight lander (Folkner et al., 2018). RiSE consists of two X-band radio transmitters and receivers. Doppler shifts of the radio link to/from Earth allow for precise measurements of the rotation of Mars, including the precession and nutation of Mars' spin axis, which are related to Mars' moment of inertia. The moment of inertia can be used to constrain Mars' interior structure (e.g., the size and state of Mars' core).

Other instruments at Mars are not inherently geodetic in nature, but some have important synergies with gravity and topography. The InSight lander's primary scientific instrument is a seismometer that has been used to constrain the size and structure of the Martian crust, mantle, and core (Khan et al., 2021; Knapmeyer-Endrun et al., 2021; Stähler et al., 2021). These local seismic data can be combined with orbital gravity and topography to provide global constraints on properties of the Martian crust. Subsurface radar sounding can be used in conjunction with gravity data to constrain composition, for example of the polar layered deposits (Broquet et al., 2020).

Fundamental questions remain about Martian history and processes despite the current knowledge described above. These questions are summarized graphically in Figure 3.2. Two broad driving science questions that are important in understanding terrestrial planet evolution and can be addressed with geodetic data at Mars are:

1. What is the geodynamic and tectonic history of Mars, and how and why does it differ from Earth's?

2. How do planetary climates respond to orbital forcing?

Below, we describe the importance of these questions, the current state of knowledge of their answers, and how new geodetic data at Mars would provide fundamental leaps in addressing them.
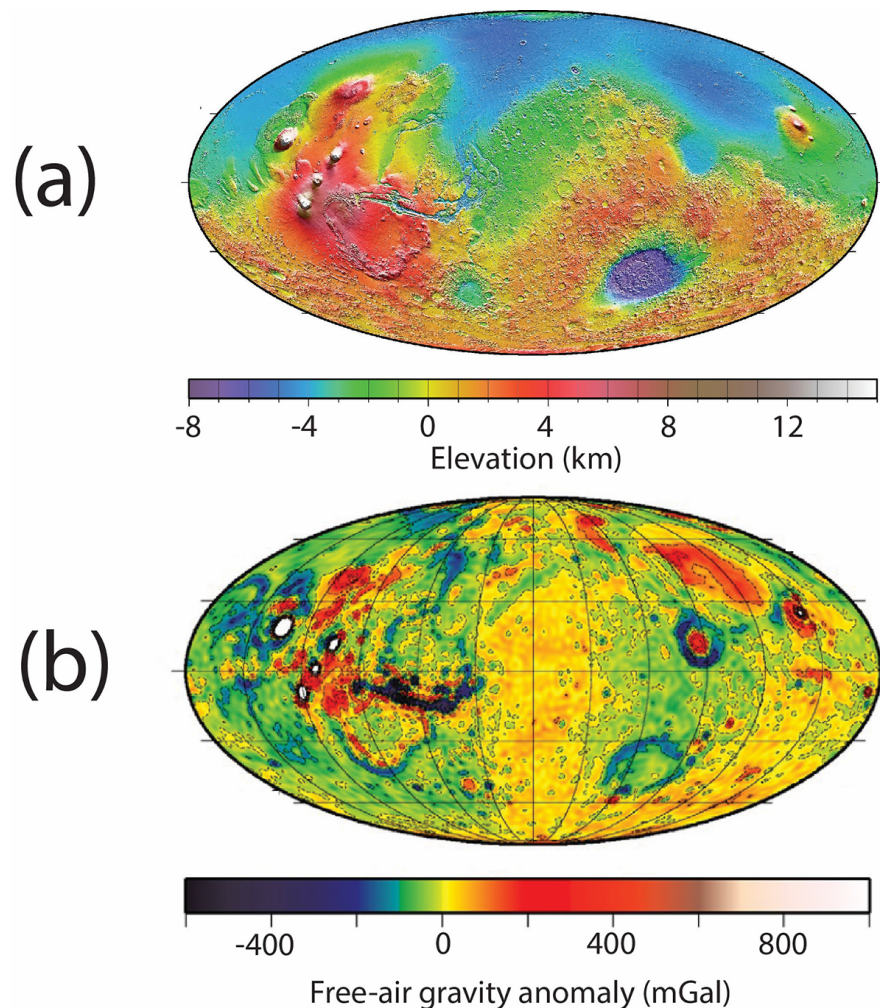
Figure 3.1: (a) Current knowledge of Martian topography, from MOLA data (Smith et al., 2001a). Note the clear presence of the global dichotomy, with low elevation in the northern hemisphere and high elevation in the southern hemisphere. (b) Current knowledge of Martian gravity, from radio tracking of individual Mars-orbiting spacecraft (Genova et al., 2016).

3.2 Mars Driving Science Question 1: What is the geodynamic and tectonic history of Mars, and how and why does it differ from Earth's?

3.2.1 The global dichotomy

The global dichotomy in topography and geology between Mars' northern and southern hemispheres—with low-elevation and young terrain in the north, and ancient, heavily cratered, high-elevation terrain in the southern hemisphere (see Figure 3.1a)—is the largest and most fundamental geophysical feature on Mars (e.g., Watters et al., 2007b). However, it is unknown what causes these observed differences between hemispheres. Because of its formation early
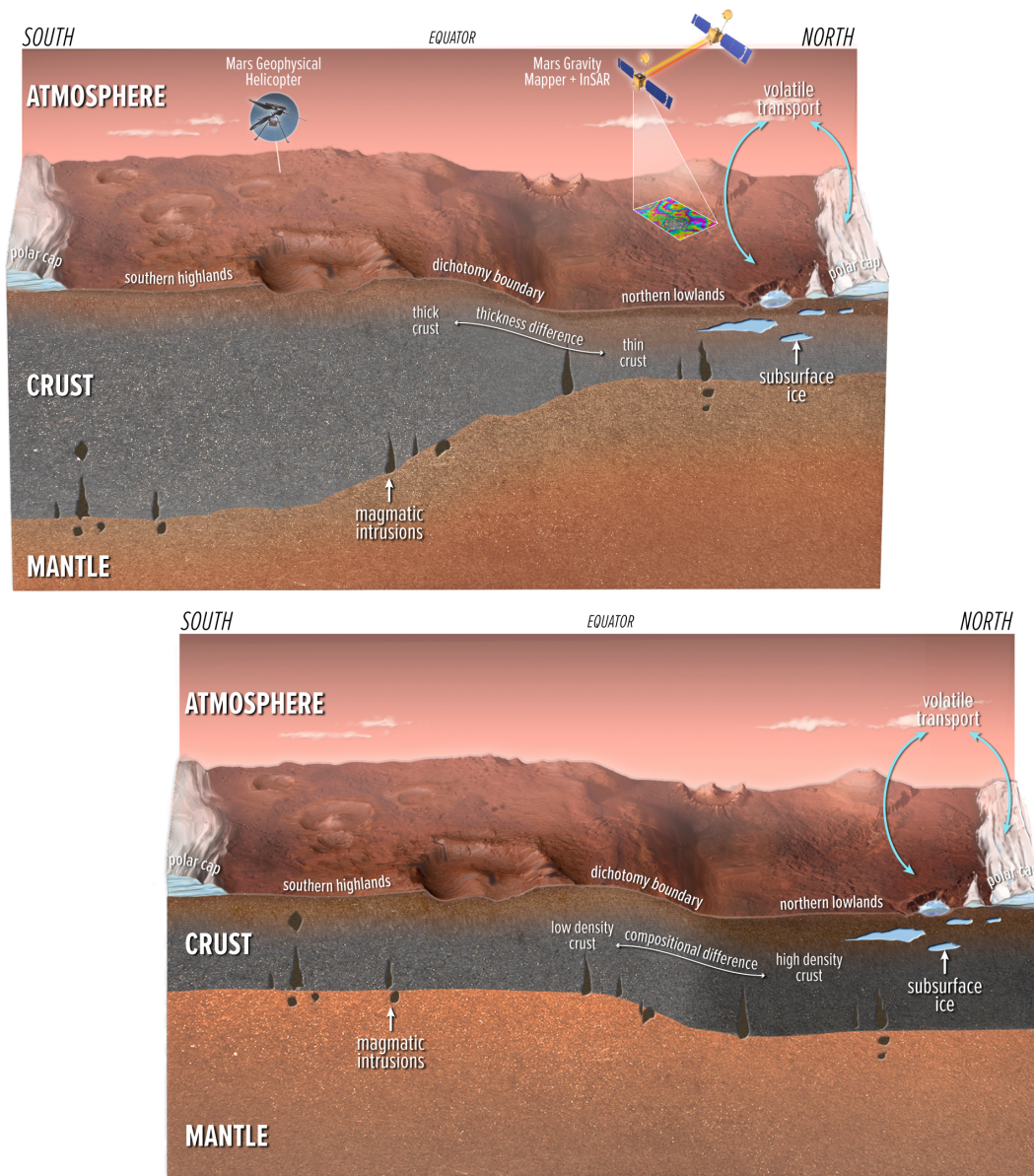
Figure 3.2: Illustration of some structures and processes on Mars that can be studied with future, realistically attainable geodetic measurements to elucidate the planet's geodynamic and climate history. Competing hypotheses on the crustal structure associated with the global dichotomy, the distribution of icy and volcanic deposits, the rates of volatile exchange between polar caps and other reservoirs, and the vigor of present-day tectonic activity can all be tested. Image credit: Charles Carter, James Tuttle Keane, Keck Institute for Space Studies.

in Martian history, the dichotomy sets the initial conditions for all subsequent planetary evolution, including controlling the location of a putative early ocean, creating substantial differences in atmospheric processes between the two hemispheres, guiding differences in climate between the two poles, and even determining where spacecraft are landed. Despite its profound importance, the formation mechanism of the Martian dichotomy remains enigmatic.

Theories of dichotomy origin include both exogenic and endogenic processes. There is not yet a consensus idea that explains all of the observed asymmetries (Citron and Roberts, 2021). The most common exogenic mechanism argued for is a giant impact into the northern hemisphere (e.g., Andrews-Hanna et al., 2008; Marinova et al., 2008; Nimmo et al., 2008; Wilhelms and Squyres, 1984), although a giant impact into the southern hemisphere (Reese et al., 2011) and multiple large impacts (Frey and Schultz, 1988) have also been proposed. Endogenic hypotheses include degree-1 mantle convection (e.g., Zhong and Zuber, 2001), asymmetric overturn from a solidifying magma ocean (Elkins-Tanton et al., 2005), and an ancient episode of plate tectonics (Sleep, 1994). A hybrid model, where a giant impact induces asymmetric mantle convection, has also been proposed (Citron et al., 2018). The reader is referred to review papers by Citron et al. (2018) and Roberts (2021) for a full discussion of current knowledge of exogenic and endogenic theories, respectively, of dichotomy formation.

An essential ingredient to understanding the Martian dichotomy is knowing if and how the dichotomy extends into the interior. In particular, precise knowledge of the distribution of crustal thickness and crustal density on the planet is required. Figure 3.3 shows example models of the crustal thickness of Mars that are all consistent with the available data. These quantities currently have large uncertainty because they are highly sensitive to model assumptions, resulting in non-unique answers (e.g., Goossens et al., 2017). For example, a crustal thickness map derived under an assumption of uniform crustal density yields a global asymmetry in crustal thickness (Figure 3.3a), with relatively thin crust in the northern hemisphere and relatively thick crust in the southern hemisphere (Zuber et al., 2000). However, it has been shown (Ojha et al., 2020; Wieczorek et al., 2022) that a global asymmetry in crustal density with no global asymmetry in crustal thickness, with denser crust in the northern hemisphere, is also consistent with current data (Figure 3.3b). Therefore, it is currently unknown if there exists an asymmetry in crustal thickness, an asymmetry in crustal density, or both on Mars. This dearth of crustal structure knowledge severely hinders our ability to understand the origin of the global dichotomy.
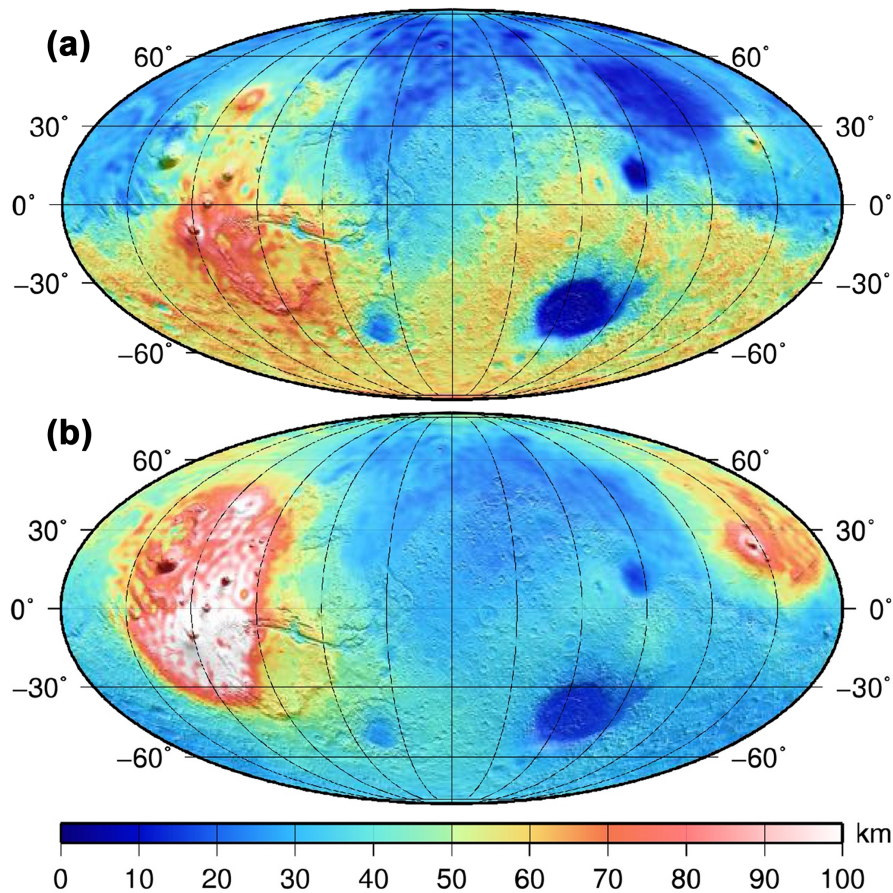
Figure 3.3: Two end-member models for the crustal thickness of Mars that are both consistent with the available geodetic data. (a) A model for the crustal thickness of Mars assuming that the crust of Mars has a uniform density (2,900 kg/m^3). This model results in a North–South hemispheric dichotomy in crustal thickness. (b) A model for the crustal thickness of Mars assuming that the crust of Mars has a laterally varying density. In this model, there is no North–South hemispheric dichotomy in crustal thickness (although there is one in crustal density). Figures from Goossens et al., 2017.

A new, sufficiently highly resolved static gravity field could be used to confidently map crustal density and crustal thickness, allowing for direct tests of hypotheses for the origin of the Martian dichotomy. At the Moon, the gravity fields derived from the GRAIL mission (Zuber et al., 2013a) were used to isolate the gravitational signature of the crust from deeper structure. By considering relatively short wavelengths (spherical harmonic degree 150 and greater), maps of crustal density, crustal thickness, and porosity were inferred (Wieczorek et al., 2013). At present, there are no worlds beyond the Earth–Moon system with gravity field measurements that permit these types of analyses without a priori assumptions that are almost certainly incorrect (e.g., assuming the crust is completely uniform in density both vertically

and laterally). At Mars, if a gravity-focused mission could be used to obtain a high-resolution static gravity field, crustal density and crustal thickness could be mapped in tandem, revealing whether the dichotomy seen at the surface corresponds to a dichotomy in crustal thickness, crustal density, or both. This attribute would provide direct tests of dichotomy origin. For example, the canonical giant impact scenario (see review in Citron, 2021) predicts hemispheric differences in both crustal thickness (because of crustal thinning from the impact) and crustal density (because the northern crust then forms from a depleted mantle). Degree-1 convection (see review in Roberts, 2021) can result in hemispheric differences in crustal thickness alone. Serpentinization can result in crustal density differences without crustal thickness differences (Quesnel et al., 2009). There are no scenarios to our knowledge that predict neither crustal density nor crustal thickness differences and are consistent with current data; if this case were to be supported by a new gravity mission, other mechanisms like dynamic topography would need to be considered.

What is the resolution of the static gravity field that would be needed to accomplish the analysis described in the preceding paragraph? To answer this question, we took the same approach as was done for the Moon (Wieczorek et al., 2013). We quantified the expected gravitational contribution of lithospheric flexure by calculating the admittance associated with flexure under a range of permitted average crustal thicknesses (Wieczorek et al., 2022). Figure 3.4 shows the results of these calculations. At spherical harmonic degree and order >174, the admittance from flexure varies by <5% with respect to current uncertainties in average crustal thickness and effective elastic thickness. Mapping crustal density across Mars would require a static gravity field with tens of degrees and orders beyond this minimum number. Therefore, knowledge of the static gravity field of Mars to spherical harmonic degree 200 or better would allow for direct tests of dichotomy formation.

The timing of dichotomy formation would be elucidated by a complete inventory of impact basins that post-date dichotomy formation. Gravity and topography data can be used to obtain this record because subsurface gravity anomalies associated with large impact basins persist longer than surface topography, especially on a world with substantial aeolian modification like Mars. An analogous investigation has been undertaken on the Moon (Neumann et al., 2015) and at Mars using the gravity data from radio tracking of orbiting spacecraft (Bottke and Andrews-Hanna, 2017). However, the Mars investigation only considered potential basins >780 km in diameter. A more highly resolved gravity dataset (topography data from MOLA is already sufficiently resolved to not be the limiting factor in this analysis) would allow for a more complete inventory of buried or otherwise erased basins at smaller diameters, and therefore place tighter age constraints on the crust on either side of the Martian dichotomy.
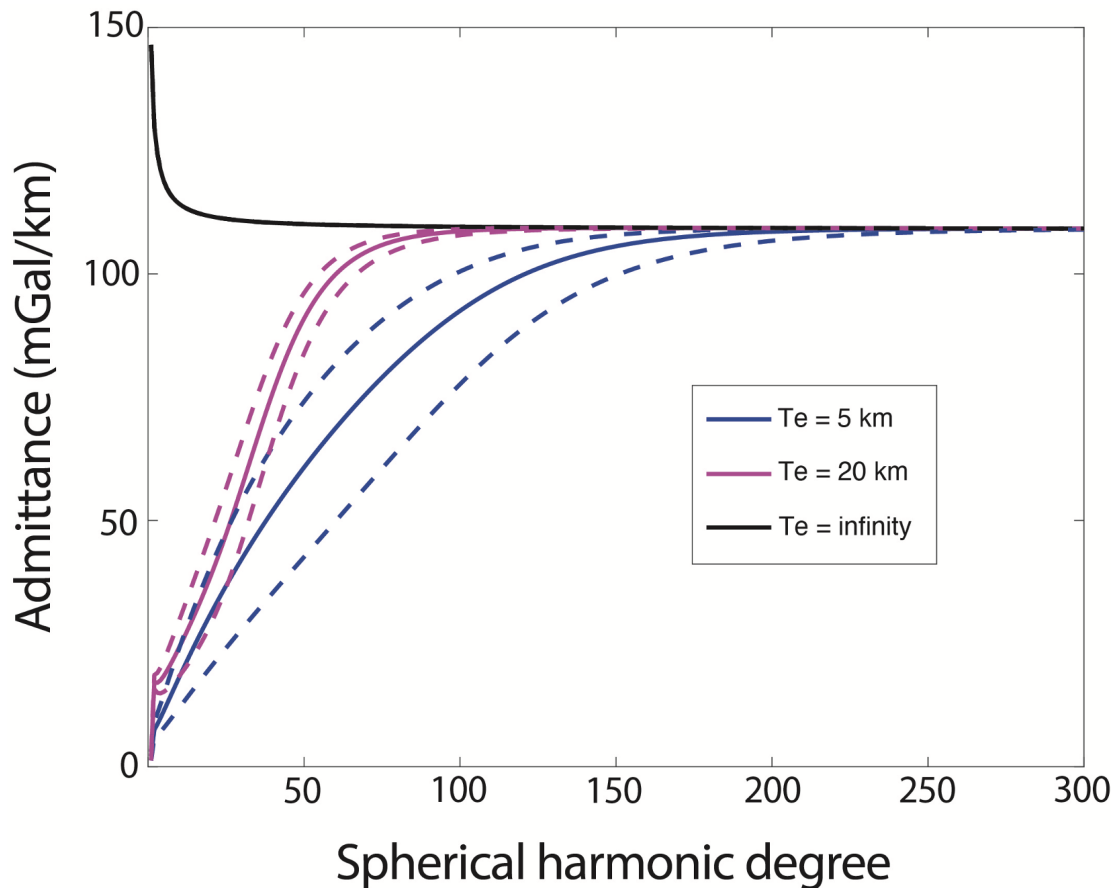
Figure 3.4: Admittance spectra for lithospheric flexure models on Mars for allowable values of average crustal thickness T_c and effective elastic thickness T_e. Solid lines represent models with $T_c = 51$ km, and dashed lines represent models with $T_c = 30$ km or 72 km, the permitted limits of T_c on Mars. All models assume crustal density 2,600 kg/m^3, mantle density 3,200 kg/m^3, Poisson's ratio 0.25, and Young's modulus 10^{11} Pa.

3.2.2   Mantle dynamics and tectonic regime

Mars presently exhibits stagnant lid tectonics, with a thick lithosphere and heat loss dominated by conduction in this outer shell. A major reason for this regime is the planet's smaller size, and thus faster cooling, compared to Earth. However, fundamental questions remain about Mars' thermal history and geodynamical vigor. Geodesy offers several ways to understand both the present geodynamic state of Mars, and the path the planet took to get to that state.

A critical unknown in assessing Mars' geodynamical vigor is whether the planet is a volcanically active world today. Although there is widespread agreement that the planet currently experiences stagnant lid tectonics, the idea that this regime must imply that Mars is a geologically dead object has been challenged. Geophysical observations are arguably best fit with a model where the Martian mantle is moderately convecting at present (Kiefer and

Li, 2009). Image analysis suggests the presence of geologically recent lava flows, arguably including a volcanic deposit that may be only tens of thousands of years old (Horvath et al., 2021). The spatial coincidence of some of the largest observed Mars seismic events (Giardini et al., 2020; Stähler et al., 2022) with the region of this potentially young lava flow hints at the possibility of active volcanism occurring on Mars today, but does not constitute proof. Geodetically measuring active surface deformation would be a key observable in testing the hypothesis that volcanic processes are occurring today on Mars, because active magma movement in the subsurface would cause predictable signals. This investigation could be accomplished with interferometric synthetic aperture radar (InSAR), as has been done with volcanoes on Earth (e.g., Pritchard and Simons, 2004). Section 6.2 discusses the use of InSAR for planetary applications. Finally, the rheology and temperature of Mars' mantle can be constrained by detecting the planet's Chandler wobble (a periodic motion of the rotational axis over time) and comparing the observed wobble period to that predicted by numerical models. Constraints on Mars' Chandler wobble have been inferred from time-variable gravity data at Mars, the only instance of this value being observationally inferred at another planet (Konopliv et al., 2020). Improvement in the uncertainties of the Martian Chandler wobble would allow for tighter constraints on mantle rheology.

Active volcanism or the lack thereof would provide constraints on Mars' current geodynamical state, but the planet's thermal history, and how quickly it evolved into that present state, is largely unknown. Constructing the planet's thermal history could be done by measuring the effective elastic thickness of the lithosphere at various times and at various points across the surface. Some investigations of this theme have been performed by considering the gravity and topography signatures associated with loading of polar ice sheets (Ojha et al., 2019; Phillips et al., 2008) and volcanic products (Belleguic et al., 2005; Broquet and Wieczorek, 2019; Ding et al., 2019; McGovern et al., 2002). However, uncertainties are very large with current datasets. For example, the recent analysis of Broquet and Wieczorek (2019) shows that at Ulysses Tholus, any effective elastic thickness at the time of loading between 20 and 200 km is allowable, and as a result of this large range, heat flows at the time of loading between 4 and 48 mW/m^2 are permitted. Other volcanoes only yield a weak minimum constraint on heat flow, with arbitrarily large heat flows allowable by current data. These results could be improved with more precise gravity data. These methodologies may be particularly compelling given that InSight's attempts to directly measure heat flow at Mars were unsuccessful.

Some studies have hypothesized the existence of plate tectonics-like processes on ancient Mars. Sleep (1994) proposed that the Martian dichotomy corresponds to plate tectonics where the northlands crust is thin and was created by processes analogous to seafloor spreading. Connerney et al. (1999) used magnetic field measurements from MGS data to argue for the presence of linear magnetic anomalies of alternating polarity in the southern highlands, which they argued could be evidence of past spreading in the presence of a changing core dynamo,

similar to seafloor striping on Earth. However, this interpretation of the magnetic data has been challenged (e.g., Ravat, 2011), and strong evidence at the surface to support seafloor spreading in this region has not been presented. Geodesy could test these hypotheses by determining how topography is regionally supported, which can be done with a global gravity field that is sufficiently precise (see Section 3.2.1) to isolate the signature of the crust (e.g., Sori et al., 2018).

3.2.3   Core dynamo and magnetization

The structure of the Martian core and the history of its ancient geodynamo are important in understanding the geodynamics of the planet, but have substantial uncertainty. Seismic detections from the InSight lander constrain the core radius to be 1,830 $\pm$ 40 km with mean density 6,000 $\pm$ 300 kg/m^3 (Stähler et al., 2021). Crustal magnetization implies the existence of a past core dynamo, but the nature and timing of that dynamo—including when it was initiated, when it ceased, whether it was intermittent, and what processes drove convection—are all debated (e.g, Acuña et al., 1999; Hood et al., 2010; Lillis et al., 2006; Mittelholz et al., 2020).

Geodesy can address these problems in two major ways. First, improved knowledge of the moment of inertia or the response of the solid planet to tidal forces, obtained by landed and/or orbital geodetic measurements, would lead to improved constraints on core size and density. Investigations under this theme have been performed for the deep interior of the Moon (Matsuyama et al., 2016; Williams et al., 2014). Second, testing the hypothesis that crustal magnetization is correlated to free-air or Bouguer gravity would lead to inferences on the source of magnetization and possible relationship to a core dynamo. This type of investigation has been performed on the Moon (Gong and Wieczorek, 2020) and, for robust results, requires knowledge of the static gravity field sufficient to isolate the gravitational signature as the crust, as described in Section 3.2.1.

Study of core structure and the history of the core dynamo is a theme that is particularly ripe for joint analysis of geodetic datasets with other geophysical datasets. Two types of data in particular, in addition to geodetic data, would be especially compelling for learning about the Martian core: seismology and magnetometry. Seismic stations additional to InSight with longer observing times would be transformative, as the single InSight lander cannot yet unambiguously constrain the presence, size, and density of an inner core (Stähler et al., 2021). Magnetic field measurements taken at low altitude or at the surface at strategically chosen locations are necessary to understand the history and timing of the core dynamo, because crustal magnetization is expected and observed to appear fundamentally different near the surface than it does at orbital altitudes (Johnson et al., 2020). A mission that could measure near-surface magnetic fields and rock density at multiple locations of interest (e.g., Noachian

and Hesperian aged lava flows, large impact craters) would be particularly useful to advance knowledge of dynamo history.

3.3 Mars Driving Science Question 2: How do planetary climates respond to orbital forcing?

3.3.1 Climate records

Mars is an excellent laboratory for studying the relationship between orbital changes and planetary climate. Planets undergo perturbations in their orbital parameters (e.g., eccentricity and longitude of perihelion) and tilt of their rotational axis (i.e., obliquity). On Earth, these variations are called Milankovitch Cycles and are thought to drive Pleistocene ice ages (Hays et al., 1976; Liu, 1992), but their importance to other geological or climate processes is debated (e.g., Goff et al., 2018). On Mars, the magnitude of orbital forcing on climate is expected to be much greater than on Earth. Mars undergoes higher amplitude changes in obliquity compared to Earth by an order of magnitude because of the lack of a large, stabilizing moon (Jakosky et al., 1995; Laskar et al., 2004), and orbital effects on climate are expected to be pronounced relative to Earth because the recent Martian climate system lacks complicating factors like oceans and surface life. As a result, it is expected that Martian climate change is dominantly controlled by orbital and obliquity variations that lead to changes in energy distribution from sunlight (Toon et al., 1980). Volatiles are expected to be driven to different latitudes depending on orbital configuration (e.g., Head et al., 2003). Several studies have proposed evidence for these orbitally driven changes in periodicities in paleoclimate records (e.g., Cutts and Lewis, 1982; Lewis et al., 2007; Sori et al., 2022), the distribution of present-day water ice (e.g., Levrard et al., 2004; Madeleine et al., 2009; Newman et al., 2005), geomorphology (e.g., Carr and Head, 2010; Levy et al., 2010), and alteration of surface minerals (Rutledge et al., 2018). However, full understanding of past Martian climate and its relation to different orbital configurations is hindered by imprecise knowledge of the location and state of climate records on Mars today.

Gravity and topography data enable understanding of Martian climate and its relationship to orbital states by constraining the spatial distribution, volume, and composition of Martian climate records. Several studies have been performed under this theme at the north and south polar layered deposits (NPLD and SPLD). MOLA topography data have been used to estimate the volume of both the NPLD and SPLD (Smith et al., 2001a), and joint inversions of gravity and topography data were key investigations showing that the SPLD are composed of nearly pure water ice (Wieczorek, 2008; Zuber et al., 2007b). However, the coarse resolution of current global gravity data hinders study of critical climate records beyond water ice in the large PLDs. More precise and higher resolution gravity data would greatly enable the analysis of other climate records at both the poles and lower latitudes.

At the poles, better gravity data would allow for reading the record of volatile deposits that represent different periods of Martian climate from the NPLD or SPLD. At the north pole, an extensive basal unit that underlies the NPLD has been proposed to represent the largest inventory of water on present-day Mars after the PLDs. Radar sounding shows the basal unit is likely ice-rich (Nerozzi and Holt, 2019), but only penetrates into the unit and allows for compositional constraints at some locations. Gravity data allows for a more representative estimate, but analysis of current data yields a highly uncertain range of allowable average ice contents between 30–80% (Ojha et al., 2019). The large uncertainty in ice content hinders attempts to model the evolution of the ice deposit, determine its age, quantify its importance in Martian climate history, and estimate its contribution to the present-day water inventory of the planet. Better gravity data would ameliorate this issue by placing tighter constraints on the unit's density. At the south pole, radar sounding has identified sequestered carbon dioxide ice (Phillips et al., 2011). It is thought that this carbon dioxide ice is massive enough such that it is comparable to the mass of carbon dioxide in the current atmosphere, and has substantial effects on Martian climate as it co-evolves with the atmosphere over timescales of millions of years (Buhler et al., 2020). However, the precise volume of this CO_2 ice—a critical quantity for understanding climate change on Mars—is unknown, and a gap in data at the south pole (sourced from spacecraft orbit inclination) prevents radar analysis from being complete. The density of CO_2 ice is substantially different from that of H_2O ice, so high-resolution gravity data is an ideal tool for addressing this problem. Based on current knowledge of the spatial scale of the detected deposit, a static gravity field where spherical harmonic degrees up to 280 or better are locally known in the south polar region would be suitable to make a significant leap in understanding the climate record represented by CO_2 ice.

One of the most exciting discoveries of recent decades on Mars is the identification of water-ice sheets outside the polar regions. These lower-latitude ice deposits represent important climate records from past orbital states and essential, accessible resources for future human explorers. These ice deposits are shallowly buried under a dry overburden layer but have been identified with a variety of orbital instruments (e.g., Morgan et al., 2021). Despite unambiguous evidence that this mid-latitude ice exists, its exact distribution, purity, and structure are debated. For example, Arcadia and Utopia Planitia have been identified as some of the most promising mid-latitude ice deposits for paleoclimate analysis and future astronaut landing sites, but the current analysis from radar sounding has not been able to uniquely distinguish whether the ice is in the form of thick, pure ice sheets (Bramson et al., 2015; Stuurman et al., 2016) or near-surface coatings (Campbell and Morgan, 2018). This ambiguity represents a critical knowledge gap for both science and human exploration. Another location of interest is the equatorial Medusa Fossae formation. The Medusa Fossae Formation has been debated to be either ice-rich (e.g., Campbell and Morgan, 2018; Watters et al., 2007a or dry and the most important source of dust in the recent Martian climate system (e.g., Ojha and

Lewis, 2018; Ojha et al., 2018). A sufficiently resolved gravity field—jointly interpreted with the radar sounding data—can break the non-uniqueness in these problems because the ice deposits are great in lateral extent (several 100s of km) and because of the large density contrast between ice and bedrock. A static gravity field where spherically harmonic degrees up to 300 or better are locally known could be used to address these issues.

All the above-described investigations—using gravity to read the climate record stored in potentially ice-rich deposits in the north polar basal unit, the south polar sequestered carbon dioxide ice, mid-latitude ice sheets, and the Medusa Fossae Formation—involve estimating the volume of both water and carbon dioxide ice. Therefore, this climate record theme also naturally leads to estimating the total volatile inventory on present-day Mars.

3.3.2   Active climate

At Mars, understanding the present is the key to the past (e.g., Dundas et al., 2018). It is difficult to understand Martian paleoclimate without a good understanding of climate processes in the present day, leading the Mars polar science community to categorize determining the mass balance of ice reservoirs as one of its highest priority scientific investigations (e.g., Smith et al., 2018). Volatile transport of both H_2O and CO_2 on seasonal and interannual timescales represent active Martian climate processes that can be studied with geodetic monitoring. Competing hypotheses on the sources, sinks, and rates of volatiles can be tested.

The seasonal transport of volatiles to and from the polar caps have been detected and constrained with time-variable gravity (Smith et al., 2009; Genova et al., 2016) and topography (Smith et al., 2001b; Xiao et al., 2022) data. These studies have shown that 10^{15}–10^{16} kg of CO_2 are seasonally exchanged between the polar deposits and the atmosphere, and have clearly demonstrated the feasibility of detecting small changes in Mars' gravity over seasonal cycles using orbiting spacecraft. However, these analyses have been limited to estimating mass exchange between the entire polar ice caps using, for example, a simple model of a cone of material centered on the pole (Smith et al., 2009). Higher resolution gravity data would allow for study of the seasonal exchange of volatiles (particularly carbon dioxide) at smaller spatial scales across the surface, elucidating regional trends in the Martian present-day climate. Quantifying CO_2 exchange at these small spatial scales would allow for inference of the thermal properties of the near surface, including the presence of shallowly buried H_2O ice (Haberle et al., 2008). We estimate that measurements at a spatial scale of 200 km (corresponding approximately to spherical harmonic degree 50) or better at monthly or better temporal resolution would be ideal for studying this process.

The mass exchange of ice across Mars represents a seasonal load and may lead to detectable elastic deformation of the lithosphere (Wagner et al., 2022). A geodetic landed instrument placed in a strategic location at the surface that is sensitive to deformation of order millimeters could observe this seasonal deflection. The magnitude of deflection is sensitive to physical

properties of the Martian interior, so observation of this deflection could in turn be used to place constraints on the rheological structure of the planet and therefore its thermal and geodynamical history.

Superposed on seasonal variations are interannual accumulation or sublimation of water-ice deposits. Of particular importance is the interannual mass flux of the PLDs. The PLDs are a record of Amazonian climate, but the ability to decode their chronology over thousands or millions of years is hampered by a poor quantitative understanding of their present-day accumulation. Many authors have attempted to constrain the interannual mass flux rate of the NPLD. However, estimated accumulation rates from current data and models are highly uncertain. Many studies propose positive accumulation rates that vary over about a factor of 10 from 10^{-4}–10^{-3} m/yr (Becerra et al., 2017; Bramson et al., 2019; Hvidberg et al., 2012; Levrard et al., 2007). Other studies have proposed substantially lower accumulation rates in the present day (Izquierdo et al., 2022; Perron and Huybers, 2009) or even net sublimation (Langevin et al., 2005). These estimates are summarized in Table 3.1. Not knowing the order of magnitude—or even the sign!—of present-day accumulation prevents us from using the NPLD stratigraphy to confidently test hypotheses on its age or whether it records astronomically forced climate (e.g., Sori et al., 2014). A similar argument holds for the SPLD (e.g., Becerra et al., 2019). Conceptually, these arguments also hold for non-PLD water-ice deposits like mid-latitude ice sheets or off-polar crater-filling ice mounds, but interannual accumulation or sublimation rates are likely even slower here than they are for the PLDs (Bramson et al., 2017; Sori et al., 2022).

Time-variable orbital gravity data of sufficient precision collected over multiple Mars years would allow for constraining the interannual accumulation or sublimation of the PLDs by looking for positive or negative trends in mass change superimposed on the seasonal cycle of volatile exchange in the polar regions. Time-variable gravity has been obtained and analyzed with detectable seasonal trends (Genova et al., 2016; Smith et al., 2009), but without sufficient precision to constrain interannual PLD accumulation rates with respect to the proposed accumulation rates described above. Precision of 10^{-11} or better in the low degree spherical harmonic coefficients (degree 2 and 3) would be required in order to meaningfully test these proposed accumulation rates, which correspond to mass balance of order less than 10^{13} kg/yr. This precision is unlikely to be achieved with radio tracking of a single orbiting spacecraft but may be plausible with a dedicated gravity mission, either with spacecraft-to-spacecraft tracking or gravity gradiometry.

Another category of climate process that may be actively occurring on Mars today are glacial processes. Real-time detection of ice creep would permit inferences on ice rheology and the efficacy of glaciers in modifying the modern Martian landscape and could allow for constraints on physical properties of the ice like impurity content and temperature structure. Icy landforms on Mars are expected to deform at rates much slower than on Earth because

of colder temperatures, but some glacial or periglacial features on Mars may deform readily enough (mm/yr to cm/yr of viscous flow rates, or visible boulder movement) to be realistically detectable (Dundas et al., 2019; Sori et al., 2016). InSAR observations would be a valuable dataset for observing and constraining these processes, as has been done on Earth (e.g., Liu et al., 2013).

Citation	Method	Inferred Accumulation Rate	Mass Balance
Banks et al. (2010)	Crater analysis	< 4 mm/yr	$< 7.8 \times 10^{12}$ kg
Becerra et al. (2017)	Climate model to match PLD stratigraphy	0.5 mm/yr	9.8×10^{11} kg
Bramson et al. (2019)	Climate model to match troughs	0.2 mm/yr	3.9×10^{11} kg
Hvidberg et al. (2012)	Climate model to match PLD stratigraphy	0.7 mm/yr	1.4×10^{12} kg
Izquierdo et al. (2022)	Climate model to match troughs	~0	~0 kg
Langevin et al. (2005)	OMEGA observations	< 0 mm/yr (i.e., net sublimation)	< 0 kg (i.e., net sublimation)
Levrard et al. (2007)	Climate model	0.9 mm/yr	1.8×10^{12} kg
Perron and Huybers (2009)	PLD stratigraphic analysis	0.02 mm/yr	3.9×10^{10} kg

Table 3.1: Hypothesized constraints on the present-day yearly net accumulation rate of the NPLD and associated net mass gain or less in one Martian year.

3.3.3 Atmospheric dynamics

Atmospheric dynamics represent mass movement and can therefore be studied with time-variable gravity data of sufficient precision and temporal baseline. The feasibility of this topic has been demonstrated with gravity from radio tracking of Mars-orbiting spacecraft, which show seasonal variations in total atmospheric mass (Smith et al., 2009). This atmospheric variability is closely tied to the seasonal exchange of carbon dioxide between the polar caps discussed in Section 3.3.2, because the atmosphere acts as a source and sink of carbon dioxide over the Martian year. Here, we describe several atmospheric science investigations that could be performed with new geodetic data in addition to the seasonal transport of carbon dioxide and related atmospheric mass variations.

Global dust storms are dynamical features in the Martian atmosphere with dominant effects on atmospheric circulation and climate in the years in which they occur (e.g., Kahre et al., 2017). However, how and why they occur in particular years is unknown. The mass transport directly

associated with dust lofting is unlikely to be realistically detectable in orbital gravity data, but pressure variations in the atmosphere can be plausibly observed. The Viking Lander 2 measured an increase of ~50 Pa in surface pressure associated with a global dust storm (Hess et al., 1980). This increase was interpreted as a change in the latitudinal extension of the Hadley cell due to the change in the radiative balance from the increase of airborne dust. This idea could be tested with time-variable observations of surface pressure variations taken by orbital gravity data. The position and extent of the large-scale atmospheric circulation would be visible for spatial structures with wavelength 1000 km (large-scale momentum meridional transport, spherical harmonic degree ~10) to 200 km (jet positions, spherical harmonic degree ~50). Using these measurements to test dust storm initiation hypotheses would likely require comparing years with and without global dust storms. Measurements of atmospheric dust content and other atmospheric properties (e.g., temperatures) would enhance the return from these measurements.

Transient eddies (synoptic-scale zonally traveling weather systems) govern the transport of heat, momentum, and volatiles at mid-to-high latitudes and likely play an important role in the dust cycle on Mars, possibly including the genesis of global dust storms (e.g., Greybush et al., 2019). The dominant zonal wavenumbers for these systems are 1 to 3 (but can be as high as 6), and their periods range from ~2 to 10 sols. Therefore, a degree and order 12 gravity field acquired at a daily timescale would allow for study of these features. Peak eddy pressure amplitudes of these systems were observed by the Viking Landers 1 and 2 to be site and 9 Pa and 24 Pa, respectively (Greybush et al., 2019). Measurements of atmospheric dust content and other atmospheric properties (e.g., temperature, surface pressure station) would enhance the return from these measurements. In particular, a direct surface pressure measurement at the surface coupled with orbitally derived gravity maps would uniquely constrain the latitudinal extent and structure of transient eddies, and in turn reveal transport modes of momentum and volatiles.

Global climate models (GCMs) are used in studies of the Martian atmosphere, including models of water and dust cycles (e.g., Navarro et al., 2014). GCMs can use gravity observations as a direct impact to retrieve the true state of the atmosphere. Weather forecast techniques are able to interpolate observations of atmospheric mass changes in space and time from gravity-derived atmospheric pressure measurements to increase accuracy Navarro et al., 2017. GCMs can use these pressure measurements to extrapolate to other meteorological variables or GCM parameters, as long as correlations exist between those variables. This concept has been proven on Earth, where the GRACE gravity dataset has been used for data assimilation. Temporal Mars gravity observations would increase the accuracy of Martian GCMs, improving knowledge of Martian atmospheric circulation.

We considered the possibility that geodetic instruments could place a useful constraint on volatile loss on Mars in real time. However, atmospheric escape on Mars is likely too slow for

this investigation to be feasible. Mars probably loses on the order of 10^8 kg of atmosphere per Mars year (Jakosky et al., 2018), corresponding to a fractional loss of the total mass of the planet of ~10^{-16}. Uncertainty in GM (the product of the gravitational constant with planetary mass) of the Moon from GRAIL is of order 10^{-8} of the value of *GM* (Williams et al., 2014). Therefore, we concluded that useful detection of the change in mass of Mars in real time is unlikely to be plausible without substantial technological development.

Many of the investigations described above in climate and atmospheric themes would require global time-variable gravity fields constructed with a certain spatial resolution and temporal sampling. At present, radio tracking of MGS, Mars Odyssey, and MRO have led to a degree and order 3 field with monthly sampling (Genova et al., 2016). The necessary spatial and temporal requirements for the climate and atmospheric investigations that we identified that require time-variable gravity data are summarized below in Figure 3.5.
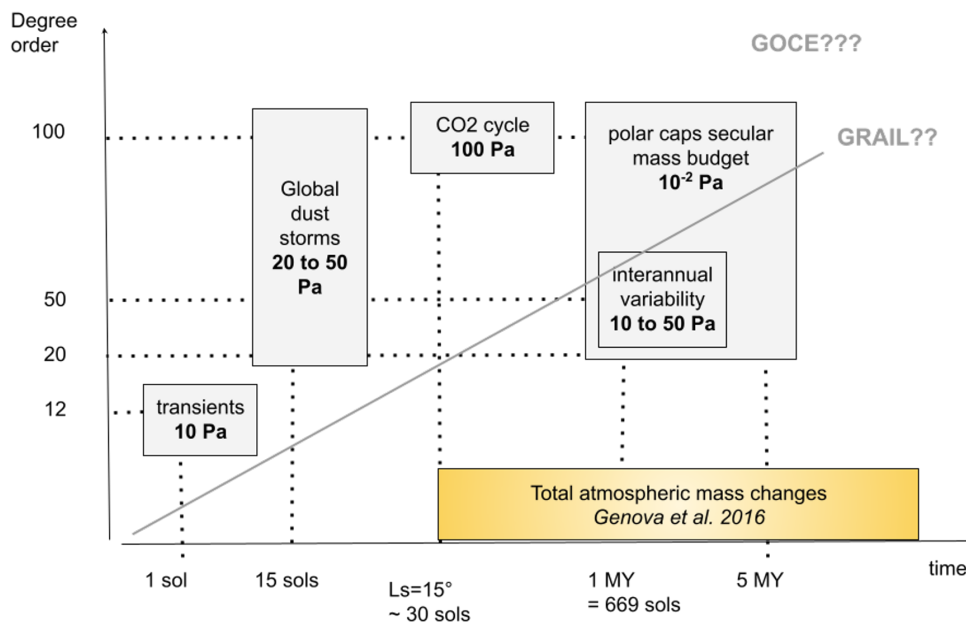
Figure 3.5: Atmospheric processes producing a change in the gravity field at different spatial and temporal scales (MY = 1 Martian year). The typical amplitudes are also given, with 10 Pa corresponding to 2.7 kg/m^2.

3.3.4   Synthesis

Dedicated collection of geodetic data at Mars would enable compelling science in geodynamics, tectonics, climate, and atmospheric science. Generally, high-resolution static gravity data could be used to address many questions in geodynamic and tectonic themes, while precise time-variable gravity data could be used to address climate and atmospheric themes. This division is a simplification, as there are some geodynamic investigations that require time-variable gravity

and some climate investigations that require high-resolution static gravity. Additionally, InSAR measurements are promising for some individual investigations in tectonics and climate. Jointly interpreting geodetic measurements with some non-geodetic measurements—like seismology and magnetometry—would be valuable in addressing some investigations. A summary showing the expected magnitude and spatial resolution of gravity signatures associated with objectives in both the Geodynamics and Climate themes that involve measurement of Mars' static gravity field is shown in Figure 3.6. The science questions identified, and the measurements needed to address them, are described in Table 3.2.

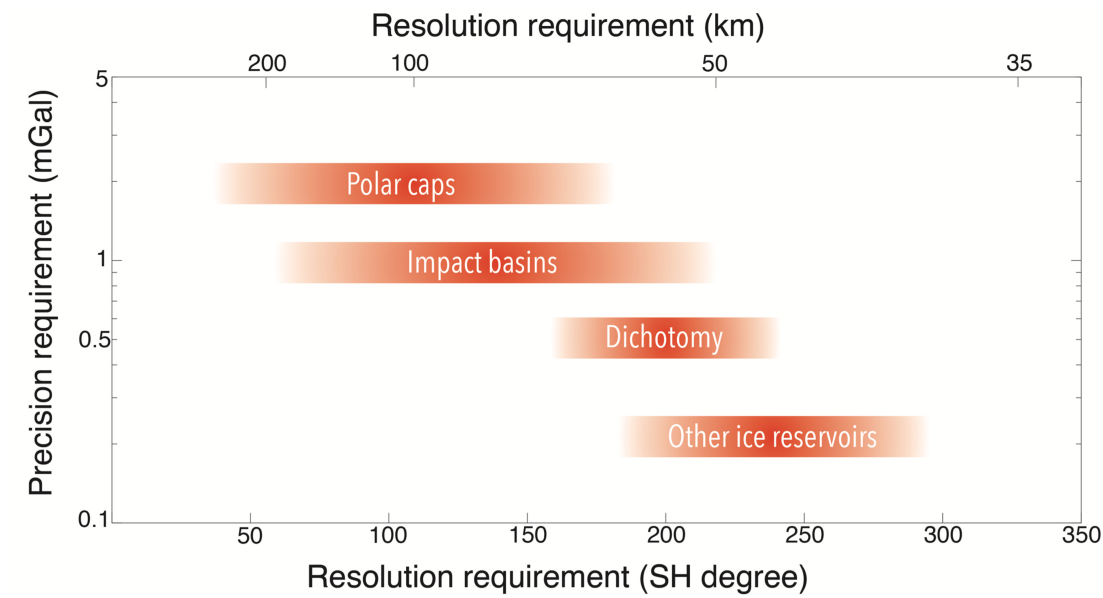**Figure 3.6:** Estimates of the precision and spatial resolution of gravity measurements required to address some topics in Mars science. For example, some ice reservoirs outside the large polar caps could be effectively studied with a static gravity field known up to degree and order ~180, whereas other ice reservoirs might require a gravity field locally known to degree and order >200.

Science Questions	Measurement Objective	Example Measurements
What is the geodynamic and tectonic history of Mars, and how and why does it differ from Earth's? (Section 4.2)	Distinguish between competing hypotheses for the nature and origin of the global dichotomy	High-resolution static gravity field to map crustal thickness and crustal density (spherical harmonic degree $\geq$ 200)
	Determine the thermal history of Mars, including whether Mars is volcanically active today	High-resolution static gravity field to map crustal thickness, crustal density, and lithospheric thickness (spherical harmonic degree $\geq$ 200), surface deformation (seasonal and secular), heat flow
	Determine the past tectonic regimes of Mars	High-resolution static gravity field to map crustal thickness and crustal density (spherical harmonic degree $\geq$ 200), seismic signals
	Determine the impact bombardment history recorded at Mars	High-resolution static gravity field to map crustal thickness and Bouguer anomalies of large craters (spherical harmonic degree $\geq$ 200)
	Determine the structure of the Martian core and the history of the core dynamo	Magnetometry (surface or near-surface), seismic signals, time-variable gravity field, rotational dynamics
How do planetary climates respond to orbital forcing? (Section 4.3)	Distinguish between competing hypotheses for the presence and volumes of icy climate records on Mars	Radar sounding, high-resolution static gravity field
	Determine how components of global circulation of the Martian atmosphere change over seasonal and interannual timescales	Time-variable gravity field (ideally for multiple Martian years), atmospheric pressure
	Determine the location and magnitude of sources and sinks of volatiles on Mars	Time-variable gravity field (ideally for multiple Martian years), high-resolution static gravity field, surface deformation (secular)

Table 3.2: Summary of Mars science questions, measurement objectives, and example measurements. Quantitative measurement requirements and candidate instrumentation for specific mission concepts at provided in tables in Section 7.

4. Venus

4.1 Introduction

Venus is arguably the planet in the solar system that is most similar to Earth: its radius and bulk density are about 95% of Earth's, and it is the closest planet to Earth in terms of distance from the Sun. Venus and Earth exhibit common geological processes, including but not limiting to volcanism, rift zones, mantle convection, atmospheric circulation, and possibly lightning. Despite these commonalities, Venus is starkly different from Earth in many ways. Venus' climate is inhospitable at the surface, with high atmospheric pressure and high temperature and an atmospheric chemistry very different from Earth's. The solid body of Venus also diverges from Earth in important ways: Earth has a system of plate tectonics, while Venus does not and instead has a tectonic regime described as a "stagnant lid," a "single plate," or a "plutonic squishy lid." Unlike Earth, Venus does not have a core dynamo or an associated internally generated magnetic field.

The single main driving science question on Venus considered here is: What is the geodynamic, tectonic, and atmospheric history of Venus, and how and why does it differ from Earth's? The details of Venus' geophysical and atmospheric processes are very much unresolved. Consequently, Venus is a high-priority science destination for the purpose of understanding the workings of our own planet and of Earth-like exoplanets. The upcoming VERITAS and EnVision missions will significantly improve knowledge of both gravity and topography on Venus. Below, we discuss ways in which geodesy may particularly illuminate three aspects of the planet—the deep interior, the lithosphere and its associated tectonics, and the atmosphere—motivated by a comparison of Venus and Earth.

4.2 Deep interior

The deep interior structure of Venus is largely unknown. Some indirect constraints come from the lack of a core-generated dynamo and associated intrinsic magnetic field—a sharp distinction from Earth that has implications for the state and size of the core, the cooling rate, and the tectonic regime (e.g., Nimmo, 2002; O'Rourke et al., 2018). Additionally, the relatively small center-of-mass–center-of-figure (COM–COF) offset constrains the mechanisms behind global resurfacing (King, 2018). However, more direct observations of the deep interior are challenging. Seismic measurements at the surface are technically difficult because of the high surface temperature. Geodetic methods may offer the best opportunity to constrain Venus' internal structure, but some geodetic analyses are relatively difficult because of the planet's slow rotation and the lack of a moon. Venus is the only terrestrial planet in the solar system with a slow, retrograde rotation, and this slow rotation results in a small hydrostatic contribution to J_2 (Dumoulin et al., 2017). As a result, future improvements to knowledge of the static low-degree gravity field of Venus are unlikely to substantially improve knowledge of the planet's deep interior.

A promising opportunity for discerning the mechanical properties of Venus' deep interior comes from considering tidal deformation of the solid body. Venus' tidal deformation is almost exclusively driven by the Sun, and it can be characterized by tidal Love numbers k, h and l, associated with the change in gravitational potential, the radial deformation, and the lateral deformation, respectively. These Love numbers generally correspond to particular spherical harmonic degrees. For example, the change in gravitational potential at degree 2 is described by the k_2 Love number. While the tide-raising potential at Venus is dominated by degree 2, the successful detection of higher-degree Love numbers would sample different ranges of depths in Venus' interior, especially in the presence of spherical asymmetries in the planet's interior structure. The Love numbers k, h, and l can be complemented by a measurement of tidal phase lag, which is inversely proportional to the planet's dissipation factor Q (see Figure 4.1).

Next-generation geodetic techniques should achieve two measurement objectives to achieve improvements in models of Venus' internal structure. First, observations of long-wavelength surface displacement with 2-cm accuracy would enable new constraints on core size, viscosity, and composition. Future technological improvements would be needed to meet this measurement objective, but could include radar retroreflectors or highly accurate InSAR observations. Second, long-duration, long-wavelength gravity monitoring would allow for study of the response of Venus' gravitational potential. This response can similarly reveal internal properties, including tidal dissipation. Such a campaign would need to span at least two solar days.
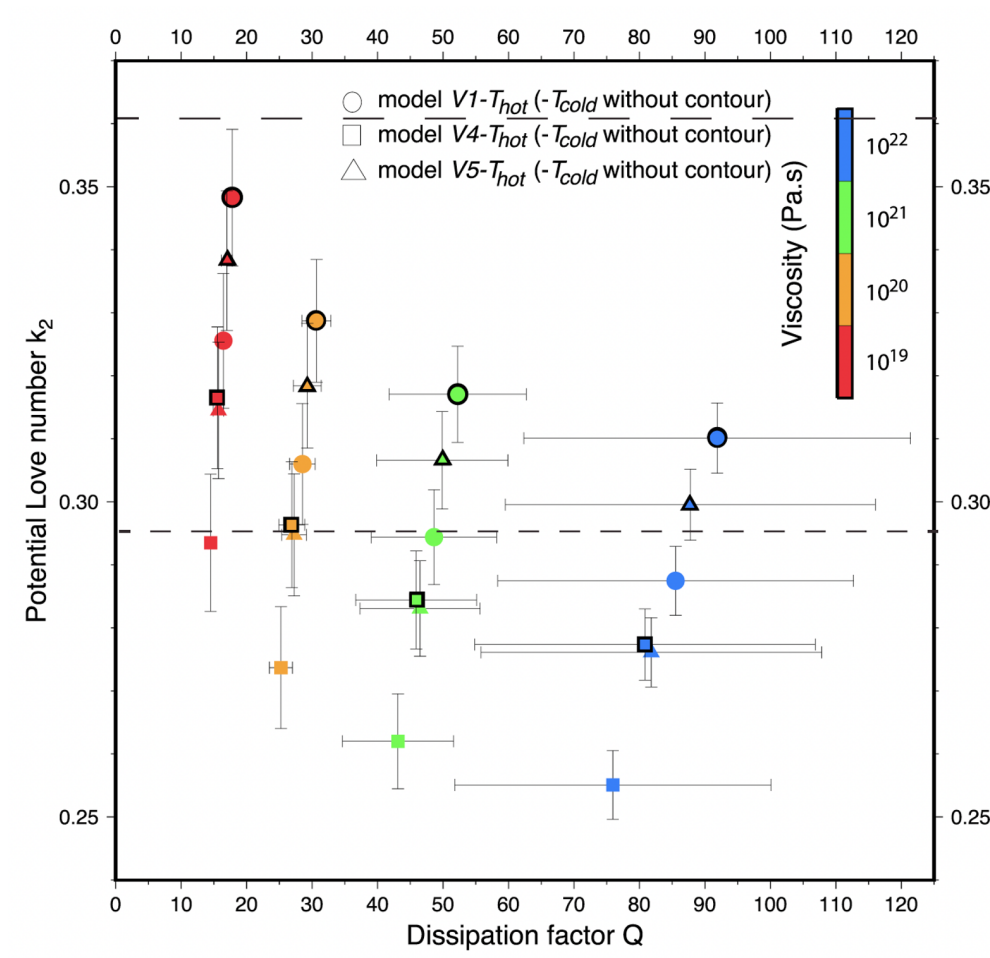
Figure 4.1: A suite of forward models yielding tidal parameters associated with various internal structures. Figure is adapted from Dumoulin et al. (2017).

4.3 Lithosphere and tectonic evolution

The surface of Venus hosts many structures that reveal the planet's geological and tectonic history—if we could decipher their origin and evolution. However, many of these structures are smaller than the current spatial resolution of the known gravity field, hindering interpretation. At its highest local degree strength, the Magellan gravity field has a horizontal resolution (spatial block size) of just under 200 kilometers (Konopliv et al., 1999). Unfortunately, many coronae, volcanoes, rift zones, craters, tesserae, and other important geologic structures exist near or below this resolution. Some of these features, like coronae, may reveal active geodynamics on Venus today (e.g., Gülcher et al., 2020). Other features, like tesserae, provide records of more ancient tectonism and deformation (e.g., Gilmore et al., 1998), and possibly even a cool, wet climate (Khawja et al., 2020). Geophysical analyses of these surface features

therefore hold great promise for elucidating the differing tectonic evolutions of Venus and Earth.

The thick atmosphere of Venus places practical limitations on the spatial resolution of a gravity field that can be derived from orbit, and therefore also on the analysis of geological features. Geological gravity signals attenuate exponentially with height, and the atmosphere limits orbital periapses. This fact should not prevent the collection of gravity data at Venus—but it makes measurement precision especially crucial for any advancement of the Venusian gravity field. The VERITAS mission will improve knowledge of the gravity field of Venus using Doppler tracking from Earth. Spacecraft-to-spacecraft tracking and gravity gradiometry could both further improve spatial resolution relative to Doppler tracking of a single orbiter (Bills et al., 2020). Gravity measurements at the surface to study local features would be challenging as a result of the high surface temperatures and pressures.

One approach that may hold promise on Venus is airborne geodesy, in which geodetic data would be collected from an atmospheric balloon. The thick atmosphere of Venus could allow airborne gravity to be an effective and efficient way to collect data over 100-km baselines (Forsberg and Olesen, 2010). A campaign like this on Venus would require accurate positioning of the sensor, and would therefore need to be embedded as part of a more expansive geodetic network.

4.4 Atmosphere

The deep atmosphere of Venus contains most of the atmospheric mass, but it is difficult to study because of an opaque cloud deck that prevents many types of remote sensing and corrosive atmospheric chemistry that limits in situ exploration. Measuring the gravitational signature of the atmospheric mass fluctuation would allow a new way to study the lowermost tens of kilometers of the atmosphere. For planets like Earth and Mars with optically thinner atmospheres, most of the solar radiation incident upon the top of the atmosphere reaches the surface. In contrast, for Venus, the vast majority of incident radiation is absorbed in the atmosphere. At present, the depth dependence of that absorption is only poorly constrained since remote sensing does not accurately recover behavior beneath the cloud deck. For the same reason, the atmospheric circulation is also poorly constrained below the cloud deck. A handful of descent profiles are available from in situ probes revealing that the angular momentum density peaks in the deep atmosphere, at ~20 km of altitude (Schubert et al., 1980).

The atmospheric thermal tide has been proposed to play an important role in Venus' rotational history. The orbital period of Venus is ~225 days. Venus rotates around its axis with a period of ~243 days in the opposite direction with respect to its orbital motion, resulting in a solar day that is ~117 days long. Shortly after early planetary radar studies revealed that Venus

was not a synchronous rotator (Carpenter, 1964), it was suggested by Gold and Soter (1969) that the observed rotation state might represent a tidal torque balance. The Sun raises both gravitational and thermal tides on Venus. The gravitational attraction of the Sun on the two tidal bulges yields two very different tidal torques.

The gravitational solid body tidal bulge is large in amplitude but has a small phase lag. In contrast, the thermal tidal bulge in the atmosphere is expected to have a small amplitude, but a large phase lag. Therefore, the torques by the Sun acting on the two bulges can be equal in magnitude and of opposite sign. This model for the origin of the rotation state of Venus has been supported by additional analyses (e.g., Correia and Laskar, 2001; Dobrovolskis and Ingersoll, 1980) but has not yet been tested by direct gravitational observations. The gravitational effect of the atmospheric thermal tide is expected to be a factor of ~10 below the sensitivity of the existing Magellan gravity data (Bills et al., 2020). However, simulations we have done suggest that they will be easily seen by the next generation Venus gravity missions. Once those gravity measurements are obtained, they will do for Venus what the GRACE mission has done for Earth—use gravitational signatures to track seasonal and inter-annual patterns of mass transport.

Atmospheric pressure variations load the surface of Venus. The surface deforms in response to the atmospheric loads leading to a perturbation in the gravity field. A spacecraft orbiting Venus that measures time-variable degree 2 coefficients would measure the sum of the solid-body tide, thermal tide, and atmospheric loading (Figure 4.2). All three contributions have important geophysical implications and, therefore, it is important to separately estimate the three effects. The total tidal amplitude has been observed by Konopliv and Yoder (1996). These authors interpreted these measurements only in terms of the gravitational solid body tide. The tidal phase lag has not yet been detected. The separation of the three effects is challenging from the degree 2 gravity measurements alone. While gravitational solid body tide is dominated by degree 2, atmospheric thermal tides have a rich harmonic spectrum. Higher degree thermal tide measurements could be used to calibrate its degree 2 contribution, which would distinguish it from the solid body tide. Venus' atmospheric time-variable gravity, if measured, would be highly complementary to lander measurements and remote sensing orbital data as it would provide global insight into Venus' deep atmosphere. Geodetic measurements of surface deformation, especially in combination with the surface atmospheric pressure data, could be used to isolate the contribution from atmospheric loading.

4.5   Synthesis

Geodetic observations at Venus hold great promise for elucidating the divergent geodynamic, thermal, and tectonic evolutions of Earth and Venus. Improvements in knowledge in the static gravity field, topography, time-variable long-wavelength gravity, and surface deformation would enable advances in understanding of the deep interior, lithosphere, surface, and atmosphere.
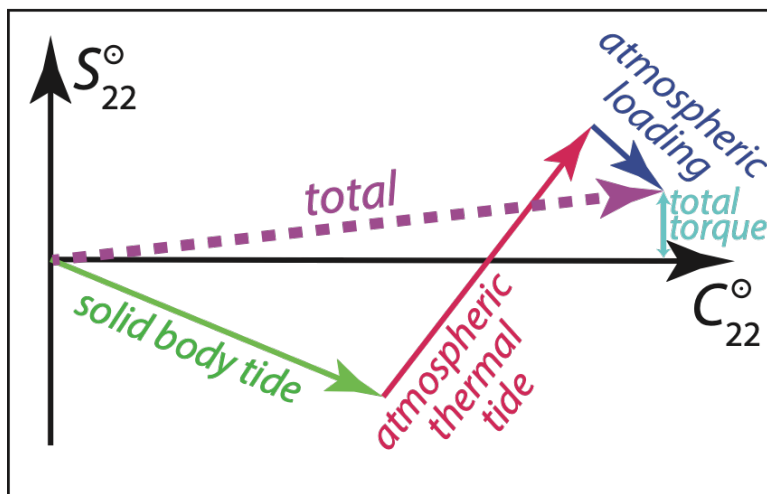
Figure 4.2: Different time-variable contributions to Venus' sectoral degree 2 gravity. The gravity components are shown in the Sun-fixed frame. The total torque is proportional to the $S_{22}^{\odot}$ component.

Many of these advances are already planned to be made with the VERITAS mission (Smrekar et al., 2022), a Venus orbiter that will collect geodetic measurements through spacecraft Doppler tracking (i.e., radio science) and an X-band interferometric radar (Cascioli et al., 2021).

Venus is one of the highest priority targets for geodesy beyond the Earth–Moon system in the coming decades. Because of the selection of the VERITAS mission, and the fact much of the science described here already falls within its mission objectives, this report places more emphasis on other worlds that do not have currently planned future geodetic observations from orbital or landed spacecraft (see Section 7). Such emphasis should not be interpreted to detract from the importance of geodetic investigations at Venus, which are essential in addressing high-priority questions in planetary science. We therefore concur with the recent finding of the Venus Exploration Analysis Group (VExAG) that VERITAS should be launched without delays.
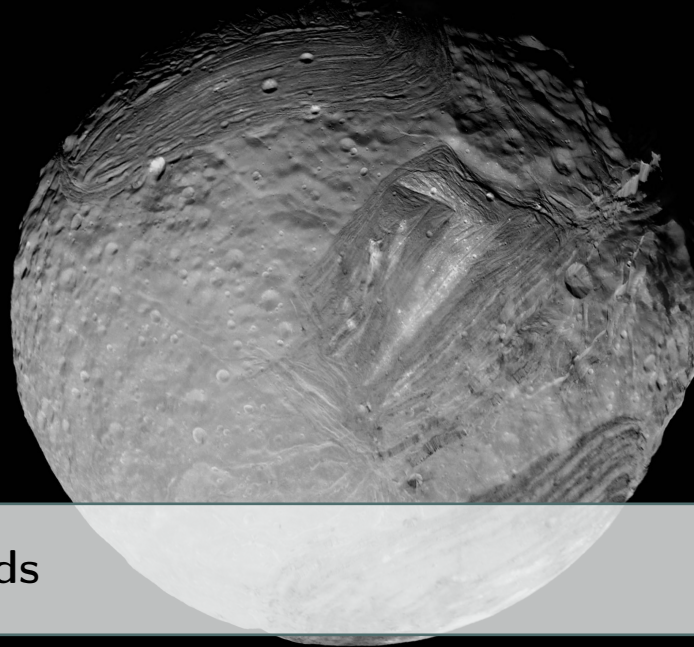
5. Other Worlds

We focused discussion on Mars, Ocean Worlds, and Venus in our workshops. This choice represented an initial guess at the planets and moons where geodesy is optimally poised to enable compelling science at feasible costs. However, all objects in the solar system would benefit to some degree from additional geodetic measurements. Here, we briefly comment on these other bodies.

The prioritization of a large flagship mission to Uranus by the recent decadal strategy report for planetary science and astrobiology represents a valuable opportunity for geodetic measurements. In the design of future missions to candidate Ocean Worlds, such as the Uranian satellites (Bierson and Nimmo, 2022; Hussmann et al., 2006), geodetic measurements should be central. Geodetic measurements are highly complementary to induction measurements, the other primary measurement for directly detecting a subsurface ocean (Cochrane et al., 2021; Weiss et al., 2021). Drawing an example from the New Horizons mission to Pluto, the flyby data provided an exceptional dataset of images and spectra but lacked geodetic observations. These datasets have provided only indirect evidence of a subsurface ocean (Cruikshank et al., 2019; Keane et al., 2016; Nimmo and Pappalardo, 2016). The lack of gravity data has left Pluto's ice shell thickness highly uncertain and the ocean's evolution over solar system history largely unknown (Bierson et al., 2018; Hammond et al., 2016; Kamata et al., 2019). The collection of gravity data at Uranus itself and gravity and topography data at the large Uranian moons (Miranda, Ariel, Umbriel, Titania, and Oberon) would enable both ice giant and Ocean World science. At Uranus, the gravity data (presumably from radio tracking of a Uranian orbiter) would elucidate the composition and internal structure of the planet, the nature and depth of atmospheric flows, and the difference in internal heat between Uranus and Neptune. The capability of analogous investigations has been shown by the Juno spacecraft at Jupiter (e.g.,

less et al., 2018). At the moons, the long-wavelength structure in topography and gravity and observations of physical libration can be used to test for the presence of subsurface liquid water oceans, as has been done at Saturnian moons from Cassini data. Four of the five major Uranian moons have been argued (Bierson and Nimmo, 2022; Hendrix et al., 2019) to plausibly have oceans persist to the present day from either past tidal heating (Miranda and Ariel) or radiogenic heating alone (Titania and Oberon). We do not recommend any particular prioritization of targets within the satellite system, other than to say that all five moons should be targeted for gravity and topography collection from a Uranian orbiter. A particularly attractive investigation for determining ocean presence in the Uranian system is combining geodetic arguments with observations of magnetic induction from a magnetometer (Cochrane et al., 2021; Weiss et al., 2021).

Titan is the only Ocean World where tidal response has been measured. The large observed value of k_2 and the large measured obliquity have been interpreted as evidence for a subsurface highly saline ocean. Because of the large distance from Saturn, permanent deformation of Titan is low. In addition, Titan's thick atmosphere hinders direct imaging of its shape. As a consequence, Titan presents a rare case where gravity is known with comparable accuracy to topography. Radar altimetry has been used to constrain Titan's shape at long wavelengths (Corlies et al., 2017). Gravity data at Titan (Durante et al., 2019) show little correlation with topography, indicating lateral heterogeneity at long wavelengths. Improving the shape and topography data will be especially critical for a future mission that seeks to understand the structure of Titan's ice shell. In addition, improving gravity data at Titan and correlating regional scale gravity anomalies to the compositional and morphologic diversity of Titan's surface will be essential to understanding the structure and evolution of Titan.

We judge Mars, Europa, Enceladus, Venus, the Uranian system, and Titan to be the most compelling and feasible geodetic targets over the next decade. This statement should not be interpreted as an assessment of the overall scientific worth of other worlds. Earth's Moon currently has the most precise and highly resolved global topography and gravity fields of any solar system object as a result of the LOLA instrument (Smith et al., 2017) and the GRAIL mission (Zuber et al., 2013b), so we concluded that new geodetic measurements at the Moon are not presently more compelling than at other targets—despite the overall high scientific importance of the Moon. Other lunar missions, like sample return from the South Pole-Aitken basin or the establishment of a lunar seismic network, should be considered to have higher priority than new global gravity or topography measurements. Similarly, Ceres has the most precise geodetic datasets of ice-rich bodies as a result of the Dawn mission (Park et al., 2020; Russell et al., 2016), and the scientific community has determined sample return and landed surface science to be the highest priorities at Ceres (Castillo-Rogez et al., 2022). Neptune and its moons are unlikely to be the target of spacecraft exploration initiated in the next decade for reasons outlined in the recent decadal strategy report for planetary science

and astrobiology. Other icy moons, like Ganymede or Callisto, hold promise for geodetic investigation (e.g., Smith et al., 2020), including from ESA's upcoming JUICE mission.

Geodetic measurements have the capability to address questions in fundamental physics, astrophysics, and heliophysics. Lunar laser ranging measurements have been used to test principles of general relativity (Williams et al., 1976, 2004, 2012), as have observations of radio photons by the Cassini spacecraft on its way to Saturn (Bertotti et al., 2003). At Mercury, range measurements to the MESSENGER spacecraft have been used to similarly test relativistic effects and constrain the oblateness of the Sun (Genova et al., 2018). These results show the capability of geodesy to address a variety of topics, and have motivated the development of a mission concept that would track the orbital evolution of the planets in real time and constrain the mass loss rate of the Sun (Smith et al., 2018).

Part II

Technology and Mission Concepts

6. Technology Developments

The scientific questions described in Sections 2–5 can be addressed with a combination of flight-proven geodetic instrumentation and technology that can be feasibly developed in the coming decade. In this section, we recommend areas of focus for technology development that would be particularly enabling for future geodetic research beyond the Earth–Moon system. The recommended areas include development of geodetic instruments (gravity gradiometers, InSAR, geodesy from aerial platforms), development of instruments that have particularly good synergy with geodesy in addressing high-priority planetary science objectives (magnetometry, seismology), and other development to spacecraft hardware and software (miniaturizing spacecraft-to-spacecraft tracking and on-board data processing).

6.1 Gravity gradiometers

Gravity gradiometry is the umbrella term for techniques where gravity gradients are measured. Gravity gradients are the second derivatives of gravitational potential and as a result are sensitive to local features. For the same reason, gravity gradients decay quickly with increasing altitude. An advantage of gravity gradiometry is that measurement noise from motion disturbances is relatively low. Therefore, gravity gradiometry can be effectively performed from moving platforms such as surface rovers or aerial vehicles while in motion (Dransfield and Zeng, 2009). On Earth, the Gravity Field and Steady-State Ocean Circulation Explorer (GOCE), ESA's gravity gradiometry mission, determined the geoid heights to 1 cm accuracy (or, equivalently 1 mGal accuracy in surface gravity) at a spatial resolution of ~100 km (e.g., van der Meijde et al., 2015). Currently, the GOCE mission provides the highest resolution

global static gravity map of the Earth from orbit, which is highly complementary to GRACE's Earth gravity solutions that are of lower spatial resolution but higher precision and span over a longer time period.

Development of superconducting gradiometers (SGG, Griggs et al., 2017; Paik et al., 1988) might enable much higher accuracy determination of static and time-variable planetary gravity fields compared to GOCE. Bills and Ermakov (2019) show that the SGG technology can provide degree 202 and 321 gravity resolutions at Mars and Venus, respectively, from a 300-km altitude orbit with one Earth year of total data collection. However, mission lifetime of SGGs may be limited because of cooling requirements. Therefore, SGGs may be best suited for cases where mission requirements favor high-resolution static gravity and mission lifetime is limited by some other factor anyway—a Europa gravity orbiter may be an example of this case. SGGs may be less well-suited where mission requirements prioritize time-variable gravity with long temporal baselines, such as for a Mars gravity orbiter that studies interannual variations in climate and atmospheric processes. We advocate for the continued development of SGGs for study of high spatial resolution static gravity fields at other planets.

6.2 InSAR

Spaceborne repeat-pass interferometric synthetic aperture radar (InSAR) is a technique that provides geodetic maps of surface displacement over time at mm-scale precision and over broad areas. By orbiting a SAR imaging instrument in almost an exactly repeating ground track, the SAR image acquired at one time can be combined with images acquired from the same vantage point at the repeating periodicity. The phase difference between any two images in a sequence records, pixel by pixel, the change in distance from the spacecraft to the pixel. The technique is mature and operational for many Earth orbiting SAR instruments, measuring a variety of geophysical phenomena, from coseismic, postseismic, and interseismic deformation, surface motions due to volcanic activity, landslides, aquifer subsidence and other, often very subtle (mm-scale) motions.

If repeating orbits can be found and maintained at other planetary bodies, InSAR has the promise of addressing similar geophysical problems as on Earth. Planetary bodies with less atmosphere and less short timescale surface changes are ideally suited to measuring mm-scale deformation over long periods of time. InSAR is sensitive to changes at the scale of the radar wavelength (cm-scale), so for planets with surface changes on faster timescales, like freezing and thawing, landslides, avalanches, or sand-dune migration, these changes are easily seen through decorrelation of the interferometric signal. At a body like Mars, InSAR could definitively answer the questions about active tectonics and volcanism, measure lithospheric flexure due to seasonal variations in polar loading of deposited and ablated CO_2, and constrain glacial flow regimes of ice. At a body like Enceladus, InSAR measurements of the Tiger Stripes could definitively quantify surface deformation and identify faulting mechanisms and

the connection between the ice shell and the ocean. InSAR is a mapping geodetic technique, and it offers an advantage in planetary remote sensing because it takes only a repeat cycle to cover the entire planet, so time is saved for missions with limited lifetime. After a year of observations, extensive observations of time-series of deformation and surface change could be collected. InSAR has only rarely been considered for Ocean Worlds, although Sandwell et al. (2004) investigated the feasibility at Europa.

Two aspects of InSAR may be particularly challenging at other planets and require further study. First, for some assumed altitudes (hundreds of km) and radar wavelengths (S-band), there is a requirement to repeat orbits to within 1 km wherever measurements are needed. Typically, a regular circular mapping orbit is desired to maximize coverage, so the InSAR orbit requirement amounts to placing the satellite in a circular repeating orbit and maintaining that ground track over the lifetime of the mission. This constraint can be a challenge with only radio tracking. Second, high data rates can be an issue and limit the area that can be covered before downlink is needed. We advocate that both these challenges be studied, especially for Mars and Enceladus that are particularly ripe targets for InSAR measurements (see Section 7).

6.3   Aerial geodesy

Gravimetry from aerial platforms such as balloons, rotorcrafts, and fixed-wing aircrafts has the advantage of surface proximity compared to orbit-based measurements. This proximity leads to a higher sensitivity to small-spatial-scale gravity anomalies. In addition, gravimetry from aerial platforms would benefit from and complement other types of observations taken at low altitudes. Compared to lander- or rover-based measurements, aerial gravimetry enables regional gravity surveys where larger areas of interest can be covered.

Aerial gravimetry presents a number of challenges. First, non-gravity-related forces acting on the aircraft need to be subtracted in order to derive the desired gravitational acceleration. On Earth, this is typically achieved with the help of the Global Positioning System (GPS), which is currently unavailable on other planets. Doppler tracking of the aerial platform from orbit can potentially replace GPS but the desired accuracy remains to be demonstrated. Gravity gradiometry has the advantage of being less affected by this motion, and if able to be performed in flight, would enable rapid coverage of areas of interest.

Alternatively, an aerial platform can be used to deliver a gravimeter to the surface and landed gravity measurements can be taken at multiple locations on the ground. The major advantage of this approach is that the gravimeter can be placed at points with different surface elevations. Collecting gravity data at different elevations and correlating these data to the gravity modeled with a digital terrain model yields estimates of regional sub-surface density. Aerial vehicles typically carry an inertial measurement unit (IMU) that measures vehicle accelerations. If the

vehicle is landed, the IMU measures surface gravity. Thus, engineering data from IMU can be used to map surface gravity changes. This process has been successfully demonstrated using IMU data from the Curiosity rover (Lewis et al., 2019).

Venus and Mars could represent compelling opportunities for geodetic observations from airborne vehicles—balloons in the case of Venus, and helicopters in the case of Mars. Such mission architectures fill an observational niche, enabling geodesy at regional scales. Aerial platforms can cover more area than a landed vehicle or rover and obtain data at higher spatial resolution than is achievable by an orbiter. At Venus, compelling target areas for geodesy could include regions were active mantle plumes or subduction is hypothesized (e.g., Gülcher et al., 2020). At Mars, compelling target areas for geodesy would include the dichotomy boundary or regions of magnetized crust (see Section 7.2).

Progress on the feasibility of this class of missions has recently been promising. An aerial vehicle has been successfully tested and flown on Mars (Balaram et al., 2021), and studies on the science that could be enabled by a future Martian rotorcraft are underway (Bapst et al., 2021). On Venus, the plausibility of geophysical observations like seismology from a balloon are being evaluated and show promise (Garcia et al., 2021; Krishnamoorthy et al., 2019). We advocate for the continued development of aerial vehicle capabilities, including the ability to carry geophysical instruments like gravimeters, gradiometers, and magnetometers.

6.4   Other geophysical datasets and geodesy

A common theme in our discussions was the value of jointly interpreting geodetic datasets with other types of geophysical observations. In particular, we identified seismology and magnetometry as especially synergistic methodologies to geodesy. Seismic analysis provides valuable constraints on crustal structure that can be folded into gravity and topography inversions to map out quantities like crustal thickness (e.g., Wieczorek et al., 2013, 2022). Magnetometry (including measuring both remnant and induced magnetic fields) can be jointly considered with geodetic data to elucidate the state of planetary cores and the histories of core dynamos.

We advocate for continued development of seismic and magnetic techniques, not only for their own sakes but for how they would improve interpretation of geodetic data. Specific areas of development that were discussed in our workshops included: development of the ability to land multiple seismometers on a planetary surface, using rocket boosters and similar materials as impactors for active seismology, and the development of a magnetometer that could be implemented on an aerial vehicle (i.e., helicopter) of appropriate magnetic cleanliness.

6.5 Opportunistic impactors for seismology and geodesy

Planetary missions often use upper stages (i.e., "boosters") to leave low-Earth orbit. These boosters are usually discarded into heliocentric orbits. We note that these boosters have provided openings for opportunistic impacts on planetary bodies, enabling active-source seismology. This technique was used during the Apollo missions, with impacts of the upper stage of the Saturn V (the SIVb) and lunar module ascent stages.

In the near future, there will be multiple boosters and vehicles heading to the Moon. The Artemis missions that will return humans to the surface of the Moon will use an Interim Cryogenic Propulsion Stage (ICPS), and ultimately the Exploration Upper Stage (EUS), to deliver Orion to cis-lunar space. There will also be a variety of smaller, robotic Commercial Lunar Payload Service (CLPS) missions heading to the Moon that may use boosters. These vehicles may ultimately be disposed of into the Earth, Moon, or a solar orbit. At present, there does not appear to be a plan to utilize these boosters as opportunistic impactors for seismology at the Moon. We also note that once spacecraft are in cis-lunar space, or on escape trajectories from the Earth–Moon system, it may be possible to use gravity assists with the terrestrial worlds to put spacecraft on trajectories with other worlds, including Mars and Venus. We will soon have active seismometers on the Moon and Titan, and we recommend that NASA consider how best to use these opportunistic impactors.

## 6.6 Miniaturizing spacecraft-to-spacecraft tracking

The gravity fields of most planetary bodies have been determined by processing Deep Space Network (DSN) Doppler tracking data. For a standard X-band telecommunication system, two-way tracking provides a Doppler accuracy of 0.03–0.1 mm/s (60-s count time). The DSN Ka-band tracking provides a Doppler accuracy better than 0.01 mm/s (60-s count time). If dual-frequency data is considered (e.g., X/Ka-up and X/Ka-down) and an Advanced Water Vapor Radiometer is available at DSN, the achievable Doppler data accuracy could be ≤ 0.005 mm/s (60-s count time). At this point, the limiting source for Doppler noise is the Earth media effect, rather than plasma noise, which typically dominates single-frequency estimates.

One way to achieve a substantial improvement in measurement accuracy is to use spacecraft-to-spacecraft tracking, because there is no medium between the two tracking platforms (such as the Earth's troposphere). For example, GRAIL's Lunar Gravity Ranging System (LGRS) provided a range-rate measurement accuracy of about 30 nm/s, or ~1000 times better than what DSN X-band tracking provides (Klipstein et al., 2013). The technology for spacecraft-to-spacecraft tracking is quite mature and has been demonstrated through the GRACE, GRAIL, and GRACE-FO missions. Achieving 30-nm/s or better measurement accuracy would require spacecraft with moderate power and pointing capabilities. We advocate for development of minimizing the size and mass of spacecraft-to-spacecraft tracking.

6.7 On-board data processing

Space electronics is undergoing a revolution as newer, smaller, and more powerful processors become available. For example, radio communication systems and radar instruments have largely become digital, software-defined systems for the generation of the waveforms, as well as all signal conditioning after sampling on reception. The power and size of these systems have also become greatly reduced, allowing less mass to be launched for a given capability, which in general means lower cost. This reduction in power, size, and cost has benefits for enabling on-board data processing.

On-board data processing involves data acquisition, storage, and compression on the spacecraft. One of the prime benefits of on-board processing is reduction of the needs for downlink, which can often be a limiting factor. This benefit can be particularly important for measurements such as radar images, where full-resolution imagery can be quite large. For example, the VERITAS mission to Venus will use on-board data processing to create images from two receiver antennas on board, then form an interferogram of these for downlink at much lower data volume than otherwise would be possible. This processing will be an enabling technology for comprehensive mapping. We advocate that similar methods should be studied and considered for repeat-pass InSAR observations at Mars or Enceladus, where data can be buffered from orbit to orbit, processed, and reduced.
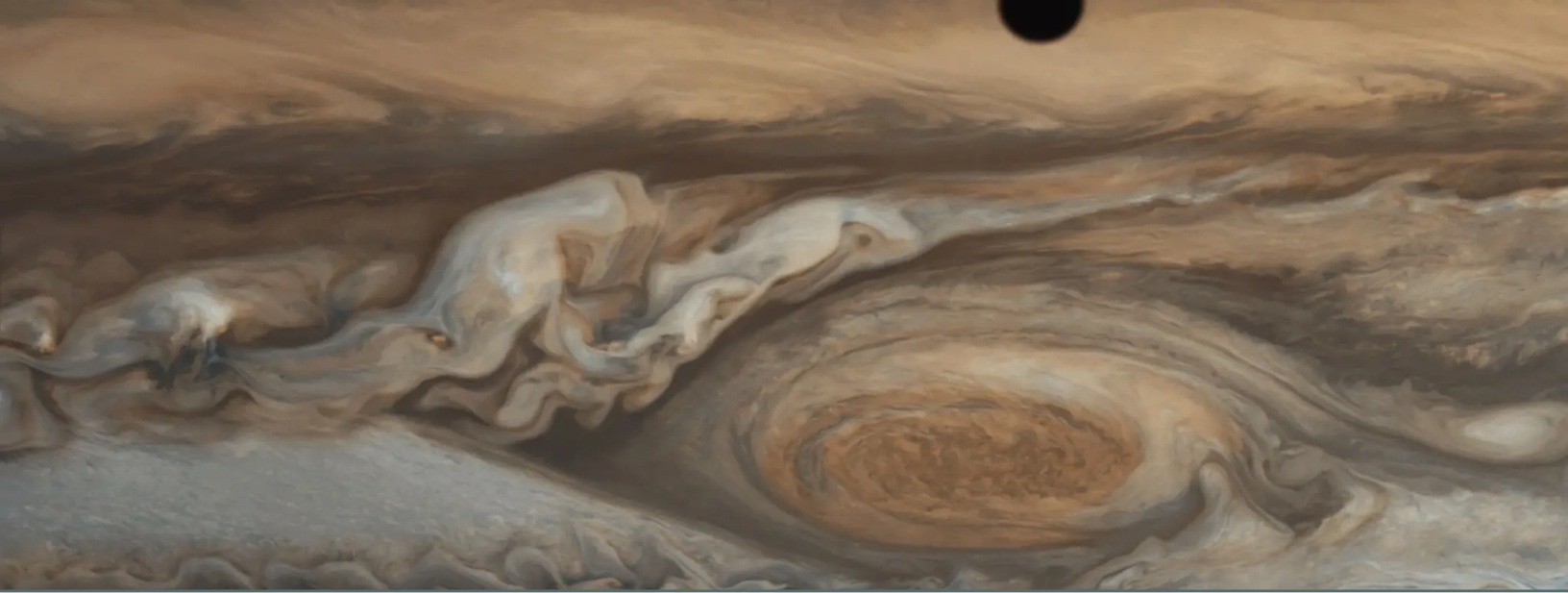
7. Compelling Mission Concepts

We discussed geodetic-themed mission concepts that would address the science described in Sections 2–5. We debated what concepts should be prioritized over the next ~10 years in planetary science. The primary consideration was science: we prioritized concepts that would enable the most compelling scientific investigations, span a range of sub-disciplines, and address the highest priorities of the planetary science community. We also considered technological feasibility, prioritizing concepts that could either be technologically ready immediately or would likely be feasible within the decade with some technology development. We considered cost. Although we did not perform formal mission concept studies, we prioritized concepts that we speculate could realistically be achieved at a cost equivalent to NASA's New Frontiers cost cap or below. Finally, we considered past, ongoing, and future selected spacecraft missions and how new geodetic measurements would fit in with those missions at individual planets or moons. We prioritized concepts where new, currently unplanned geodetic data would be most effective at addressing compelling science.

We recommend that four mission concepts be considered the highest priority for geodetic planetary science. These four concepts are shown in Table 7.1 (not in any prioritized order), and include a Mars Gravity Mapper and InSAR, Mars Geophysical Helicopter, Enceladus Geophysical Orbiter, and Europa Orbiter. We conclude that the Mars dual-spacecraft orbiter and the Enceladus geophysical orbiter are most technologically ready for the immediate future, whereas the Mars geophysical helicopter and the Europa orbiter may require some technological development over the next decade.

Concept	Description	Science Motivation
Mars Gravity Mapper and InSAR (Section 7.1)	An orbital mission at Mars that collects gravity data using spacecraft-to-spacecraft tracking with two spacecraft and collects InSAR data.	• Test hypotheses on the origin of the Martian global dichotomy. • Global and regional climate observer. • Quantify the vigor of present-day geologic activity.
Mars Geophysical Helicopter (Section 7.2)	A mobile aerial platform (i.e., a "helicopter") at the Martian surface with geophysics-focused instrumentation including a gravimeter and magnetometer.	• Fills "sweet spot" between orbiter and rover science, enabling regional geophysics. • Test hypotheses on the Martian global dichotomy. • Test hypotheses on the Martian core dynamo.
Enceladus Geophysical Orbiter (Section 7.3)	A geophysical orbiter at Enceladus that collects topography, gravity, and deformation measurements.	• Determine the interior structure of Enceladus. • Characterize the origin, evolution, and extent of tectonism on Enceladus. • Characterize habitable niches within Enceladus.
Europa Orbiter (Section 7.4)	An orbiter at Europa with a gravity gradiometer and magnetometer.	• Synergy with Europa Clipper to probe the interior structure of Europa. • Characterize the interior structure of Europa, including mapping the ice shell, ocean, and seafloor.

Table 7.1: Four highest priority, compelling, next-generation planetary geodesy mission concepts identified by this workshop.

These recommendations should not be interpreted to mean that other planets and moons in the solar system are not scientifically compelling objects, as discussed in Section 5. Rather,

our assessment is that Mars, Enceladus, and Europa represent the most attractive targets for geodetic exploration over the next decade when considering both the scientific potential and the landscape of other planned spacecraft missions. We very likely would have prioritized a Venus mission if not for recent Venus-focused mission selections by NASA and ESA, which will result in substantially improved topography and gravity datasets compared to current data. Venus missions focused on regional geodesy—perhaps from an airborne platform—should be strongly considered after NASA's VERITAS mission provides global geophysical context through its collection of topography and gravity data (Smrekar et al., 2022).

Below, we describe the four recommended mission concepts in greater detail. We focus on the scientific objectives and investigations that would be addressed by each mission and what types of instruments would achieve them. We recommend that all four ideas be formally studied for cost and feasibility.

7.1 Mars Gravity Mapper and InSAR

High-precision global gravity data of Mars is one of the highest-priority measurements necessary to address the evolution of rocky planets and the relationship of planetary climate to orbit. To address the motivating science questions about rocky planet evolution, it is necessary to measure Mars' global gravity field to a spatial resolution equivalent to spherical harmonic degree 200 (equivalent to a spatial resolution of ~100 km) or better. To address the motivating science questions about planetary climate, it is necessary to measure Mars' time-variable gravity field for at least two Mars years. Some questions require low-degree (degree and order 2 or better) sampling at daily timescales, and others require medium degree (degree and order 50 or better) sampling at ~monthly timescales. These divisions are approximate, as some geodynamical questions could be addressed with time-variable gravity and some climate questions could be addressed with high-precision static gravity. Some individual investigations have stricter requirements than spherical harmonic degree 200 and collection for 1 Mars year. Science objectives are listed below in Table 7.2.

Spacecraft-to-spacecraft tracking is the preferred option for an orbital Mars gravity mission (Figure 7.1). Microwave ranging systems have been flight-proven multiple times on the GRACE, GRAIL, and GRACE-FO missions (e.g., Klipstein et al., 2013). Although the Martian atmosphere would prevent spacecraft from operating at the low altitudes flown by GRAIL at the Moon, a dedicated gravity orbiter would still yield substantial improvement over the known gravity field at Mars. In addition to microwave ranging, laser ranging interferometry at optical wavelengths has been demonstrated by the GRACE-FO mission (Kornfeld et al., 2019). This instrumentation holds promise for significant increase in the precision of individual ranging measurements, and should be considered for the inter-spacecraft ranging system via a spacecraft-to-spacecraft tracking architecture at Mars. Because of the value in climate-themed investigations that require long temporal baselines to collect time-variable gravity data,

superconducting gravity gradiometers at Mars is not prioritized—as they have limited lifetimes because of the need to be kept at cryogenic temperatures (Section 6.1). A superconducting gravity gradiometer would hold promise for increased precision in individual measurements but likely would have a shorter operational lifetime because of cryocooling requirements. However, gradiometers may be optimal for other worlds (see Section 7.4).
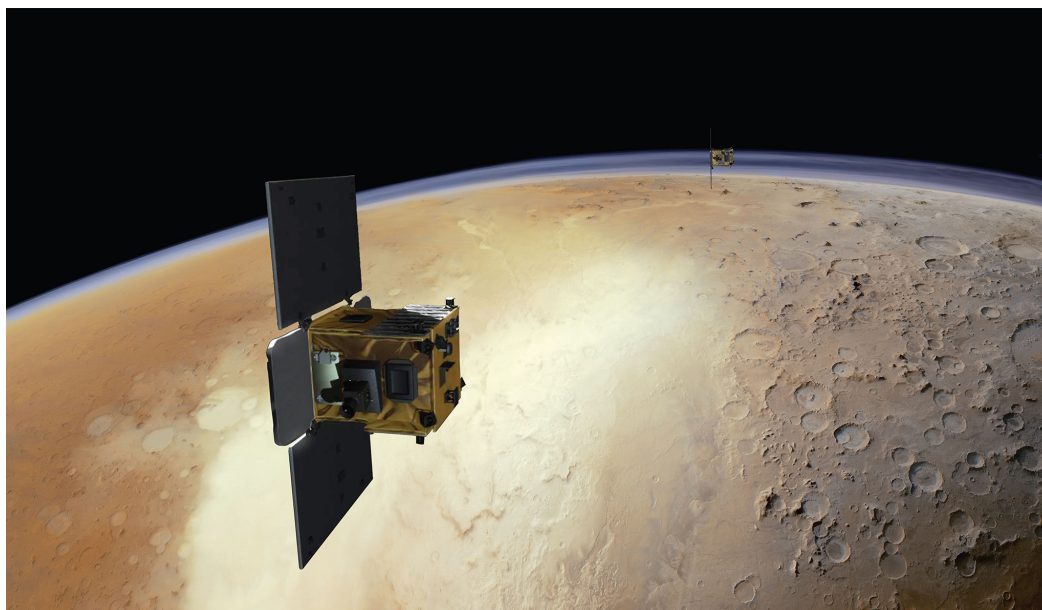
Figure 7.1: Artist rendering of a GRAIL/GRACE-like spacecraft pair orbiting Mars. Image credit: Hellas Basin from Mars Express (ESA / DLR / FU Berlin / Justin Cowart), GRAIL (NASA / JPL-Caltech / MIT), composited by James Tuttle Keane.

InSAR may have transformative potential at Mars, similar to the way it has revolutionized terrestrial geology and geophysics. InSAR measurements of surface displacement would be sensitive to seasonal volatile cycles and possibly tectonic or volcanic activity, enabling quantitative studies of the geological activity of Mars today. This instrumentation is timely with the detection of endogenic seismic activity ("Marsquakes") by the InSight mission.

We encourage formal studies of a Mars gravity mapper with or without an INSAR instrument. Specific questions that should be studied include:

1. What is the optimal orbital strategy to achieve goals related to both geodynamics and climate? Obtaining gravity data at high spatial resolution lends itself to data collection at low altitudes, whereas monitoring the Martian climate for long timescales implies a preference for higher, more stable altitudes. Is there an orbital architecture that involves data collection at multiple altitudes to optimally address the science investigations in aggregate?

Science Themes	Science Objectives	Candidate Instruments	Mission Architecture
1. *Planetary Evolution:* **Understand the geodynamic and tectonic history of Mars, and how and why it differs from Earth's**	• Distinguish between competing hypotheses for the nature and origin of the Martian global dichotomy. • Determine the thermal history and past tectonic regimes of Mars. • Determine the impact bombardment history recorded at Mars.	• **Gravity science** for measuring static gravity field (spherical harmonic degree/order ~200 or better) and time-dependent gravity field (daily sampling of degree 2 or better and monthly sampling of degree 50 or better for 2 Mars years). • **InSAR** for measuring active, sub-centimeter scale deformation over a Mars year.	Mars dual orbiters with spacecraft-to-spacecraft tracking using microwave or optical laser interferometric ranging, with stable, near-polar orbits at low altitudes for sampling high-resolution static gravity field and high altitudes for monitoring time-variable gravity field
2. *Climate:* **Understand how planetary climates respond to orbital changes**	• Distinguish between competing hypotheses for the presence and volume of icy climate records on Mars. • Determine how the components of global circulation of the Martian atmosphere change over seasonal and interannual timescales. • Determine the location and quantify the magnitude of sources and sinks of volatiles on Mars.		

Table 7.2: Summary of the science themes, objectives, candidate instruments, and notional architecture for a Mars Gravity Mapper and InSAR concept.

2. What are the trade-offs between using a microwave ranging system (as was done on GRAIL, GRACE, and GRACE-FO) and optical laser ranging interferometry (as shown in a technology demonstration on GRACE-FO)? Is the added precision of optical laser ranging worth the added risk represented by the fact that it has been flown on fewer spacecraft missions?

3. Is there a need to augment spacecraft position accuracy of a gravity mission at Mars based on spacecraft-spacecraft tracking beyond radio tracking of the two spacecraft from Earth?

4. Can InSAR be added to a gravity mapping mission at Mars at a Discovery level cost? If not, can InSAR be done at Mars as a standalone mission at a lower-than-Discovery level (~$300 million) cost?

We recommend a spacecraft-to-spacecraft tracking orbital gravity mission at Mars be formally studied and flown as soon as possible. Such a mission would be extremely scientifically compelling with or without an InSAR instrument.

7.2 Mars Geophysical Helicopter

The success of the Ingenuity helicopter (Balaram et al., 2021) deployed from the Perseverance rover opens new possibilities for aerial instrumentation near the surface of Mars. Helicopters hold promise for addressing science at length scales in a "sweet spot" between that of rovers and orbiters (Figure 7.2). In particular, helicopters can take measurements hundreds of meters above the surface (compared to meters for rovers and hundreds of kilometers for orbiters), and can traverse hundreds of kilometers across the Martian surface during the lifetime of a single mission (compared to kilometers for rovers). We identified two broad science themes that could be effectively addressed by a geophysically focused helicopter at Mars.

First, a helicopter could focus on the origin and evolution of the Martian dichotomy. As argued in Sections 3.2.1 and 7.1, a gravity orbiter would provide a compelling view of the Martian dichotomy via the construction of global crustal thickness and crustal density maps. An advantage of a helicopter architecture is that an aerial vehicle could study the dichotomy boundary in great detail. The traverses enabled by a helicopter (hundreds of kms over a mission lifetime) would allow for a single mission to meaningfully cross the dichotomy boundary and take measurements on both sides of the boundary with the same set of instruments. A gravimeter would allow for measurement of crustal density by taking gravity measurements at strategically chosen locations across a range of altitudes, similar to how the Curiosity navigation accelerometers were used to infer the density and composition of material in Gale crater (Lewis et al., 2019). The dichotomy boundary also closely follows some hypothesized shorelines of an ancient Martian ocean, so a helicopter mission that crosses the dichotomy boundary would also naturally study ocean history. For example, gravity measurements could
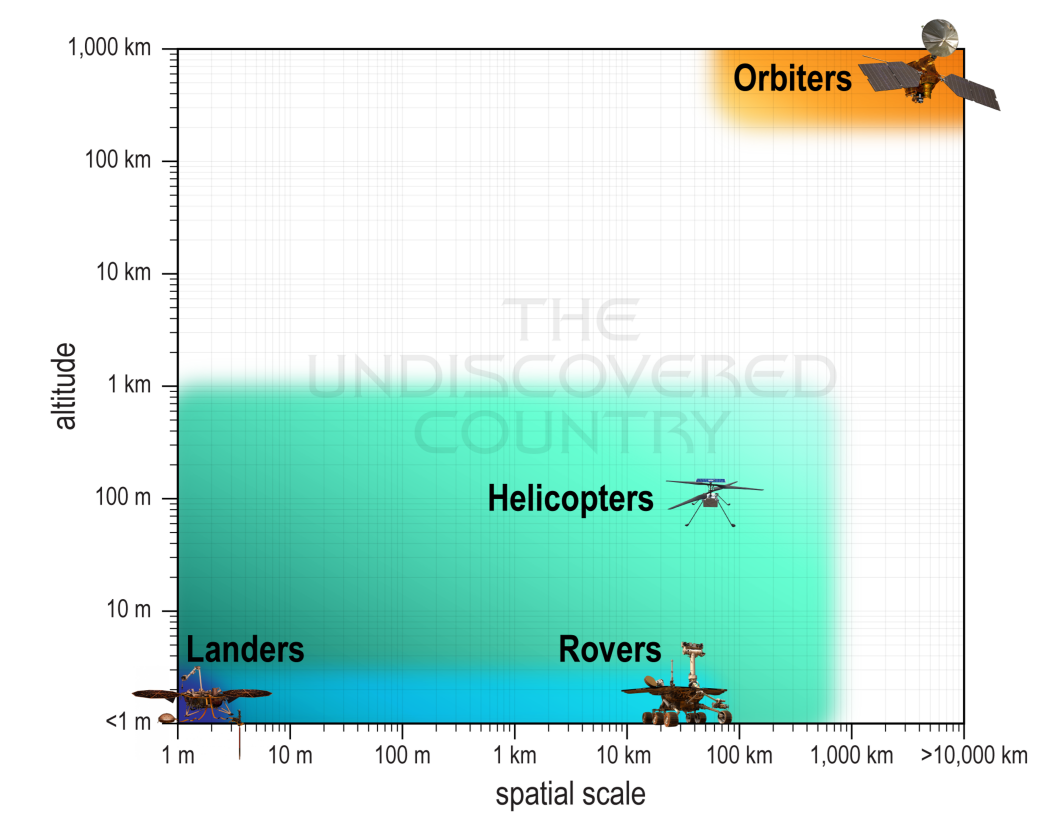
Figure 7.2: Plot showing the approximate altitudes and lateral spatial scales that can be studied by rovers, helicopters, and orbiters on Mars.

be used to test formation hypotheses on features like putative mud volcanoes (Dapremont and Wray, 2021). The geophysical gravity and magnetometry (see paragraph below) measurements should be supplemented by visible images and a VNIR spectrometer to provide context and study composition and geomorphology.

Second, a helicopter could focus on the history of magnetization in the Martian crust and the history of the core dynamo (Figure 7.3). Crustal magnetization is a particularly compelling observable to study with an aerial vehicle because of the capability it provides to sample the potential field at different altitudes. It is known that magnetic observations near the surface will reveal structure not observable from orbit (e.g., Johnson et al., 2020). A magnetometer on a helicopter could test hypotheses on dynamo cessation (e.g., Mittelholz et al., 2020) by measuring magnetization of lava flows and basin ejecta, and determine if polarity reversals are recorded in melt sheets by measuring the magnetic field at different altitudes in and near impact basins (Chaffee and Tikoo, 2021). A difference in crustal magnetization may be an important component of the global dichotomy, so there is promise that the magnetic theme could be addressed in tandem with the dichotomy theme. However, the magnetized southern

highlands far from the dichotomy boundary should also be considered as a possible region for the magnetic theme.
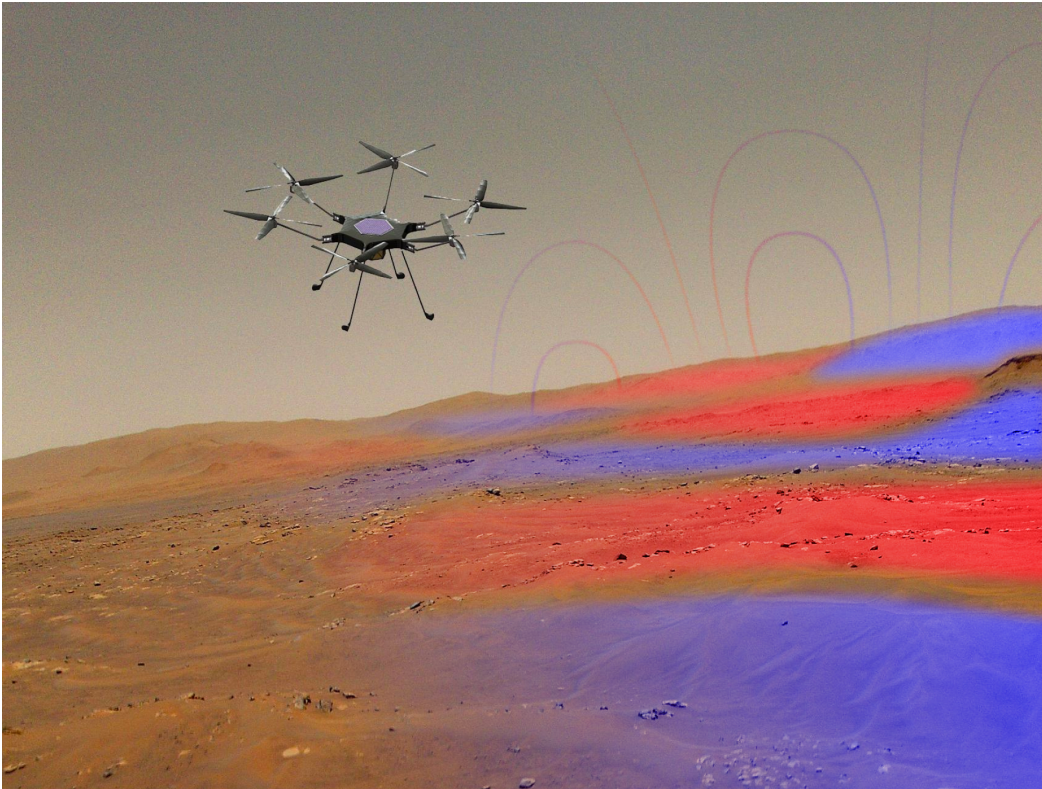
Figure 7.3: Artist concept of a Mars Geophysical Helicopter, measuring magnetic and/or gravity fields (colored red/blue) at a range of length and height scales. Image credit: NASA/JPL-Caltech, James Tuttle Keane

Possible science objectives for a Mars geophysical helicopter are listed in Table 7.3. We identified the following questions that should be addressed by a formal mission concept study in order to address the capability that a helicopter could meet these objectives:

1. What is the ideal location to send a geophysically themed Martian helicopter? Is there a traverse that efficiently allows study of both the evolution of the dichotomy boundary and the history of the core dynamo?

2. What is the realistic magnetic cleanliness of a Martian helicopter? Would a magnetometer need to be separated from the vehicle on a boom, and if so by how much distance? Would a boom allow the magnetometer to take measurements while the helicopter is flying?

3. Can a gravimeter with the required precision be flown on a helicopter while meeting the mass requirements for vehicle flight?

Finally, we note that a helicopter inherently triggers a high amount of inspiration and public interest in a way that goes beyond other types of missions. This factor should be considered as a benefit to a potential Mars geophysical helicopter. We encourage continued study of helicopter capabilities on Mars.

Science Themes	Science Objectives	Candidate Instruments	Mission Architecture
1. *Dichotomy:* **Understand the origin and evolution of the global dichotomy and the dichotomy boundary**	• Characterize crustal structure north and south of the dichotomy boundary • Test for the existence of ancient ocean shorelines • Test hypothesis that aqueous alteration is the cause of the crustal magnetization dichotomy	• **Gravimeter** for measuring gravity field with precision 0.1 mGal and inverting for bulk density with uncertainty ~10 kg/m^3 • **Magnetometer** for measuring crustal magnetization and magnetization associated with lava flows and impact melt sheets • **Visible camera** for providing geological context • **VNIR** for compositional and mineralogical constraints	Mars aerial vehicle that strategically traverses 100s of kms across the dichotomy boundary and/or magnetized highlands, sampling potential fields at different altitudes and elevations
2. *Core:* **Characterize the nature and timing of the core dynamo**	• Quantify magnetization in northern lowlands and/or southern highlands • Quantify magnitude and direction of magnetic field at the surface at specific points in Martian history • Determine if polarity reversals are recorded		

Table 7.3: Summary of the science themes, objectives, candidate instruments, and notional architecture for a Mars Geophysical Helicopter concept.

7.3 Enceladus Geophysical Orbiter

The Cassini mission revealed Enceladus to be an incredibly dynamic and potentially habitable Ocean World. Nonetheless, major questions remain about its internal structure, energy budget, and nature of potentially habitable niches. We identified an Enceladus geophysical orbiter—equipped with a variety of geophysical instruments (gravity science, visible and thermal imaging cameras, InSAR, and a magnetometer)—as an exceptionally compelling concept for addressing critical knowledge gaps left after Cassini, while also paving the way and providing essential context for future "life-finding" investigations.

The Enceladus geophysical orbiter concept (Figure 7.4) would have the three science objectives, centered around structure, energy, and habitability (Table 7.4).
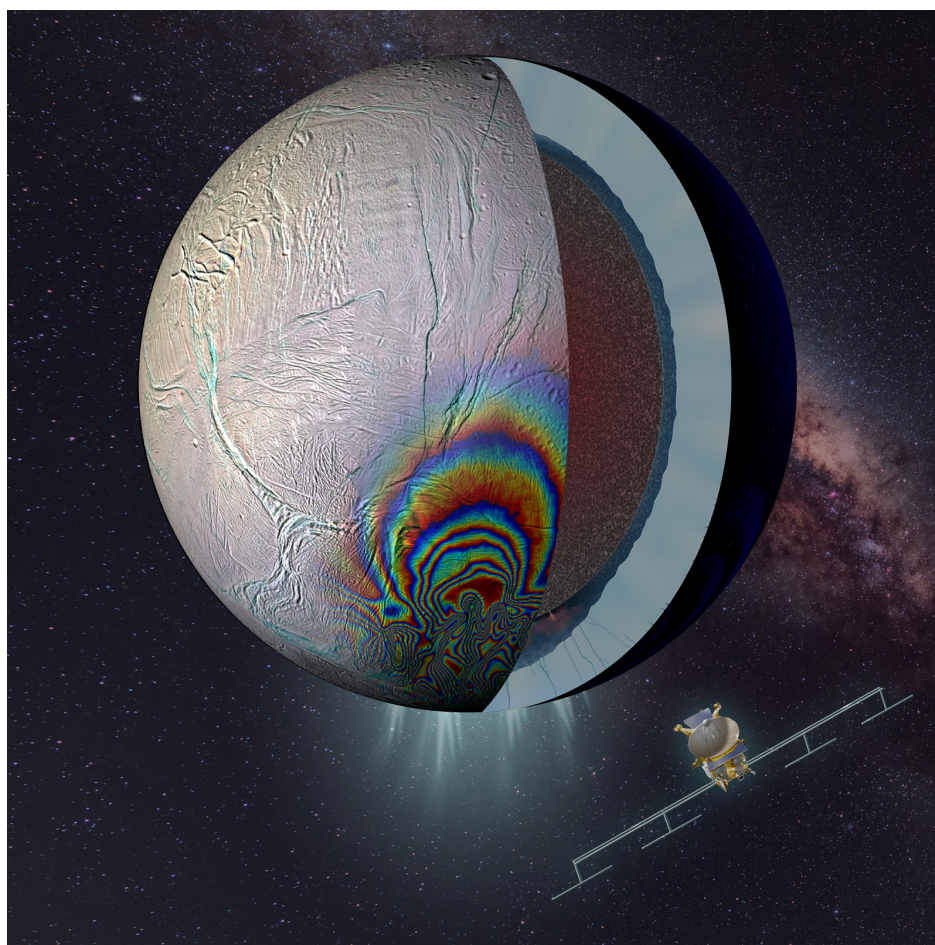

Figure 7.4: Artist concept of an Enceladus Geophysical Orbiter, revealing the interior structure of Enceladus and measuring active deformation associated Enceladus' Tiger Stripes and south polar terrain. The synthetic InSAR inteferogram draped on the surface of Enceladus is derived from models from Běhounkovà et al. (2017). Image credit: NASA / JPL-Caltech / James Tuttle Keane.

Science Themes	Science Objectives	Candidate Instruments	Mission Architecture
1. *Structure:* **Determine the global internal structure properties of Enceladus**	• Measure the mean shell thickness, density, and its regional variations. • Determine the structure and composition of the ocean. • Determine the physical state of the core (monolithic vs. rubble pile).	• **Gravity science** for measuring static gravity field (up to spherical harmonic degree/order ~30) and time-dependent gravity field (real and imaginary k_2). • **Imaging** for recovering topography of regions illuminated by the Sun (and possibly Saturn), and for monitoring plume/jet activity.	
2. *Energy:* **Determine the global energy budget of Enceladus**	• Determine if the satellite is in thermal equilibrium. • Quantify the total tidal heat dissipated by measuring the tidal phase lag.	• **InSAR** for measuring active, sub-centimeter scale deformation over the tidal cycle. • **Thermal instrument** for measuring surface temperatures and constraining the heat flow out of Enceladus.	Enceladus orbiter, with stable, periodic orbit (inclination ~50°), uniformly sampling Enceladus' tidal cycle, with an altitude of ~150 km.
3. *Habitability:* **Characterize habitable niches within Enceladus**	• Determine the rates of mass and energy exchange between the icy shell, ocean, and rocky interior	• **Magnetometer** for performing magnetic induction experiment.	

Table 7.4: Summary of the science themes, objectives, candidate instruments, and notional architecture for an Enceladus Geophysical Orbiter concept.

	Results	Key Challenges	Future Steps
1. **Radar design proof**	S-band radar with 800-m baseline.	None noted.	Develop a better understand the scattering properties of the surface in greater detail as a function of frequency.
2. **Orbit properties and maintenance proof**	Mid-latitude stable orbits exist with ~60° inclination and altitude 170–210 km. Repeat time is ~30.5 hours, sufficiently out-of-phase with tidal period (33 hours). The South Polar Region is visible from this latitude with reasonable look angles.	These InSAR orbits require small daily orbit maintenance maneuver to revisit the same spot with 800 m accuracy. ΔV for orbit maintenance is <1 m/s per day, but this ultimately adds up to limit mission lifetime.	Perform a more detailed analysis to determine if ΔV for orbit maintenance can be reduced.
3. **InSAR instrument design and resources proof**	InSAR: total mass: ~50 kg; total power: ~250 W peak with low duty cycle; cost consistent with similar missions.	InSAR will require on-board processing to reduce data $1,000\times$ to 2 Gbits per day (max for 8-hour DSN pass).	Develop a proof of concept for InSAR data processing algorithm. Define the full set of complementary science payloads and investigations, to create a complete mission concept. Investigate opportunities for science instrument partnerships based on past precedent.
4. **Mission technical concept proof**	Baseline instruments included representative imaging camera, thermal infrared imager, magnetometer, gravity science. Total spacecraft wet mass is ~6,200 kg with 1,000 m/s Saturn Orbit Insertion, 900 m/s for pump-down and Enceladus orbit insertion, and 400 m/s ΔV for orbit maintenance Does not fit on Falcon Heavy recoverable, but 80% launch mass margin on Falcon Heavy expendable.	Trajectory assumed has 9-year cruise to Saturn + 3-year pump-down. This is a long time to wait for science! Falcon Heavy expendable has not been an option in past Discovery and New Frontiers opportunities. This may be a cost upper, but is mission-enabling	Refine trajectory to reduce cruise time and ΔV for orbit insertion. Develop full spacecraft full point design with new trajectory to refine mass and cost. Explore options in orbit insertion concepts (e.g., aerocapture at Titan).
5. **Mission cost proof**	Spacecraft alone is almost half of total cost due to large propulsion system and supporting structure. Mission is consistent with New Frontiers Class. Note: did not include any contributions from partners.	Unknowns: cost upper for on-board processing, Falcon Heavy expendable launch vehicle, other payload costs and resources.	Investigate areas of cost reduction in follow-on facilitated discussion. Campaign for mission-enabling Falcon Heavy expendable option in next mission opportunities.

Table 7.5: Summary of results, challenges, and next-steps from JPL Enceladus geophysical orbiter InSAR feasibility study.

These objectives motivate a well-instrumented spacecraft in a stable, periodic orbit around Enceladus, with an altitude of ~100–300 km. The baseline instruments would include a gravity science package for measuring static gravity up to spherical harmonic degree/order ~30 and time-varying gravity, a geodetic camera or laser altimeter for determining Enceladus' shape, InSAR for measuring active sub-centimeter scale deformation over Enceladus' tidal cycle, a thermal instrument for measuring surface temperatures and heat flow, and a magnetometer for performing a magnetic induction experiment. Ermakov et al. (2021) provides many of the necessary measurement requirements for such an Enceladus mission.

Motivated by the KISS workshop, JPL performed a concept feasibility study for an Enceladus geophysical orbiter. Of all the proposed measurements for an Enceladus Geophysical Orbiter, InSAR is by far the most challenging at Enceladus as it has stringent mission design requirements. Thus, the central goal of this study was to evaluate the feasibility of flying an InSAR at Enceladus that is capable of measuring sub-centimeter scale deformation over Enceladus' 33-hour tidal cycle. JPL's Team-X (a concurrent engineering, rapid mission concept development team) was tasked with answering the following five questions:

1. Does a radar design exist that achieves the desired science requirements?

2. Does a repeat orbit exist with adequate tidal sampling, and can it be maintained to the required accuracy?

3. Are the instrument technical resources and cost in-family with historical missions?

4. Does a mission concept exist that can fly this payload and fit within technical constraints?

5. Is the cost class of such a mission consistent with the Discovery, New Frontiers, or Flagship mission classes?

Table 7.5 summarizes the results of this JPL study. In short: instruments, orbits, and mission designs exist that suggest that InSAR is feasible at Enceladus. This concept appears consistent with a medium-sized, New Frontiers class mission. There are two overarching key challenges. First, InSAR produces a substantial amount of raw data—far more than is feasible to return to Earth—meaning that on-board data processing (i.e., creating interferograms on board) may be enabling. Second, getting into Enceladus orbit and maintaining that orbit for InSAR requires a substantial amount of fuel, and thus a massive spacecraft. Heavy lift launch vehicles, like Falcon Heavy Expendable, may be enabling.

While the JPL InSAR feasibility study is compelling, and suggests that an Enceladus geophysical orbiter may be viable, we encourage the community to perform more detailed concept studies for an Enceladus geophysical orbiter. We identified the following specific questions to be studied:

1. What are the trade-offs between geodetically tracking a single spacecraft from Earth vs spacecraft that track one another (e.g., GRACE, GRAIL)?

2. What is the feasibility of operating InSAR at Enceladus? InSAR has stringent operational requirements (e.g., spacecraft orbit control), which will substantially impact overall mission design. Additionally, is it possible to perform on-board data processing to reduce the data volume necessary to transmit to Earth?

7.4 Europa Geophysical Orbiter

Europa is a priority target for NASA's exploration of the solar system and the search for life. The forthcoming Europa Clipper mission will revolutionize understanding of this icy Ocean World. However, it is important to note that Europa Clipper will not be capable of addressing all of the priority science questions at Europa by virtue of its Jupiter-centric orbit. As noted in the Midterm review of the previous Decadal Survey:

> "[Europa Clipper] preserves much of the [Jupiter Europa Orbiter] Europa science proposed to the decadal—estimates from the project science office are 73 percent—but the major loss is to the geophysical science objectives; without being in orbit it is challenging to establish the interior structure of Europa." (Page 69 of *Vision into Voyages for Planetary Science in the Decade 2013–2022: A Midterm Review*.)

There is much to be gained from in situ, orbital measurements at Europa.

The workshop developed a notional Europa Geophysical Orbiter concept (Figure 7.5) that would address the outstanding priority science questions at Europa left after the Europa Clipper mission. The science objectives for such a mission (Table 7.6) are nearly identical to those for the Enceladus Geophysical Orbiter. However, despite these apparent similarities, there are rather dramatic differences between these two worlds, which ultimately would drive equally dramatic differences between mission architectures (Table 7.7).

We note that we prioritized measurements that would not be accomplished by Europa Clipper. For example, we anticipate that Europa Clipper would measure Europa's shape to high precision. If Europa Clipper cannot measure Europa's shape to the same precision as the gravity field specified above, then this concept would need an additional instrument to characterize Europa's shape (e.g., a laser altimeter).

The single biggest challenge for a Europa Geophysical Orbiter is the radiation risk in Europa orbit. Previous estimates, such as those done for the Europa Lander concept, suggest that it may be feasible to survive in Europa orbit for approximately one month before radiation ultimately renders the spacecraft inoperative. Because of this limitation, it seems improbable that a traditional single or dual spacecraft gravity science mission would be capable of
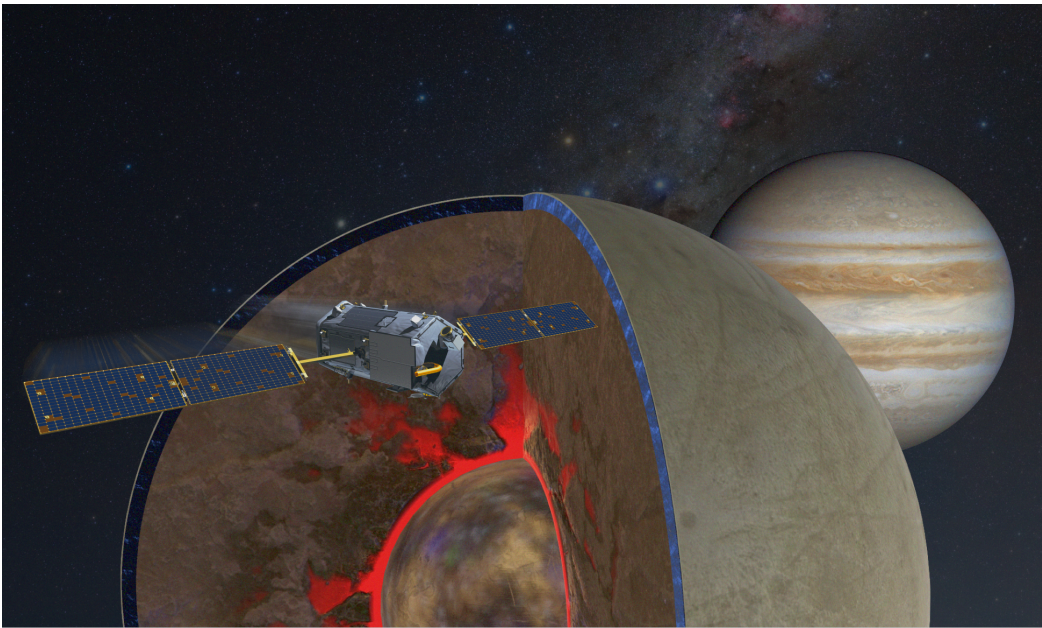
Figure 7.5: Artist concept of a Europa Geophysical Orbiter, revealing the interior structure of Europa. Image credit: NASA / JPL-Caltech / James Tuttle Keane.

accomplishing the science objectives rapidly. Superconductive gravity gradiometers show substantial promise for enabling recovery of gravity fields to high precision in a shorter duration than traditional spacecraft tracking techniques. However, such an instrument has never been flown before.

Science Themes	Science Objectives	Candidate Instruments	Mission Architecture
1. *Structure:* **Determine the global internal structure properties of Europa**	• Measure the mean shell thickness, density, and its regional variations. • Determine the structure and composition of the ocean. • Determine the physical state of the core (monolithic vs. rubble pile).	• **Gravity science** for measuring static gravity field (up to spherical harmonic degree/order ~100) and time-dependent gravity field (real and imaginary k_2). • **Magnetometer** for performing magnetic induction experiment over a range of frequencies.	Europa orbiter with stable, low-altitude, high-inclination orbit, uniformly sampling Europa's tidal cycle (85 hours). Mission duration is likely limited by radiation to be ~1 month.
2. *Energy:* **Determine the global energy budget of Europa**	• Determine if the satellite is in thermal equilibrium. • Quantify the total tidal heat dissipated by measuring the tidal phase lag.		
3. *Habitability:* **Characterize habitable niches within Europa**	• Determine the rates of mass and energy exchange between the icy shell, ocean, and rocky interior		

Table 7.6: Summary of the science themes, objectives, candidate instruments, and notional architecture for a Europa Geophysical Orbiter concept.

		Enceladus	Europa
Science aspects	Bulk composition	**Comparable amounts of water and rock**	**Mostly rock**
	Surface mobility	Evidence for tidal fractures and **very likely active today**.	Evidence for surface mobility and tidal fractures in the geologic record, although it **may be inactive today**.
	Deep interior	Possible porous, hydrated core.	Rocky core, plausibly with a metallic core.
	Ocean stability	**Ephemeral, cyclic, or long-lived ocean?**.	**Long-lived ocean?** Tidal and radiogenic heating can maintain an ocean over geologic time.
	Geologic activity	**Active cryovolcanic eruptions** with clear connection to tidal forcing and tectonics.	**Active cryovolcanism is debated**, and if present, does not have a clear relationship to tidal forcing or tectonic processes.
Implementation aspects	Magnetic induction	**Very challenging** due to Saturn's magnetic field geometry and contamination due to the plumes—although there may be a weak eccentricity signal.	**Very effective** due to Jupiter's magnetic field geometry. Induction provides strong constraints on the ocean thickness and salinity.
	Orbital stability	**Relatively hard to orbit**, due to the paucity of stable, low-altitude, polar orbits.	**Relatively easy to orbit.**
	Radiation environment	**Benign radiation environment.**	**High radiation risk**, requiring mitigation, and ultimately limiting mission duration (~1 month).

Table 7.7: Key differences between Enceladus and Europa, both from a scientific perspective and a mission implementation perspective.

8. Conclusions and Future Directions

New geodetic measurements have transformative potential in planetary science. At Mars, geodetic measurements would be particularly compelling in addressing questions related to rocky planet evolution and planetary climate. At Enceladus and Europa, geodetic measurements would be particularly compelling in addressing questions related to Ocean World interior structure, mass and energy transport, and habitability. Geodesy at Venus is equally scientifically compelling, but less of a focus in this report because the collection of new global topography and gravity data is already planned with the recent selection of NASA's VERITAS mission.

Two geodetic mission concepts in particular represent "low hanging fruit": missions that would yield massive scientific return and could be flown in the near future with minimal additional technological development. **(1) A dual spacecraft mission that collects gravity data at Mars** with spacecraft-spacecraft tracking through microwave or optical ranging and **(2) an orbiter at Enceladus** that collects gravity data through radio tracking and topography data through altimetry would address the major scientific themes listed in the previous paragraph on both worlds. Observations of surface deformation through InSAR measurements at both Mars and Enceladus is compelling, probably viable, and should be considered as additions to both mission concepts, but likely requires some technological development and needs to be formally studied for cost trade-offs.

There are two additional geodetic mission concepts we recommend be studied, but likely require a greater degree of technological development than the concepts described previously. **(3) A helicopter-like vehicle with aerial mobility on the Martian surface** that can collect gravity and magnetic data at strategically chosen locations would be able to address

questions related to the origin of the Martian crust and the history of the planet's core dynamo. **(4) An orbiter at Europa** that collects global gravity data with a superconducting gravity gradiometer and magnetic data with a magnetometer would allow for detailed study of Europa's interior structure and ocean, and be ideally complimentary to Europa Clipper.

Geodetic measurements have powerful potential throughout the solar system, and should be prioritized at other planets in the same way that they have at the Earth and Moon.
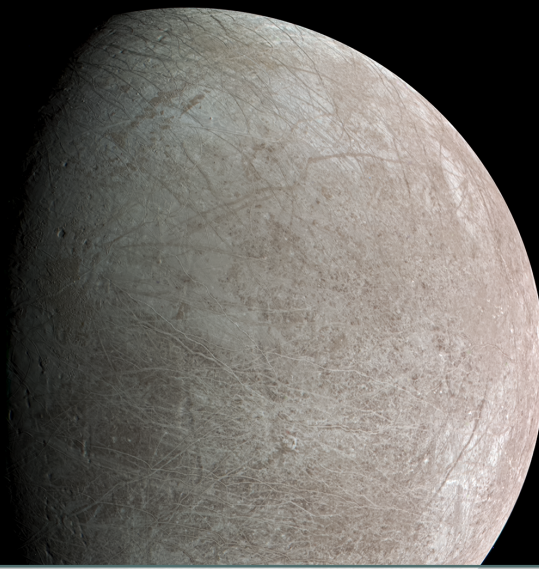
References

Acuña, M. H. et al. (1999). "Global distribution of crustal magnetization discovered by the Mars Global Surveyor MAG/ER experiment". In: *Science* 284.5415, pp. 790–793. DOI: 10.1126/science.284.5415.790.

Akiba, R., A. I. Ermakov, and B. Militzer (2022). "Probing the icy shell structure of Ocean Worlds with gravity-topography admittance". In: *Planet. Sci. J.* 3.1, p. 53. DOI: 10.3847/psj/ac4d2b.

Amit, H. et al. (2020). "Cooling patterns in rotating thin spherical shells—Application to Titan's subsurface ocean". In: *Icarus* 338, p. 113509. DOI: 10.1016/j.icarus.2019.113509.

Anderson, J. D. et al. (1998). "Europa's differentiated internal structure: inferences from four Galileo encounters". In: *Science* 281, pp. 2019–2022. DOI: 10.1126/science.281.5385.2019.

Andrews-Hanna, J. C., M. T. Zuber, and W. B. Banerdt (2008). "The Borealis basin and the origin of the Martian crustal dichotomy". In: *Nature* 453, pp. 1212–1215. DOI: 10.1038/nature07011.

Baland, R.-M. et al. (2014). "Titan's internal structure inferred from its gravity field, shape, and rotation state". In: *Icarus* 237, pp. 29–41. DOI: 10.1016/j.icarus.2014.04.007.

Balaram, J., M. Aung, and M.P. Golombek (2021). "The ingenuity helicopter on the Perseverance rover". In: *Space Sci. Rev.* 217, p. 56. DOI: 10.1007/s11214-021-00815-w.

Banks, M. E. et al. (2010). "Crater population and resurfacing of the Martian north polar layered deposits". In: *J. Geophys. Res. Planets* 115.E08006. DOI: 10.1029/2009je003523.

Bapst, J. et al. (2021). "Mars science helicopter: Compelling science enabled by an aerial platform". In: *Bulletin of the American Astronomical Society* 53.4, p. 361. DOI: 10.3847/1538-3881/ab2865.

Becerra, P., M. M. Sori, and S. Byrne (2017). "Signals of astronomical forcing in the exposure topography of the north polar layered deposits of Mars". In: *Geophys. Res. Lett.* 44.2, pp. 62–70. DOI: 10.1002/2016gl071197.

Becerra, P. et al. (2019). "Timescales of the climate record in the south polar ice cap of Mars". In: *Geophys. Res. Lett.* 46.12, pp. 7268–7277. DOI: 10.1029/2019gl083588.

Běhounkovà, M. et al. (2017). "Plume Activity and Tidal Deformation on Enceladus Influenced by Faults and Variable Ice Shell Thickness". In: *Astrobiology* 17.12, pp. 1357–1371. DOI: 10.1089/ast.2016.1629.

Běhounkovà, M. et al. (2021). "Tidally Induced Magmatic Pulses on the Oceanic Floor of Jupiter's Moon Europa". In: *Geophys. Res. Lett.* 48.24, e2020GL090077. DOI: 10.1029/2020gl090077.

Belleguic, V., P. Lognonné, and M. A. Wieczorek (2005). "Constraints on the Martian lithosphere from gravity and topography data". In: *J. Geophys. Res. Planets* 110.E11005. DOI: 10.1029/2005je002437.

Bertotti, B., L. Iess, and P. Tortora (2003). "A test of general relativity using radio links with the Cassini spacecraft". In: *Nature* 425.6956, pp. 374–376. DOI: 10.1038/nature01997.

Besserer, J. et al. (2013). "Convection-driven compaction as a possible origin of Enceladus's long wavelength topography". In: *J. Geophys. Res. Planets* 118.E08002, pp. 1–20. DOI: 10.1002/jgre.20079.

Beuthe, M. (2013). "Spatial patterns of tidal heating". In: *Icarus* 223.2, pp. 308–329. DOI: 10.1016/j.icarus.2012.11.020.

Beuthe, M. (2018). "Enceladus's crust as a non-uniform thin shell: I tidal deformations". In: *Icarus* 302.2, pp. 145–174.

Beuthe, M. (2019). "Enceladus's crust as a non-uniform thin shell: II tidal dissipation". In: *Icarus* 332.1, pp. 66–91. DOI: 10.1016/j.icarus.2019.05.035.

Bierson, C. J. and F. Nimmo (2016). "A test for Io's magma ocean: Modeling tidal dissipation with a partially molten mantle". In: *J. Geophys. Res. Planets* 121.11, pp. 2211–2224. DOI: 10.1002/2016je005005.

Bierson, C. J., F. Nimmo, and W. B. McKinnon (2018). "Implications of the observed Pluto–Charon density contrast". In: *Icarus* 309.2, pp. 207–219. DOI: 10.1016/j.icarus.2018.03.007.

Bierson, C. J. and F. Nimmo (2022). "A note on the possibility of subsurface oceans on the Uranian satellites". In: *Icarus* 373.1, p. 114776. DOI: 10.1016/j.icarus.2021.114776.

Bills, B. G. and A. I. Ermakov (2019). "Simple models of error spectra for planetary gravitational potentials as obtained from a variety of measurement configurations". In: *Planet. Space Sci.* 179, p. 104744. DOI: 10.1016/j.pss.2019.104744.

Bills, B. G. et al. (2020). "Gravitational signatures of atmospheric thermal tides on Venus". In: *Icarus* 340, p. 113568. DOI: 10.1016/j.icarus.2019.113568.

Bland, M. T. and C. M. Elder (2022). "Silicate volcanism on Europa's seafloor and implications for habitability". In: *Geophys. Res. Lett.* 49, e2021GL096939. DOI: 10.1029/2021gl096939.

Blankenship, D. D. et al. (2009). "Radar sounding of Europa's subsurface properties and processes: The view from Earth". In: *Europa* 631, pp. 631–654. DOI: 10.2307/j.ctt1xp3wdw.33.

Bottke, W. F. and J. C. Andrews-Hanna (2017). "A post-accretionary lull in large impacts on early Mars". In: *Nature Geosci.* 10, pp. 344–348. DOI: 10.1038/ngeo2937.

Bouffard, M. et al. (2017). "A particle-in-cell method for studying double-diffusive convection in the liquid layers of planetary interiors". In: *J. Comput. Phys.* 346, pp. 552–571. DOI: 10.1016/j.jcp.2017.06.028.

Bramson, A. M. et al. (2015). "Widespread excess ice in Arcadia Planitia Mars". In: *Geophys. Res. Lett.* 42, pp. 6566–6574. DOI: 10.1002/2015gl064844.

Bramson, A. M., S. Byrne, and J. Bapst (2017). "Preservation of midlatitude ice sheets on Mars". In: *J. Geophys. Res. Planets* 122, pp. 2250–2266. DOI: 10.1002/2017je005357.

Bramson, A. M. et al. (2019). "A migration model for the polar spiral troughs of Mars". In: *J. Geophys. Res. Planets* 124, pp. 1020–1043. DOI: 10.1029/2018je005806.

Broquet, A. and M. A. Wieczorek (2019). "The gravitational signature of Martian volcanoes". In: *J. Geophys. Res. Planets* 124, pp. 2054–2086. DOI: 10.1029/2019je005959.

Broquet, A., M. A. Wieczorek, and W. Fa (2020). "Flexure of the lithosphere beneath the north polar cap of Mars: Implications for ice composition and heat flow". In: *Geophys. Res. Lett.* 47, e2019GL086746. DOI: 10.1029/2019gl086746.

Buhler, P. B. et al. (2020). "Coevolution of Mars's atmosphere and massive south polar CO_2 ice deposit". In: *Nature Astron.* 4, pp. 364–371. DOI: 10.1002/essoar.10512516.1.

Čadek, O. et al. (2019). "Long-term stability of Enceladus' uneven ice shell". In: *Icarus* 319, pp. 476–484. DOI: 10.1016/j.icarus.2018.10.003.

Campbell, B. A. and G. A. Morgan (2018). "Fine-scale layering of Mars polar deposits and signatures of ice content in nonpolar material from multiband SHARAD data processing". In: *Geophys. Res. Lett.* 45, pp. 1759–1766. DOI: 10.1002/2017gl075844.

Carnahan, E. et al. (2021). "New insights into temperature-dependent ice properties and their effect on ice shell convection for icy Ocean Worlds". In: *Earth Planet. Sci. Lett.* 563, p. 116886. DOI: 10.1016/j.epsl.2021.116886.

Carpenter, R. L. (1964). "Study of Venus by CW radar". In: *Astronom. J.* 69, pp. 2–11. DOI: 10.1086/109872.

Carr, M. H. and J. W. III Head (2010). "Geologic history of Mars". In: *Earth Planet. Sci. Lett.* 294, pp. 185–203. DOI: 10.1016/j.epsl.2009.06.042.

Cascioli, G. et al. (2021). "The determination of the rotational state and interior structure of Venus with VERITAS". In: *Planet. Sci. J.* 2, p. 220. DOI: 10.1002/essoar.10506298.1.

Castillo-Rogez, J. C. and J. I. Lunine (2010). "Evolution of Titan's rocky core constrained by Cassini observations". In: *Geophys. Res. Lett.* 37, p. L20205. DOI: 10.1029/2010gl044398.

Castillo-Rogez, J. C. et al. (2022). "Concepts for the future exploration of dwarf planet Ceres' habitability". In: *Planet. Sci. J.* 3, p. 41. DOI: 10.3847/psj/ac34ee.

Chaffee, T. M. and S. M. Tikoo (2021). "Size thresholds for unidirectional remanence within lunar magnetic anomalies". In: *Lunar Planet. Sci. Conf.* 52nd, p. 2548.

Chen, E. M. A., F. Nimmo, and G. A. Glatzmaier (2014). "Tidal heating in icy satellite oceans". In: *Icarus* 229, pp. 11–30. DOI: 10.1016/j.icarus.2013.10.024.

Choblet, G. et al. (2017). "Powering prolonged hydrothermal activity inside Enceladus". In: *Nature Astron.* 1, pp. 841–847. DOI: 10.1038/s41550-017-0289-8.

Citron, R. I., M. Manga, and E. Tan (2018). "A hybrid origin of the Martian crustal dichotomy: Degree-1 convection antipodal to a giant impact". In: *Earth Planet. Sci. Lett.* 491, pp. 58–66. DOI: 10.1016/j.epsl.2018.03.031.

Citron, R. I. (2021). "Forging the Mars crustal dichotomy: the giant impact hypothesis". In: *Mars Geological Enigmas*. Chap. 16, pp. 475–498. DOI: 10.1016/b978-0-12-820245-6.00016-1.

Citron, R. I. and J. H. Roberts (2021). "Hemispheres together: Toward understanding the crustal dichotomy on Mars". In: *Mars Geological Enigmas*, pp. 473–474. DOI: 10.1016/B978-0-12-820245-6.00024-0.

Cochrane, C. J. et al. (2021). "In Search of Subsurface Oceans within the Uranian Moons". In: *J. Geophys. Res. Planets* 126, e2021JE006956. DOI: 10.1029/2021je006956.

Collins, G. C. et al. (2022). "Episodic Plate Tectonics on Europa: Evidence for Widespread Patches of Mobile?lid Behavior in the Antijovian Hemisphere". In: *J. Geophys. Res. Planets* 127, e2022JE007492. DOI: 0.1002/essoar.10511967.1.

Connerney, J. E. P. et al. (1999). "Magnetic lineations in the ancient crust of Mars". In: *Science* 284, pp. 794–798. DOI: 10.1126/science.284.5415.794.

Corlies, P. et al. (2017). "Titan's topography and shape at the end of the Cassini mission". In: *Geophys. Res. Lett.* 44, pp. 11754–11761. DOI: 10.1002/2017gl075518.

Correia, A. C .M. and J. Laskar (2001). "The four final rotation states of Venus". In: *Nature* 411, pp. 767–770. DOI: 10.1038/35081000.

Cruikshank, D. P. et al. (2019). "Recent cryovolcanism in virgil fossae on Pluto". In: *Icarus* 330, pp. 155–168. DOI: 10.1016/j.icarus.2019.04.023.

Culberg, R., D. M. Schroeder, and G. Steinbrügge (2022). "Double ridge formation over shallow water sills on Jupiter's moon Europa". In: *Nature Comm.* 13, pp. 1–10. DOI: 10.1038/s41467-022-29458-3.

Cutts, J. A. and B. H. Lewis (1982). "Models of climate cycles recorded in the Martian polar layered deposits". In: *Icarus* 50, pp. 216–244. DOI: 10.1016/0019-1035(82)90124-5.

Dapremont, A. M. and J. J. Wray (2021). "Igneous or mud volcanism on Mars? The case study of Hephaestus Fossae". In: *J. Geophys. Res. Planets* 126, e2020JE006390. DOI: 10.1029/2020je006390.

Degruyter, W. and M. Manga (2011). "Cryoclastic origin of particles on the surface of Enceladus". In: *Geophys. Res. Lett.* 38, p. L16201. DOI: 10.1029/2011gl048235.

Ding, M. et al. (2019). "Variations in Martian lithospheric strength based on gravity/topography analysis". In: *J. Geophys. Res. Planets* 124, pp. 3095–3118. DOI: 10.1029/2019je005937.

Dobrovolskis, A. R. and A. P. Ingersoll (1980). "Atmospheric tides and the rotation of Venus I. Tidal theory and the balance of torques". In: *Icarus* 41, pp. 1–17. DOI: 10.1016/0019-1035(80)90156-6.

Dombard, A. J. and A. M. Sessa (2019). "Gravity measurements are key in addressing the habitability of a subsurface ocean in Jupiter's moon Europa". In: *Icarus* 325, pp. 31–38. DOI: 10.1016/j.icarus.2019.02.025.

Dransfield, M. and Y. Zeng (2009). "Airborne gravity gradiometry: Terrain corrections and elevation error". In: *Geophysics* 74, pp. I37–I42. DOI: 10.1190/1.3170688.

Dumoulin, C. et al. (2017). "Tidal constraints on the interior of Venus". In: *J. Geophys. Res. Planets* 122, pp. 1338–1352. DOI: 10.1002/2016je005249.

Dundas, C. M. et al. (2018). "Future Mars exploration: The present is the key to the past". In: *MEPAG meeting*.

Dundas, C. M. et al. (2019). "Active boulder movement at high Martian latitudes". In: *Geophys. Res. Lett.* 46, pp. 5075–5082. DOI: 10.1029/2019gl082293.

Durante, D. et al. (2019). "Titan's gravity field and interior structure after Cassini". In: *Icarus* 326, pp. 123–132. DOI: 10.1016/j.icarus.2019.03.003.

Elkins-Tanton, L. T., P. C. Hess, and E. M. Parmentier (2005). "Possible formation of ancient crust on Mars through magma ocean processes". In: *J. Geophys. Res. Planets* 110, E12S01. DOI: 10.1029/2005je002480.

Ermakov, A. I. et al. (2021). "A recipe for the geophysical exploration of Enceladus". In: *Planet. Sci. J.* 2, p. 157. DOI: 10.3847/25c2cfeb.b65f2c4c.

Findley, W. N., J. S. Lai, and K. Onaran (1976). *Creep and relaxation of nonlinear viscoelastic materials with an introduction to linear viscoelasticity*. Dover, New York. DOI: 10.1115/1.3424077.

Folkner, W. M. et al. (2018). "The rotation and interior structure experiment on the InSight mission to Mars". In: *Space Sci. Rev.* 214.1-4, p. 100. DOI: 10.1007/s11214-018-0581-3.

Forsberg, R. and A. V. Olesen (2010). "Airborne gravity field determination". In: *Sciences of geodesy-I*. Springer, Berlin, Heidelberg, pp. 83–104. DOI: 10.1007/978-3-642-11741-1_3.

Frey, H. and R.A. Schultz (1988). "Large impact basins and the mega-impact origin for the crustal dichotomy on Mars". In: *Geophys. Res. Lett.* 15, pp. 229–232. DOI: 10.1029/gl015i003p00229.

Garcia, R. F. et al. (2021). "An active source seismo-acoustic experiment using tethered balloons to validate instrument concepts and modelling tools for atmospheric seismology". In: *Geophys. J. International* 225, pp. 186–199. DOI: 10.1093/gji/ggaa589.

Genova, A. et al. (2016). "Seasonal and static gravity field of Mars from MGS, Mars Odyssey and MRO radio science". In: *Icarus* 272, pp. 228–245. DOI: 10.1016/j.icarus.2016.02.050.

Genova, A. et al. (2018). "Solar system expansion and strong equivalence principle as seen by the NASA MESSENGER mission". In: *Nature Comm.* 9, p. 289. DOI: 10.1038/s41467-017-02558-1.

Giardini, D. et al. (2020). "The seismicity of Mars". In: *Nature Geosci.* 13, pp. 205–212. DOI: 10.1038/s41561-020-0539-8.

Gilmore, M. S. et al. (1998). "Style and sequence of extensional structures in tessera terrain, Venus". In: *J. Geophys. Res.* 103, pp. 16813–16840. DOI: 0.1029/98JE01322.

Gissinger, C. and L. Petitdemange (2019). "A magnetically driven equatorial jet in Europa's ocean". In: *Nature Astron.* 3, pp. 401–407. DOI: 10.1038/s41550-019-0713-3.

Glein, C. R. et al. (2018). "The geochemistry of Enceladus: Composition and controls". In: *Enceladus and the icy moons of Saturn*. The University of Arizona Press. DOI: 10.2458/azu_uapress_9780816537075-ch003.

Goff, J. A., S. Zahirovic, and D. Müller (2018). "No evidence for Milankovitch cycles influence on abyssal hills at intermediate, fast, and superfast spreading rates". In: *Geophys. Res. Lett.* 45, pp. 10305–10313. DOI: 10.1029/2018gl079400.

Gold, T. and S. Soter (1969). "Atmospheric tides and the resonant rotation of Venus". In: *Icarus* 11, pp. 356–366. DOI: 10.1016/0019-1035(69)90068-2.

Goldsby, D. L. and D. L. Kohlstedt (2001). "Superplastic deformation of ice: Experimental observations". In: *J. Geophys. Res. Solid Earth* 106, pp. 11017–11030. DOI: 10.1029/2000jb900336.

Gomez Casajus, L. et al. (2021). "Updated Europa gravity field and interior structure from a reanalysis of Galileo tracking data". In: *Icarus* 358, p. 114187. DOI: 10.1016/j.icarus.2020.114187.

Gong, S. and M. A. Wieczorek (2020). "Is the lunar magnetic field correlated with gravity or topography?" In: *J. Geophys. Res. Planets* 125, e2019JE006274. DOI: 10.1029/2019je006274.

Goossens, S. et al. (2017). "Evidence for a low bulk crustal density for Mars from gravity and topography". In: *Geophys. Res. Lett.* 44, pp. 7686–7694. DOI: 10.1002/2017gl074172.

Greybush, S. J., H. E. Gillespie, and R. J. Wilson (2019). "Transient eddies in the TES/MCS Ensemble Mars Atmosphere Reanalysis System (EMARS)". In: *Icarus* 317, pp. 158–181. DOI: 10.1016/j.icarus.2018.07.001.

Griggs, C. E. et al. (2017). "Sensitive superconducting gravity gradiometer constructed with levitated test masses". In: *Physical Review Applied* 8, p. 064024. DOI: 10.1103/physrevapplied.8.064024.

Gülcher, A. J. P. et al. (2020). "Corona structures driven by plume-lithosphere interactions and evidence for ongoing plume activity on Venus". In: *Nature Geosci.* 13, pp. 547–554. DOI: 10.31223/x5jk88.

Haberle, R. M. et al. (2008). "The evolution of the Martian atmosphere: A reviewThe effect of ground ice on the Martian seasonal CO_2 cycle". In: *Planet. Space Sci.* 56, pp. 251–255. DOI: 10.1016/j.pss.2007.08.006.

Hammond, N. P., A. C. Barr, and E. M. Parmentier (2016). "Recent tectonic activity on Pluto driven by phase changes in the ice shell". In: *Geophys. Res. Lett.* 43, pp. 6775–6782. DOI: 10.1002/2016gl069220.

Hay, H. C. F. C. and I. Matsuyama (2017). "Numerically modelling tidal dissipation with bottom drag in the oceans of Titan and Enceladus". In: *Icarus* 281, pp. 342–356. DOI: 10.1016/j.icarus.2016.09.022.

Hay, H. C. F. C. and I. Matsuyama (2019). "Nonlinear tidal dissipation in the subsurface oceans of Enceladus and other icy satellites". In: *Icarus* 319, pp. 68–85. DOI: 10.1016/j.icarus.2018.09.019.

Hays, J. D., J. Imbrie, and N. J. Shackleton (1976). "Variations in the Earth's orbit: Pacemaker of the ice ages". In: *Science* 194, pp. 1121–1132. DOI: 10.1126/science.198.4316.528.b.

Head, J. W. et al. (2003). "Recent ice ages on Mars". In: *Nature* 426, pp. 797–802. DOI: 10.1038/nature02114.

Hemingway, D. J. et al. (2018). "The Interior of Enceladus". In: *Enceladus and the Icy Moons of Saturn*. Ed. by P.M. Schenk et al., pp. 219–244. DOI: 10.2458/azu_uapress_9780816537075-ch004.

Hemingway, D. J. and T. Mittal (2019). "Enceladus's ice shell structure as a window on internal heat production". In: *Icarus* 332, pp. 111–131. DOI: 10.1016/j.icarus.2019.03.011.

Hemingway, D. J., M. L. Rudolph, and M. Manga (2020). "Cascading parallel fractures on Enceladus". In: *Nature Astronomy* 4, pp. 234–239. DOI: 10.1038/s41550-019-0958-x.

Hendrix, A. R. et al. (2019). "The NASA roadmap to Ocean Worlds". In: *Astrobiology* 19, pp. 1–14. DOI: 10.1089/ast.2018.1955.

Hess, S. L. et al. (1980). "The annual cycle of pressure on Mars measured by Viking Landers 1 and 2". In: *Geophys. Res. Lett.* 7, pp. 197–200. DOI: 10.1029/gl007i003p00197.

Hood, L. L. et al. (2010). "Magnetic anomalies near Apollinaris Patera and the Medusa Fossae Formation in Lucas Planum, Mars". In: *Icarus* 208, pp. 118–131. DOI: 10.1016/j.icarus.2010.01.009.

Horvath, D. G. et al. (2021). "Evidence for geologically recent explosive volcanism in Elysium Planitia, Mars". In: *Icarus* 365, p. 114499. DOI: 10.1016/j.icarus.2021.114499.

Howett, C. J. A. et al. (2011a). "High heat flow from Enceladus' south polar region measured using 10–600 cm^{-1} Cassini/CIRS data". In: *J. Geophys. Res. Planets* 116, E03003. DOI: 10.1029/2010je003718.

Howett, C. J. A. et al. (2011b). "High heat flow from Enceladus' south polar region measured using 10-600 cm^{-1} Cassini/CIRS data". In: *Journal of Geophysical Research: Planets* 116, E3003. DOI: 10.1029/2010je003718.

Hsu, H. W. et al. (2015). "Ongoing hydrothermal activities within Enceladus". In: *Nature* 519, pp. 207–210. DOI: 10.1038/nature14262.

Hussmann, H., T. Spohn, and K. Wieczerkowski (2002). "Thermal equilibrium states of Europa's ice shell: Implications for internal ocean thickness and surface heat flow". In: *Icarus* 156, pp. 143–151.

Hussmann, H., F. Sohl, and T. Spohn (2006). "Subsurface oceans and deep interiors of medium-sized outer planet satellites and large trans-neptunian objects". In: *Icarus* 185, pp. 258–273. DOI: 10.1016/j.icarus.2006.06.005.

Hvidberg, C. S. et al. (2012). "Reading the climate record of the Marian polar layered deposits". In: *Icarus* 221, pp. 405–419. DOI: 10.1016/j.icarus.2012.08.009.

Iess, L. et al. (2012). "The Tides of Titan". In: *Science* 337, pp. 457–459. DOI: 10.1126/science.1219631.

Iess, L. et al. (2014). "The Gravity Field and Interior Structure of Enceladus". In: *Science* 344, pp. 78–80. DOI: 10.1126/science.1250551.

Iess, L. et al. (2018). "Measurement of Jupiter's asymmetric gravity field". In: *Nature* 555, pp. 220–222. DOI: 10.1038/nature25776.

Ingersoll, A. P. and M. Nakajima (2016). "Controlled boiling on Enceladus. 2. Model of the liquid-filled cracks". In: *Icarus* 272, pp. 319–326. DOI: 10.1016/j.icarus.2015.12.040.

Izquierdo, K. et al. (2022). "Mass balance of Martian polar ice from Bayesian fit to trough migration paths". In: *Lunar Planet. Sci. Conf.* 53, p. 1706.

Jackson, I., U. H. Faul, and R. Skelton (2014). "Elastically accommodated grain-boundary sliding: New insights from experiment and modeling". In: *Physics of the Earth and Planetary Interiors* 228, pp. 203–210. DOI: 10.1016/j.pepi.2013.11.014.

Jakosky, B. M., B. G. Henderson, and M. T. Mellon (1995). "Chaotic obliquity and the nature of the Martian climate". In: *J. Geophys. Res.* 100, pp. 1579–1584. DOI: 10.1029/94je02801.

Jakosky, B. M. et al. (2018). "Loss of the Martian atmosphere to space: Present-day loss rates determined from MAVEN observations and integrated loss through time". In: *Icarus* 315, pp. 146–157. DOI: 10.1016/j.icarus.2018.05.030.

Johnson, B. C. et al. (2016). "Formation of the Orientale lunar multiring basin". In: *Science* 354, pp. 441–444. DOI: 10.1126/science.aag0518.

Johnson, B. C. et al. (2017). "Porosity and salt content determine if subduction can occur in Europa's ice shell". In: *J. Geophys. Res. Planets* 122, pp. 2765–2778. DOI: 10.1002/2017je005370.

Johnson, C. L. et al. (2020). "Crustal and time-varying magnetic fields at the InSight landing site on Mars". In: *Nature Geosci.* 13, pp. 199–204. DOI: 10.1038/s41561-020-0537-x.

Johnston, S. A. and L. G. J. Montési (2014). "Formation of ridges on Europa above crystallizing water bodies inside the ice shell". In: *Icarus* 237, pp. 190–201. DOI: 10.1016/j.icarus.2014.04.026.

Journaux, B. et al. (2020). "Large Ocean Worlds with high-pressure ices". In: *Space Science Reviews* 216, pp. 1–36. DOI: 10.1007/s11214-019-0633-7.

Kahre, M. A. et al. (2017). "The Mars dust cycle". In: pp. 295–337. DOI: 10.1017/9781139060172.010.

Kalousová, K. and C. Sotin (2018). "Melting in high-pressure ice layers of large ocean worlds - implications for volatiles transport". In: *Geophysical Research Letters* 45, pp. 8096–8103. DOI: 10.1029/2018gl078889.

Kalousová, K. and C. Sotin (2020). "Dynamics of Titan's high-pressure ice layer". In: *Earth and Planetary Science Letters* 545, p. 116416. DOI: 10.5194/epsc2020-82.

Kamata, S. et al. (2019). "Pluto's ocean is capped and insulated by gas hydrates". In: *Nature Geosci.* 12, pp. 407–410. DOI: 10.1038/s41561-019-0369-8.

Kang, W. et al. (2022). "How does salinity shape ocean circulation and ice geometry on Enceladus and other icy satellites?" In: *Science Advances* 8, eabm4665. DOI: 10.21203/rs.3.rs-143806/v1.

Kaspi, Y. et al. (2018). "Jupiter's atmospheric jet streams extend thousands of kilometres deep". In: *Nature* 555, pp. 223–226. DOI: 10.1038/nature25793.

Kattenhorn, S. A. and T. Hurford (2009). "Tectonics of Europa". In: *Europa*. Springer, pp. 199–236. DOI: 10.2307/j.ctt1xp3wdw.15.

Kattenhorn, S. A. and L. M. Prockter (2014). "Evidence for subduction in the ice shell of Europa". In: *Nature Geosci.* 7, pp. 762–767. DOI: 10.1038/ngeo2245.

Keane, J. T. et al. (2016). "Reorientation and faulting of Pluto due to volatile loading within Sputnik Planitia". In: *Nature* 540, pp. 90–93. DOI: 10.1038/nature20120.

Khan, S. A. et al. (2008). "Geodetic measurements of postglacial adjustments in Greenland". In: *J. Geophys. Res. Solid Earth* 113, B02402. DOI: 10.1029/2007JB004956.

Khan, A. et al. (2021). "Upper mantle structure of Mars from InSight seismic data". In: *Science* 373, pp. 434–438. DOI: 10.1126/science.abf296.

Khawja, S. et al. (2020). "Tesserae on Venus may preserve evidence of fluvial erosion". In: *Nature Communications* 11, p. 5789. DOI: 10.1038/s41467-020-19336-1.

Khurana, K. K. et al. (2009). "Electromagnetic Induction from Europa's Ocean and the Deep Interior". In: *Europa*, pp. 571–586. DOI: 10.2307/j.ctt1xp3wdw.30.

Kiefer, W. S. and Q. Li (2009). "Mantle convection controls the observed lateral variations in lithospheric thickness on present-day Mars". In: *Geophys. Res. Lett.* 36, p. L18203. DOI: 10.1029/2009gl039827.

King, S.D. (2018). "Venus resurfacing constrained by geoid and topography". In: *J. Geophys. Res. Planets* 123, pp. 1041–1060. DOI: 10.1002/2017je005475.

Kite, E. S. and A. M. Rubin (2016). "Sustained eruptions on Enceladus explained by turbulent dissipation in tiger stripes". In: *Proc. Natl. Acad. Sci.* 113, p. 201520507. DOI: 10.1073/pnas.1520507113.

Kivelson, M. G. et al. (2000). "Galileo magnetometer measurements: A stronger case for a subsurface ocean at Europa". In: *Science* 289, pp. 1340–1343. DOI: 10.1126/science.289.5483.1340.

Klipstein, W. M. et al. (2013). "The lunar gravity ranging system for the Gravity Recovery and Interior Laboratory (GRAIL) mission". In: *Space Sci. Rev.* 178, pp. 57–76. DOI: 10.1007/978-1-4614-9584-0_4.

Knapmeyer-Endrun, B. et al. (2021). "Thickness and structure of the martian crust from InSight seismic data". In: *Science* 373, pp. 438–443. DOI: 10.1126/science.abf8966f.

Koh, Z. W. et al. (2022). "Assessing the detectability of Europa's seafloor topography from Europa Clipper's gravity data". In: *Planet. Sci. J.* 3.1, p. 197. DOI: doi.org/10.3847/ps j/ac82aa.

Konopliv, A. S. and C. F. Yoder (1996). "Venusian k_2 tidal Love number from Magellan and PVO tracking data". In: *Geophys. Res. Lett.* 23.23, pp. 1857–1860. DOI: 10.1029/96gl01 589.

Konopliv, A. S., W. B. Banerdt, and W. L. Sjogren (1999). "Venus gravity: 180th degree and order model". In: *Icarus* 139.1, pp. 3–18. DOI: 10.1006/icar.1999.6086.

Konopliv, A. S. et al. (2011). "Mars high resolution gravity fields from MRO, Mars seasonal gravity, and other dynamical parameters". In: *Icarus* 211.2, pp. 401–428. DOI: 10.1016/j .icarus.2010.10.004.

Konopliv, A. S. et al. (2020). "Detection of the Chandler wobble of Mars from orbiting spacecraft". In: *Geophys. Res. Lett.* 47.10, e2020GL090568.

Kornfeld, R. P. et al. (2019). "GRACE-FO: The gravity recovery and climate experiment follow-on mission". In: *J. Spacecraft and Rockets* 56.4, pp. 931–951. DOI: 10.2514/1.A34326.

Krishnamoorthy, S. et al. (2019). "Aerial seismology using balloon-based barometers". In: *IEEE Trans. Geosci. Remote Sensing* 57.12, pp. 10191–10201. DOI: 10.1109/tgrs.2019 .2931831.

Kvorka, J. et al. (2018). "Does Titan's long-wavelength topography contain information about subsurface ocean dynamics?" In: *Icarus* 310, pp. 149–164. DOI: 10.1016/j.icarus.2017 .12.010.

Kvorka, J. and O. Čadek (2022). "A numerical model of convective heat transfer in Titan's subsurface ocean". In: *Icarus* 376, p. 114853. DOI: 10.1016/j.icarus.2021.114853.

Lainey, V. et al. (2009). "Strong tidal dissipation in Io and Jupiter from astrometric observations". In: *Nature* 459, pp. 957–959. DOI: /10.1038/nature08108.

Langevin, Y. et al. (2005). "Summer evolution of the north polar cap of Mars as observed by OMEGA/Mars Express". In: *Science* 307, pp. 1581–1584. DOI: 10.1126/science.110943 8.

Laskar, J. et al. (2004). "Long term evolution and chaotic diffusion of the insolation quantities of Mars". In: *Icarus* 170, pp. 343–364. DOI: 10.1016/j.icarus.2004.04.005.

Lau, H. C. P. et al. (2017). "Tidal tomography constrains Earth's deep-mantle buoyancy". In: *Nature* 551, pp. 321–326. DOI: 10.1038/nature24452.

Lemasquerier, D. et al. (2017). "Libration?driven flows in ellipsoidal shells". In: *J. Geophys. Res. Planets* 122, pp. 1926–1950. DOI: 10.1002/2017je005340.

Lemoine, F. G. et al. (2001). "An improved solution of the gravity field of Mars (GMM-2b) from Mars Global Surveyor". In: *J. Geophys. Res. Planets* 106, pp. 23359–23376. DOI: 10.1029/2000je001426.

Levrard, B. et al. (2004). "Recent ice-rich deposits formed at high-latitudes on Mars by sublimation of unstable equatorial ice during low obliquity". In: *Nature* 431.7012, pp. 1072–1075. DOI: 10.1038/nature03055.

Levrard, B. et al. (2007). "Recent formation and evolution of northern Martian polar layered deposits as inferred from a global climate model". In: *Journal of Geophysical Research: Planets* 112.E6, E06012. DOI: 10.1029/2006je002772.

Levy, J., J. W. Head, and D. R. Marchant (2010). "Concentric crater fill in the northern mid-latitudes of Mars: Formation processes and relationships to similar landforms of glacial origin". In: *Icarus* 207.2, pp. 390–404. DOI: 10.1016/j.icarus.2010.03.036.

Lewis, E. and R. Perkin (1986). "Ice pumps and their rates". In: *Journal of Geophysical Research: Oceans* 91.C7, pp. 11756–11762. DOI: 10.1029/jc091ic10p11756.

Lewis, K. W. et al. (2007). "Quasi-periodic bedding in the sedimentary rock record of Mars". In: *Science* 322.5907, pp. 1532–1535. DOI: 10.1126/science.1161870.

Lewis, K. W. et al. (2019). "A surface gravity traverse on Mars indicates low bedrock density at Gale crater". In: *Science* 363.6428, pp. 535–537. DOI: 10.1126/science.aau3683.

Liao, Y., F. Nimmo, and J. A. Neufeld (2020). "Heat production and tidally driven fluid flow in the permeable core of Enceladus". In: *J. Geophys. Res. Planets* 125.3, e2019JE006209. DOI: 10.1029/2019JE006209.

Lillis, R. J. et al. (2006). "Unusual magnetic signature of the Hadriaca Patera volcano: Implications for early Mars". In: *Geophys. Res. Lett.* 33.3, p. L03202. DOI: 10.1029/2005 GL024242.

Liu, H.-S. (1992). "Frequency variations of the Earth's obliquity and the 100-kyr ice-age cycles". In: *Nature* 358.6385, pp. 397–399. DOI: 10.1038/358397a0.

Liu, L. et al. (2013). "Surface motion of active rock glaciers in the Sierra Nevada, California, USA: Inventory and a case study using InSAR". In: *The Cryosphere* 7.4, pp. 1109–1119. DOI: 10.5194/tc-7-1109-2013.

Lobo, A. H. et al. (2021). "A pole-to-equator ocean overturning circulation on Enceladus". In: *Nature Geosci.* 14, pp. 185–189. DOI: 10.1038/s41561-021-00706-8.

Madeleine, J.-B. et al. (2009). "Amazonian northern mid-latitude glaciation on Mars: A proposed climate scenario". In: *Icarus* 203.2, pp. 390–405. DOI: 10.1016/j.icarus.2009.01.019.

Malamud, U. and D. Prialnik (2016). "A 1-D evolutionary model for icy satellites, applied to Enceladus". In: *Icarus* 268, pp. 1–11. DOI: 10.1016/j.icarus.2015.12.045.

Manga, M. and C. Michaut (2017). "Formation of lenticulae on Europa by saucer-shaped sills". In: *Icarus* 286, pp. 261–269. DOI: 10.1016/j.icarus.2016.10.009.

Marinova, M. M., O. Aharonson, and E. Asphaug (2008). "Mega-impact formation of the Mars hemispheric dichotomy". In: *Nature* 453, pp. 1216–1219. DOI: 10.1038/nature07070.

Matsuyama, I. et al. (2016). "GRAIL, LLR, and LOLA constraints on the interior structure of the Moon". In: *Geophysical Research Letters* 43, pp. 8365–8375. DOI: 10.1002/2016gl069952.

Matsuyama, I. et al. (2018). "Ocean tidal heating in icy satellites with solid shells". In: *Icarus* 312, pp. 208–230. DOI: 10.1016/j.icarus.2018.04.01.

McCarthy, C. and R. F. Cooper (2016). "Tidal dissipation in creeping ice and the thermal evolution of Europa". In: *Earth and Planetary Science Letters* 443, pp. 185–194. DOI: 10.1016/j.epsl.2016.03.006.

McEwen, A. S. et al. (2007). "Mars Reconnaissance Orbiter's High Resolution Imaging Science Experiment (HiRISE)". In: *Journal of Geophysical Research: Planets* 112.E5. DOI: 10.1029/2005je002605.

McGovern, P. J. et al. (2002). "Localized gravity/topography admittance and correlation spectra on Mars: Implications for regional and global evolution". In: *Journal of Geophysical Research: Planets* 107.E12. DOI: 10.1029/2002je001854.

McKinnon, W. B. (2013). "The shape of Enceladus as explained by an irregular core: Implications for gravity, libration, and survival of its subsurface ocean". In: *J. Geophys. Res. Planets* 118, pp. 1775–1788. DOI: 10.1002/jgre.20122.

Melosh, H. J. et al. (2004). "The temperature of Europa's subsurface water ocean". In: *Icarus* 168, pp. 498–502. DOI: 10.1016/j.icarus.2003.11.026.

Meyer, J. and J. Wisdom (2007). "Tidal heating in Enceladus". In: *Icarus* 188, pp. 535–539. DOI: 10.1016/j.icarus.2007.03.001.

Mittelholz, A. et al. (2020). "Timing of the Martian dynamo: New constraints for a core field 4.5 and 3.7 Ga ago". In: *Sci. Adv.* 6, eaba0513. DOI: 10.1126/sciadv.aba0513.

Moore, W. B. and G. Schubert (2003). "The tidal response of Ganymede and Callisto with and without liquid water oceans". In: *Icarus* 166, pp. 223–226. DOI: 10.1016/j.icarus.2003.07.001.

Morgan, G. A. et al. (2021). "Availability of subsurface water-ice resources in the northern mid-latitudes of Mars". In: *Nature Astro.* 5, pp. 230–236. DOI: 10.1038/s41550-020-01290-z.

Nakajima, M. and A. P. Ingersoll (2016). "Controlled boiling on Enceladus. 1. Model of the vapor-driven jets". In: *Icarus* 272, pp. 309–318. DOI: 10.1016/j.icarus.2016.02.027.

Navarro, T. et al. (2014). "Global Climate Modeling of the Martian water cycle with improved microphysics and radiatively active water ice clouds". In: *J. Geophys. Res. Planets* 119, pp. 1479–1495. DOI: 10.1002/2013je004550.

Navarro, T. et al. (2017). "The challenge of atmospheric data assimilation on Mars". In: *Earth Space Sci.* 4, pp. 690–722. DOI: 10.1002/2017ea000274.

Nerozzi, S. and J. W. Holt (2019). "Buried ice and sand caps at the north pole of Mars: Revealing a record of climate change in the cavi unit with SHARAD". In: *Geophys. Res. Lett.* 46, pp. 7278–7286. DOI: 10.1029/2019gl082114.

Neumann, G. A. et al. (2015). "Lunar impact basins revealed by Gravity Recovery and Interior Laboratory measurements". In: *Science Adv.* 1, e1200852. DOI: 10.1126/sciadv.1500852.

Neveu, M., S. J. Desch, and J. C. Castillo-Rogez (2017). "Aqueous geochemistry in icy world interiors: Equilibrium fluid, rock, and gas compositions, and fate of antifreezes and radionuclides". In: *Geochimica et Cosmochimica Acta* 212, pp. 324–371. DOI: 10.1016/j.gca.2017.06.023.

Newman, C. E., S. R. Lewis, and P. L. Read (2005). "The atmospheric circulation and dust activity in different orbital epochs on Mars". In: *Icarus* 174, pp. 135–160. DOI: 10.1016/j.icarus.2004.10.023.

Nimmo, F. (2002). "Why does Venus lack a magnetic field?" In: *Geology* 30, pp. 987–990. DOI: 10.1130/0091-7613(2002)030<0987:wdvlam>2.0.co;2.

Nimmo, F. et al. (2007). "Shear heating as the origin of the plumes and heat flux on Enceladus". In: *Nature* 447, pp. 289–291. DOI: 10.1038/nature05783.

Nimmo, F. et al. (2008). "Implications of an impact origin for the martian hemispheric dichotomy". In: *Nature* 453, pp. 1220–1223. DOI: 10.1038/nature07025.

Nimmo, F. and B. G. Bills (2010). "Shell thickness variations and the long-wavelength topography of Titan". In: *Icarus* 208, pp. 896–904. DOI: 10.1016/j.icarus.2010.02.020.

Nimmo, F. and R. T. Pappalardo (2016). "Ocean Worlds in the outer solar system". In: *J. Geophys. Res. Planets* 121, pp. 1378–1399. DOI: 10.1002/2016je005081.

O'Rourke, J. G., C. Gillmann, and P. Tackley (2018). "Prospects for an ancient dynamo and modern crustal remanent magnetism on Venus". In: *Earth and Planetary Science Letters* 502, pp. 46–56. DOI: 10.1016/j.epsl.2018.08.055.

Ojha, L. and K. Lewis (2018). "The density of the Medusa Fossae Formation: Implications for its composition, origin, and importance in Martian history". In: *Journal of Geophysical Research: Planets* 123.6, pp. 1368–1379. DOI: 10.1130/abs/2017am-297627.

Ojha, L. et al. (2018). "The Medusa Fossae Formation as the single largest source of dust on Mars". In: *Nature Communications* 9.1, pp. 1–9. DOI: 10.1038/s41467-018-05291-5.

Ojha, L., S. Nerozzi, and K. Lewis (2019). "Composition constraints on the north polar cap of Mars from gravity and topography". In: *Geophysical Research Letters* 46.15, pp. 8671–8679. DOI: 10.1029/2019gl082294.

Ojha, L., E. Mazarico, and S. Goossens (2020). "Is there a crustal thickness dichotomy on Mars?" In: *Lunar and Planetary Science Conference* 51.

Paik, H.-J. et al. (1988). "Global gravity survey by an orbiting gravity gradiometer". In: *EOS Transactions* 69, pp. 1601–1611. DOI: 10.1029/88eo01211.

Panning, M. P. et al. (2018). "Expected seismicity and the seismic noise environment of Europa". In: *Journal of Geophysical Research: Planets* 123.1, pp. 163–179. DOI: 10.1002/2017je005332.

Park, R. S. et al. (2020). "Evidence of non-uniform crust of Ceres from Dawn's high-resolution gravity data". In: *Nature Astron.* 4.8, pp. 748–755. DOI: 10.1038/s41550-020-1019-1.

Patterson, G. W. et al. (2018). "The Geology of Enceladus". In: *Enceladus and the Icy Moons of Saturn*. Ed. by Paul M Schenk et al. University of Arizona Press, pp. 95–125. DOI: 10.2458/azu_uapress_9780816537075-ch006.

Perron, J. T. and P. Huybers (2009). "Is there an orbital signal in the polar layered deposits on Mars?" In: *Geology* 37.2, pp. 155–158. DOI: 10.1130/g25143a.1.

Phillips, R. J. et al. (2008). "Mars north polar deposits: Stratigraphy, age, and geodynamical response". In: *Science* 320.5876, pp. 1182–1185. DOI: 10.1126/science.1157546.

Phillips, R. J. et al. (2011). "Massive CO_2 ice deposits sequestered in the south polar layered deposits of Mars". In: *Science* 332.6025, pp. 838–841. DOI: 10.1126/science.1203091.

Porco, C. C. et al. (2006). "Cassini observes the active south pole of Enceladus". In: *Science* 311.5766, pp. 1393–1401. DOI: 10.1126/science.1123013.

Pritchard, M. E. and M. Simons (2004). "An InSAR-based survey of volcanic deformation in the central Andes". In: *Geochem., Geophys., Geosys.* 5.8. DOI: 10.1029/2003gc000610.

Quesnel, Y. et al. (2009). "Serpentinization of the martian crust during Noachian". In: *Earth and Planetary Science Letters* 277, pp. 184–193. DOI: Serpentinizationofthemartian crustduringNoachia.

Quick, L. C., L. S. Glaze, and S. M. Baloga (2017). "Cryovolcanic emplacement of domes on Europa". In: *Icarus* 284, pp. 477–488. DOI: 10.1016/j.icarus.2016.06.029.

Randolph-Flagg, N. G., T. Mittal, and D. Hemingway (2020). "Tidal pumping and heating of Enceladus's porous core". In: *Ocean Sciences Meeting*, MG24A–2197.

Rathbun, J. A. et al. (2004). "Mapping of Io's thermal radiation by the Galileo photopolarimeter-radiometer (PPR) instrument". In: *Icarus* 169, pp. 127–139. DOI: 10.1016/j.icarus.2003.12.021.

Ravat, D. (2011). "Interpretation of Mars southern highlands high amplitude magnetic field with total gradient and fractal source monitoring: New insights into the magnetic mystery of Mars". In: *Icarus* 214, pp. 400–412. DOI: 10.1016/j.icarus.2011.05.004.

Reese, C. C., C. P. Orth, and V. S. Solomatov (2011). "Impact megadomes and the origin of the Martian crustal dichotomy". In: *Icarus* 213, pp. 433–442. DOI: 10.1016/j.icarus.2011.03.028.

Renaud, J. P. and W. G. Henning (2018). "Increased tidal dissipation using advanced rheological models: Implications for Io and tidally active exoplanets". In: *The Astrophysical Journal* 857.2, p. 98. DOI: 10.3847/1538-4357/aab784.

Roberts, J. H. and F. Nimmo (2008). "Near-surface heating on Enceladus and the south polar thermal anomaly". In: *Geophys. Res. Lett.* 35 (9), p. L09201. DOI: 10.1029/2008gl033725.

Roberts, J. H. (2015). "The fluffy core of Enceladus". In: *Icarus* 258, pp. 54–66. DOI: 10.1016/j.icarus.2015.05.033Action.

Roberts, J. H. (2021). "Endogenic origin of the Martian hemispheric dichotomy". In: *Mars Geological Enigmas*. Chap. 17, pp. 475–498. DOI: 10.1016/b978-0-12-820245-6.00017-3.

Rovira-Navarro, M. et al. (2019). "Do tidally-generated inertial waves heat the subsurface oceans of Europa and Enceladus?" In: *Icarus* 321, pp. 126–140. DOI: 10.1016/j.icarus.2018.11.010.

Rovira-Navarro, M. et al. (2022). "The Tides of Enceladus' porous core". In: *J. Geophys. Res. Planets* 127, e2021JE007117. DOI: 10.1029/2021je007117.

Ruiz, J. (2005). "The heat flow of Europa". In: *Icarus* 177, pp. 438–446. DOI: 10.1016/j.icarus.2005.03.021.

Russell, C. T. et al. (2016). "Dawn arrives at Ceres: Exploration of a small, volatile-rich world". In: *Science* 353, pp. 1008–1010. DOI: 10.1126/science.aaf4219.

Schmidt, B. E. et al. (2011). "Active formation of chaos terrain over shallow subsurface water on Europa". In: *Nature* 479.7374, pp. 502–505. DOI: 10.1038/nature10608.

Schmidt, B. E. (2020). "The astrobiology of Europa and the Jovian System". In: *Planetary Astrobiology*. Springer, pp. 185–215. DOI: 10.2458/azu_uapress_9780816540068-ch008.

Schmitt, R. W (1994). "Double diffusion in oceanography". In: *Annual Review of Fluid Mechanics* 26, pp. 255–285. DOI: 10.1146/annurev.fl.26.010194.001351.

Schubert, G. et al. (1980). "Structure and circulation of the Venus atmosphere". In: *Journal of Geophysical Research: Space Physics* 85.A13, pp. 8007–8025. DOI: 10.1029/JA085iA13p08007.

Schubert, G., F. Sohl, and H. Hussmann (2009). "Interior of Europa". In: *Europa*. University of Arizona Press, p. 353. DOI: 10.2307/j.ctt1xp3wdw.20.

Simons, M. and P. A. Rosen (2015). "Interferometric Synthetic Aperture Radar geodesy". In: *Treatise on Geophysics*. 2nd. Elsevier Press, pp. 339–385. DOI: 10.1016/b978-0444527248-6/00059-6.

Sleep, N. H. (1994). "Martian plate tectonics". In: *Journal of Geophysical Research: Planets* 99.E3, pp. 5639–5655. DOI: 10.1029/94je00216.

Smith, D. E. et al. (2001a). "Mars Orbiter Laser Altimeter: Experiment summary after the first year of global mapping of Mars". In: *Journal of Geophysical Research: Planets* 106.E10, pp. 23689–23722. DOI: 10.1029/2000JE00136.

Smith, D. E., M. T. Zuber, and G. A. Neumann (2001b). "Seasonal variations of snow depth on Mars". In: *Science* 294, pp. 2141–2146. DOI: 10.1126/science.1066556.

Smith, D. E. et al. (2009). "Time variations of Mars' gravitational field and seasonal changes in the masses of the polar caps". In: *J. Geophys. Res.* 114, E05002. DOI: 10.1029/2008je003267.

Smith, D. E. et al. (2017). "Summary of the results from the Lunar Orbiter Laser Altimeter after seven years in lunar orbit". In: *Icarus* 283, pp. 70–91.

Smith, D. E. et al. (2018). "Trilogy, a planetary geodesy mission concept for measuring the expansion of the solar system". In: *Planet. Space Sci.* 153, pp. 127–133. DOI: 10.1016/j.pss.2018.02.003.

Smith, D. E. et al. (2020). "Callisto: A guide to the origin of the Jupiter system". In: *Decadal survey on planetary science and astrobiology 2023–2032 white paper*. DOI: 10.3847/25c2cfeb.8ef223f3.

Smrekar, S. et al. (2022). "VERITAS (Venus Emissivity, Radio Science, InSAR, Topography, and Spectroscopy): A Discovery mission". In: *2022 IEEE Aerospace Conference (AERO)*, pp. 1–20. DOI: 10.5194/epsc2020-447.

Soderblom, J. M. et al. (2015). "The fractured Moon: Production and saturation of porosity in the lunar highlands from impact cratering". In: *Geophysical Research Letters* 42.17, pp. 6939–6944. DOI: 10.1002/2015gl065022.

Soderlund, K. M. et al. (2014). "Ocean-driven heating of Europa's icy shell at low latitudes". In: *Nature Geoscience* 7.1, pp. 16–19. DOI: 10.1038/ngeo2021.

Soderlund, K. M. (2019). "Ocean dynamics of outer solar system satellites". In: *Geophysical Research Letters* 46.15, pp. 8700–8710. DOI: 10.1029/2018gl081880.

Soderlund, K. M. et al. (2020). "Ice-ocean exchange processes in the Jovian and Saturnian satellites". In: *Space Science Reviews* 216.4, p. 80. DOI: 10.1007/s11214-020-00706-6.

Solomatov, V. S. (1995). "Scaling of temperature-and stress-dependent viscosity convection". In: *Physics of Fluids* 7.1, pp. 266–274. DOI: 10.1063/1.868624.

Sori, M. M. et al. (2014). "A procedure for testing the significance of orbital tuning of the Martian polar layered deposits". In: *Icarus* 235, pp. 136–146. DOI: 10.1016/j.icarus.2014.03.009.

Sori, M. M. et al. (2016). "Viscous flow rates of icy topography on the north polar layered deposits of Mars". In: *Geophysical Research Letters* 43.2, pp. 541–549. DOI: 10.1002/2015gl067298.

Sori, M. M. et al. (2018). "Isostatic compensation of the lunar highlands". In: *J. Geophys. Res. Planets* 123.3, pp. 646–665. DOI: 10.1002/2017je005362.

Sori, M. M. et al. (2022). "Orbital forcing of Martian climate revealed in a south polar outlier ice deposit". In: *Geophys. Res. Lett.* 49.4, e2021GL097450. DOI: 10.1029/2021gl097450.

Sotin, C. et al. (2009). "Tides and tidal heating on Europa". In: *Europa*. University of Arizona Press, pp. 85–118. DOI: 10.2307/j.ctt1xp3wdw.10.

Souček, O. et al. (2016). "Effect of the tiger stripes on the deformation of Saturn's moon Enceladus". In: *Geophys. Res. Lett.* 43.14, pp. 7417–7423. DOI: 10.1002/2016gl069415.

Souček, O. et al. (2019). "Tidal dissipation in Enceladus' uneven, fractured ice shell". In: *Icarus* 328, pp. 218–231. DOI: 10.1016/j.icarus.2019.02.012.

Spencer, J. R. and F. Nimmo (2013). "Enceladus: An active ice world in the Saturn system". In: *Annual Review of Earth and Planetary Sciences* 41, pp. 693–717. DOI: 10.1146/annurev-earth-050212-124025.

Spencer, J. R. et al. (2018). "Plume Origins and Plumbing: Ocean to Surface". In: *Enceladus and the Icy Moons of Saturn*. Ed. by P. M. Schenk et al. Tucson, Arizona: University of Arizona Press, pp. 163–174. DOI: 10.2458/azu_uapress_9780816537075-ch008.

Squyres, S. W. et al. (1983). "The evolution of Enceladus". In: *Icarus* 53.2, pp. 319–331. DOI: 10.1016/0019-1035(83)90152-5.

Stähler, S. C. et al. (2021). "Seismic detection of the martian core". In: *Science* 373.6550, pp. 443–448. DOI: 10.5194/egusphere-egu21-13310.

Stähler, S. C. et al. (2022). "Tectonics of Cerberus Fossae unveiled by marsquakes". In: *Nature Astron.* DOI: 10.1038/s41550-022-01803-y.

Stuurman, C. M. et al. (2016). "SHARAD detection and characterization of subsurface water ice deposits in Utopia Planitia, Mars". In: *Geophys. Res. Lett.* 43.18, pp. 9484–9491. DOI: 10.1002/2016gl070138.

Tapley, B. D. et al. (2004). "The gravity recovery and climate experiment: Mission overview and early results". In: *Geophys. Res. Lett.* 31.9, p. L09607. DOI: 10.1029/2004GL019920.

Tapley, B. D. et al. (2019). "Contributions of GRACE to understanding climate change". In: *Nature Climate Change* 9.5, pp. 358–369. DOI: 10.1038/s41558-019-0456-2.

Thomas, P. C. et al. (2016). "Enceladus's measured physical libration requires a global subsurface ocean". In: *Icarus* 264, pp. 37–47. DOI: 10.1016/j.icarus.2015.08.037.

Tobie, G. (2003). "Tidally heated convection: Constraints on Europa's ice shell thickness". In: *Journal of Geophysical Research: Planets* 108.E11, p. 5124. DOI: 10.1029/2003je002099.

Toon, O. B. et al. (1980). "The astronomical theory of climatic change on Mars". In: *Icarus* 44.3, pp. 552–607. DOI: 10.1016/0019-1035(80)90130-x.

Tyler, R. H. (2008). "Strong ocean tidal flow and heating on moons of the outer planets". In: *Nature* 456.7222, pp. 770–772. DOI: 10.1038/nature07571.

Tyler, R. (2011). "Tidal dynamical considerations constrain the state of an ocean on Enceladus". In: *Icarus* 211.1, pp. 770–779. DOI: 10.1016/j.icarus.2010.10.007.

Van der Meijde, M. et al. (2015). "GOCE data, models, and applications: A review". In: *International Journal of Applied Earth Observation and Geoinformation* 35, pp. 4–15. DOI: 10.1016/j.jag.2013.10.001.

Van Hoolst, T., R. M. Baland, and A. Trinh (2013). "On the librations and tides of large icy satellites". In: *Icarus* 226, pp. 299–315. DOI: 10.1016/j.icarus.2013.05.036.

Vance, S. et al. (2007). "Hydrothermal systems in small ocean planets". In: *Astrobiology* 7, pp. 987–1005. DOI: 10.1089/ast.2007.0075.

Vance, S. D. et al. (2018). "Geophysical Investigations of Habitability in Ice-Covered Ocean Worlds". In: *J. Geophys. Res. Planets*, pp. 180–205. DOI: 10.1002/2017je005341.

Vance, S. D. et al. (2021). "Magnetic induction responses of Jupiter's ocean moons including effects from adiabatic convection". In: *J. Geophys. Res. Planets* 126, e2020JE006418. DOI: 10.1002/essoar.10502420.2.

Wagner, N. L. et al. (2022). "Quantifying lithospheric deflection caused by seasonal mass transport from the polar layered deposits on Mars". In: *Lunar Planet. Sci. Conf. 53rd*, p. 2352.

Watters, T. R. et al. (2007a). "Radar sounding of the Medusa Fossae Formation Mars: Equatorial ice or dry, low-density deposits?" In: *Science* 318, pp. 1125–1128. DOI: 10.1126/science.1148112.

Watters, T. R., P. J. McGovern, and R. P. Irwin III (2007b). "Hemispheres apart: The crustal dichotomy on Mars". In: *Ann. Rev. Earth Planet. Sci.* 35, pp. 621–652. DOI: 10.1146/annurev.earth.35.031306.140220.

Watts, A. B. (2001). *Isostasy and flexure of the lithosphere*. Cambridge University Press. DOI: 10.1017/CBO9780511527430.

Weiss, B. P. et al. (2021). "Searching for subsurface oceans on the moons of Uranus using magnetic induction". In: *Geophysical Research Letters* 48.11, e2021GL094758. DOI: 10.1002/essoar.10507412.1.

Wieczorek, M. A. (2008). "Constraints on the composition of the Martian south polar cap from gravity and topography". In: *Icarus* 196.2, pp. 506–517. DOI: 10.1016/j.icarus.2007.10.026.

Wieczorek, M. A. et al. (2013). "The crust of the Moon as seen by GRAIL". In: *Science* 339.6120, pp. 671–675.

Wieczorek, M. A. et al. (2022). "InSight constraints on the global character of the Martian crust". In: *Journal of Geophysical Research: Planets* 127.1, e2022JE007298. DOI: 10.1029 /2022JE00729.

Wilhelms, D. E. and S. W. Squyres (1984). "The Martian hemispheric dichotomy may be due to a giant impact". In: *Nature* 309.5965, pp. 138–140. DOI: 10.1038/309138a0.

Williams, J. G. et al. (1976). "New test of the equivalence principle from lunar laser ranging". In: *Physical review letters* 36.21, pp. 551–554. DOI: 10.1103/PhysRevLett.36.551.

Williams, J. G., S. G. Turyshev, and D. H. Boggs (2004). "Progress in lunar laser ranging tests of relativistic gravity". In: *Physical review letters* 93.26, p. 261101. DOI: 10.1103/ph ysrevlett.93.261101.

Williams, J. G. et al. (2006). "Lunar laser ranging science: Gravitational physics and lunar interior and geodesy". In: *Advances in Space Research* 37, pp. 67–71. DOI: 10.1016/j.as r.2005.05.013.

Williams, J. G., S. G. Turyshev, and D. H. Boggs (2012). "Lunar laser ranging tests of the equivalence principle". In: *Classical and Quantum Gravity* 29.18, p. 184004. DOI: 10.1088/0264-9381/29/18/184004.

Williams, J. G. et al. (2014). "Lunar interior properties from the GRAL mission". In: *Journal of Geophysical Research: Planets* 119.7, pp. 1546–1578. DOI: 10.1002/2013JE004559.

Wolfenbarger, N. S. et al. (2022). "Brine volume fraction as a habitability Metric for Europa's ice shell". In: *Geophysical Research Letters* 49.5, e2022GL100586. DOI: 10.1002/essoar .10512037.2.

Xiao, H. et al. (2022). "Spatio-temporal level variations of the Martian seasonal south polar cap from co-registration of MOLA profiles". In: *Journal of Geophysical Research: Planets* 127.5, e2022JE007196. DOI: 10.1029/2022je007196.

Zeng, Y. and M. F. Jansen (2021). "Ocean circulation on Enceladus with a high- versus low-salinity ocean". In: *Planetary Science Journal* 2.4, p. 151. DOI: 10.3847/psj/ac1114.

Zhong, S. and M. T. Zuber (2001). "Degree-1 mantle convection and the crustal dichotomy on Mars". In: *Earth and Planetary Science Letters* 189.1-2, pp. 75–84. DOI: 10.1016/s00 12-821x(01)00345-4.

Zhong, S. et al. (2012). "Can tidal tomography be used to unravel the long-wavelength structure of the lunar interior?" In: *Geophys. Res. Lett.* 39, p. L15201. DOI: 10.1029/201 2gl052362.

Zhu, P. et al. (2017). "The influence of meridional ice transport on Europa's ocean stratification and heat content". In: *Geophys. Res. Lett.* 44, pp. 5969–5977. DOI: 10.1002/2017gl072996.

Zuber, M. T. (2001). "The crust and mantle of Mars". In: *Nature* 412, pp. 220–227. DOI: 10.1038/35084163.

Zuber, M. T. et al. (2007a). "Mars Reconnaissance Orbiter radio science gravity investigation". In: *J. Geophys. Res.* 112, E05S07. DOI: 10.1029/2006JE002833.

Zuber, M. T. et al. (2007b). "Density of Mars' south polar layered deposits". In: *Science* 317, pp. 1718–1719. DOI: 10.1126/science.1146995.

Zuber, M. T. et al. (2013a). "Gravity field of the Moon from the Gravity Recovery and Interior Laboratory (GRAIL) mission". In: *Science* 339, pp. 668–671. DOI: 10.1126/science.1231507.

Zuber, M. T. et al. (2013b). "Gravity Recovery and Interior Laboratory (GRAIL): Mapping the lunar interior from crust to core". In: *Space Sci. Rev.* 178, pp. 3–24. DOI: 10.1007/978-1-4614-9584-0_2.

Zuber, M. T. et al. (2016). "Gravity field of the Orientale basin from the Gravity Recovery and Interior Laboratory Mission". In: *Science* 354.6311, pp. 438–441. DOI: 10.1126/science.aag0519.
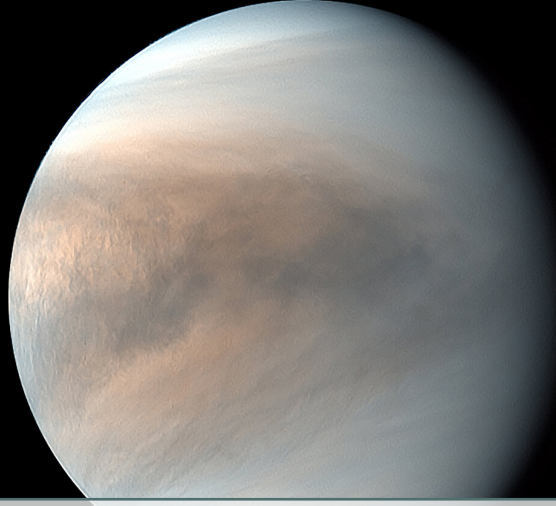
Appendix 1: Glossary of Geodetic Observables

Static Gravity: The gravity field of a planet is most commonly expressed in terms of an expansion in spherical harmonic functions:

$$U\left(\lambda, \phi, r\right) = \frac{GM}{r} \sum_{n=2}^{\infty} \sum_{m=0}^{n} \left[\left(\frac{R_0}{r}\right)^n \left(\bar{C}_{nm} cosm\lambda + \bar{S}_{nm} sinm\lambda\right) \bar{P}_{nm} sin\phi \right] \quad \text{(A1.1)}$$

where U is the gravitational potential, n is the degree, m is order, λ is longitude, ϕ is latitude, r is planetary radius, C_{nm} and S_{nm} are the normalized spherical harmonic coefficients of the gravity field, and R_0 is the reference radius of the gravity field model (which is not necessarily equal to the mean radius of the planet). The variance spectrum V of gravity can be found as follows:

$$V_n^{gg} = \sum_{m=0}^{n} \bar{C}_{nm}^2 + \bar{S}_{nm}^2 \quad \text{(A1.2)}$$

The coefficient Root-Mean-Square (RMS) spectrum M can be found as follows:

$$M_n^{gg} = \left(\frac{v_n^{gg}}{2n+1}\right)^{\frac{1}{2}} \quad \text{(A1.3)}$$

Variance and RMS spectra are used to study how the amplitude of gravity changes as a function of spatial wavelength $\lambda \approx 2\pi R/\sqrt{n(n+1)}$.

Gravity anomalies: Gravity anomalies represent differences between observed gravity and the gravity predicted by some assumed interior model. For the case of the **free-air anomaly**, the modeled gravity is that of a body in hydrostatic equilibrium. Hydrostatic equilibrium is the state in which the gravitational force throughout the body is balanced by the pressure gradient, centrifugal force and the tidal force (for a tidally locked satellite). The **Bouguer anomaly** is the difference between the observed gravity and that of the observed shape assuming the body has a uniform density. In other words, it is the gravity field of a body that removes the predicted gravitational effects of topography. It is sometimes practical to use a version of a Bouguer anomaly for a multilayer body, in which different layers have different uniform densities. This type of Bouguer anomaly represents the differences between the observed gravity and the gravity of the multilayer body where all the internal density interfaces are in hydrostatic equilibrium, and the outer surface is the observed irregular surface. The **isostatic anomaly** is the difference between the observed gravity and that predicted by an isostatic model. It is computed by perturbing the inner density interface to satisfy isostatic equilibrium (e.g., Watts, 2001). In practice, the isostatic equilibrium model relies on assumptions, such as an assumption about crustal density or the mechanism of compensation (e.g., Airy isostasy). Crustal thickness and density maps of a planet are often constructed by minimizing some misfit of the Bouguer or isostatic anomaly.

Gravity gradients: Gravity gradients are second derivatives of gravitational potential or directional derivative of the gravity force. Due to the second differentiation, the gravity gradients are more localized near the source of the anomalies. The standard unit accepted in geodesy is Eotvos (E). One Eotvos is 10^{-9} s^{-2}. Gravity gradients are fully characterized by the gravity gradient tensor or the Eotvos tensor, which has six independent components. The techniques for measuring gravity gradients are collectively called "gradiometry".

Time-variable gravity: Processes in a planet's solid interior, oceans, and/or atmospheres can lead to temporal changes in that planet's gravity field. These processes can be secular, periodic, or stochastic. An example of a secular change is the melting of the ice sheet in Antarctica and Greenland, which causes the Earth's gravity to decrease from year to year in these regions. An example of a periodic change is the gravity change associated with seasonal hydrological cycles observed by GRACE spacecraft. An example of a stochastic change is the change associated with an earthquake.

Tides and tidal Love numbers: Tides are responses of a planet to a non-uniform gravity field. Love numbers *h*, *k*, and *l* (each operating at spherical harmonic degrees *n* and order *m*) collectively and quantitatively describe how a planet's shape changes in response to tides. The Love numbers depend on factors like a planet's rigidity and interior structure. This tidal response has frequency dependance. The response at zero frequency is sometimes called the "static response" or "fluid response." The Love numbers at zero frequency are called fluid Love numbers ($k_{n,f}$) or static Love numbers. The response at non-zero frequencies are called

"dynamic tides." Planets and moons do not instantaneously react to tides unless they are perfectly elastic: there is a lag in the tidal response. The amplitude of this tidal lag also depends on the frequency of the forcing. Tidal lag can be given separately from the Love numbers, in which case the Love numbers are real numbers. Alternatively, tidal lag can be encoded into the Love numbers, in which case the Love numbers are complex numbers. The Love numbers h, k, and l at spherical harmonic degree n and order m control the deformation of a planet in the radial r, north N, and east E directions in response to a potential U_tidal via the equations:

$$\Delta U_{nm} = k_{nm} U^\text{tidal}_{nm}$$
$$\Delta r_{nm} = \frac{h_{nm}}{g} U^\text{tidal}_{nm}$$
$$\Delta N_{nm} = \frac{l_{nm}}{g} \frac{\partial U^\text{tidal}_{nm}}{\partial \phi} \tag{A1.4}$$
$$\Delta E_{nm} = \frac{l_{nm}}{g cos\phi} \frac{\partial U^\text{tidal}_{nm}}{\partial \lambda}$$

Loading and loading Love numbers: Loading represents a force applied to a planet's surface. Loading is conceptually similar to tides, but the tidal force is applied throughout the volume of a planet, whereas loading is applied to the surface of a planet. An example of loading is the loading of a lithosphere due to a freshly formed volcano on the surface.

Shape: Shape is the overall geometric figure of a planet. Planetary shape can provide important constraints on the body's interior. Rotation makes the shapes of planets oblate. A uniform density planet would be more oblate compared to a planet with density concentrated at depth (i.e., is differentiated). For a tidally locked satellite, planetary gravity makes the satellite's shape a triaxial ellipsoid. The satellite's shape would be more spherical the closer its density distribution is to a uniform distribution. Similar to gravity, the planetary shape r can be expanded in spherical harmonics:

$$r\left(\lambda, \phi\right) = R \sum_{n=0}^{\infty} \sum_{m=0}^{n} \left[\left(\bar{A}_{nm} cos m\lambda + \bar{B}_{nm} sin m\lambda\right) \bar{P}_{nm} sin\phi\right] \tag{A1.5}$$

Topography: Topography is the difference between the observed planetary shape and the hypothetical shape the body would have if it were in a state of perfect hydrostatic equilibrium. Note the distinction between "shape" and "topography," which are sometimes informally used interchangeably. For example, if Enceladus was in hydrostatic equilibrium, its shape would be a triaxial ellipsoid, with the longest axis pointing toward Saturn. If perfectly smooth, this

triaxial ellipsoid would have no topography despite its deviation from a sphere. Sometimes, it is difficult to separate the topography from shape, because it is not possible to separate the hydrostatic planet's response to rotation and static tide from the non-hydrostatic effects (for example, as caused by internal convection).

Surface deformation: Planetary surfaces can deform in response to various applied forces such as a tidal force, surface loading, or subsurface loading. Surface deformation can be thought of as time-variable planetary shape.

Obliquity: Obliquity is the angle between the planet's spin vector and the normal to its orbit, often called the axial tilt. Obliquity can periodically vary with time. Tidal friction can cause a body's obliquity to damp to a so-called Cassini state, where the obliquity value is related to the body's moment of inertia.

Libration: Libration is a periodic change in the rotation rate of a planetary body in response to external torques. Libration amplitude has been measured for the Earth's Moon, Phobos, Mercury, Mimas and Enceladus. The libration amplitude is inversely proportional to the moment of inertia of the librating body. For tidally locked satellites, libration amplitude measurement reveals whether or not the outer ice shell is decoupled from the interior by subsurface liquid water ocean. With an ocean, the smaller moment of inertia of the shell leads to a larger libration amplitude.

Appendix 2: Geodesy in the Planetary Science and Astrobiology Decadal Survey

This table includes all of the Strategic Research items identified by the Planetary Science and Astrobiology Decadal Survey, "Origins, Worlds, and Life: A Decadal Strategy for Planetary Science and Astrobiology 2023–2032" (OWL for short), that include an aspect relevant to geodetic measurements (e.g., measuring shapes, gravity fields, deformation, rotational states, interior structures, etc.). Note that this does not mean that geodesy is irrelevant to other questions or priorities in the Decadal Survey—just that they are not explicitly called out.

Question 10: Dynamic Habitability Where in the solar system do potentially habitable environments exist, what processes led to their formation, and how do planetary environments and habitable conditions co-evolve over time?	Q10.3 WATER AVAILABILITY: WHAT CONTROLS THE AMOUNT OF AVAILABLE WATER ON A BODY OVER TIME?	**Identify the amounts and locations of any past or present liquid water beneath or emplaced on the surfaces of Enceladus, Europa, Titan, Ceres, and candidate ocean worlds of Neptune and Uranus** using radar, gravity, topography, magnetic field (induction), and surface spectral measurements, combined with models of tidal deformation and the formation and evolution of surface features.
	Q10.6 WHAT CONTROLS THE ENERGY AVAILABLE FOR LIFE?	**Determine the geophysical parameters that control past and present material fluxes in rocky subsurfaces, such as porosity, permeability, heat flux, volcanic flux, and tectonics** by geophysical measurement, drilling/coring, change-detection experiments, seismic experiments, and modelling.
Question 11: Search for Life Elsewhere Is there evidence of past or present life in the solar system beyond Earth and how do we detect it?	Q11.4 LIFE CHARACTERIZATION: WHAT IS THE NATURE OF LIFE ELSEWHERE, IF IT EXISTS?	**Prepare for characterizing life in the subsurface of ocean worlds** by determining the heterogeneity of thicknesses of ice shells via planetary mission data as well as validating and deploying emerging technologies for life characterization, and maturing technology for accessing the subsurface for exploration, by work in the field and in the laboratory.

Scientific Themes	Priority Science Questions	Main Questions	Strategic Research
	Question 1: Evolution of the Protoplanetary Disk What were the initial conditions in the solar system? What processes led to the production of planetary building blocks, and what was the nature and evolution of these materials?	Q1.3 WHAT PROCESSES LED TO THE PRODUCTION OF PLANETARY BUILDING BLOCKS I.E., PLANETESIMALS?	**Clarify the mechanisms that enabled accretion of objects beyond the "fragmentation barrier" size (~1 m)** through determination of the structure, porosity, magnetization size and shapes of grains on small bodies by return of comet surface samples; in situ imaging, strength and gravity measurements of comets, Centaurs, or Kuiper belt objects; ground- and space-based telescopic observations; accretion modeling; and laboratory petrological and paleomagnetic analyses of returned and terrestrially collected samples
		Q2.1 HOW DID THE GIANT PLANETS FORM?	**Determine the bulk composition and internal structure of Uranus and Neptune** via gravity, magnetic field, and atmospheric profile measurements by spacecraft, as well as Doppler seismology.
			Constrain physical properties and boundary conditions (i.e., tropospheric temperatures, shapes, rotation rates) for structure models of Uranus and Neptune via gravity, magnetic field, and atmospheric profile measurements by spacecraft, remote sensing by spacecraft and ground/space-based telescopes.
		Q2.2 WHAT CONTROLLED THE COMPOSITIONS OF THE MATERIAL THAT FORMED THE GIANT PLANETS?	**Understand how compositional gradients in the atmosphere and interior of Jupiter, Saturn, Uranus, and Neptune affect the determination of bulk planetary composition** based on observed atmospheric composition, using gravity, magnetic field, and atmospheric profile measurements by spacecraft, Doppler seismology, and laboratory/theoretical studies of physical processes (e.g., turbulent diffusion, moist convection, precipitation, and helium rain).
			Determine fundamental properties of the midsize uranian moons through gravity, magnetic field, and geodetic measurements (by spacecraft), surface composition measurements (by remote sensing from spacecraft and ground-/space-based telescopes), and geological characterization (based on remote sensing by spacecraft, including imaging of the hemispheres unseen by Voyager 2).

A) Origins	**Question 2: Accretion in the Outer Solar System** How and when did the giant planets and their satellite systems originate, and did their orbits migrate early in their history? How and when did dwarf planets and cometary bodies orbiting beyond the giant planets form, and how were they affected by the early evolution of the solar system?	Q2.3 HOW DID SATELLITES AND RINGS FORM AROUND THE GIANT PLANETS DURING THE ACCRETION ERA?	**Determine fundamental properties of Neptune's moon Triton** through gravity, magnetic field, and geodetic measurement (by spacecraft), surface composition measurements (by remote sensing from spacecraft and ground-/space-based telescopes), and geological characterizatio (based on remote sensing by spacecraft, including imaging of the hemisphere poor seen by Voyager 2).
			Determine Callisto's state of differentiation to constrain the accretiona conditions of large icy moons via spacecraft geodesy (shape), gravity, pole position, and magnetic field and associate charged particle measurements (the latter necessary for proper interpretation).
		Q2.5 HOW DID PROCESSES IN THE EARLY OUTER SOLAR SYSTEM PRODUCE THE STRUCTURE AND COMPOSITION (SURFACE AND INTERIOR) OF PLUTO AND THE TRANS-NEPTUNIAN OBJECTS?	**Characterize the basic properties (size, mass, shape, cratering, rings, binarity) of diverse TNOs and related bodies (Centaurs, comets)** via remote sensing by spacecraft and ground- /space-based telescopic observations
		Q2.6 HOW DID THE ORBITAL STRUCTURE OF THE TRANS-NEPTUNIAN BELT, THE OORT CLOUD, AND THE SCATTERED DISK ORIGINATE, AND HOW DID GRAVITATIONAL INTERACTIONS IN THE EARLY OUTER SOLAR SYSTEM LEAD TO SCATTERING AND EJECTION?	**Determine the rotational, physical, chemical, geological, and interior properties of a diversity of primitive smal bodies (TNOs) in the outer solar system** with spacecraft and/or ground-/space-based observations.
			Determine the rotational, physical, chemical, geological, and interior properties of a diversity of irregular satellites, Trojans, Centaurs, and comets as well as investigate their ring system(s and/or activity with spacecraft and/or ground-/space-based observations.
			Characterize the rotational, physical, chemical, geological, and interior properties of Interstellar Objects and comparison with small bodies in the sola system with spacecraft and/or ground-/space-based observations.
		Q3.1 HOW AND WHEN DID ASTEROIDS AND INNER SO-LAR SYSTEM PROTOPLAN-ETS FORM?	**Determine what secondary processes hav led to the diversity of asteroids and pla etary feedstocks** by conducting geochem cal, petrological, and geophysical investig tions of meteorites, asteroids, and sample returned from asteroids.

	Question 3: Origin of Earth and Inner Solar System Bodies How and when did the terrestrial planets, their moons, and the asteroids accrete, and what processes determined their initial properties? To what extent were outer solar system materials incorporated?	Q3.3 HOW DID THE EARTH-MOON SYSTEM FORM?	**Determine the internal structure of the Moon with sufficient resolution to constrain its bulk composition and initial thermal state** using geophysical measurements obtained from spacecraft and/or a seismic network and other in situ analyses.
			Differentiate between giant impact concepts by developing model predictions for observable properties of the Moon and Earth and comparing them with lunar compositional and geophysical data.
		Q3.4 WHAT PROCESSES YIELDED MARS, VENUS, AND MERCURY AND THEIR VARIED INITIAL STATES?	**Determine the interior structure and bulk composition of Venus** by seismic observations, constraints on the moment of inertia and gravity field from spacecraft and Earth-based radar measurements, and through atmospheric and surface observations.
	Question 4: Impacts and Dynamics How has the population of solar system bodies changed through time due to collisions and dynamical interactions? How has bombardment varied across the solar system? How have collisions affected the evolution and properties of planetary bodies?	Q4.4 HOW DO THE PHYSICS AND MECHANICS OF IMPACTS PRODUCE DISRUPTION OF AND CRATERING ON PLANETARY BODIES?	**Determine how impacts crush porous structures and materials on comets and asteroids in microgravity** by characterizing the density variations beneath impact craters based on impact experiments, high-resolution gravity measurements, and remote sensing observations
		Q5.1 HOW DIVERSE ARE THE COMPOSITIONS AND INTERNAL STRUCTURES WITHIN AND AMONG SOLID BODIES?	**Probe the internal structures of the Moon, Mars, and Mercury** by establishing a geophysical (seismic/magnetometer) network on the former two bodies and making the first surface seismic/magnetometer measurements on the latter.
			Investigate the properties of subsurface water or magma oceans and melt reservoirs within Europa, Io, Titan, Enceladus, Triton and the Uranian Moons via electromagnetic sounding (active/passive) or induction, or geodetic measurements from orbiting or landed spacecraft.
			Investigate magmatism, and the effects of interior processes on surface compositions of planetesimals (specifically large asteroids and dwarf planets) via high-resolution imaging, spectroscopy and topography.

B) Worlds and Processes			
		Q5.4 HOW HAVE SURFACE CHARACTERISTICS AND COMPOSITIONS OF SOLID BODIES BEEN MODIFIED BY, AND RECORDED, SURFACE PROCESSES AND ATMOSPHERIC INTERACTIONS?	**Search for evidence of weathering or the presence of ancient water on Venus** by characterizing the chemical compositions and mineralogy of surface rocks paired with high-resolution imaging and topography using global and local scale measurements.
			Investigate the fundamental processes that govern hydrologic cycles by investigating Titan's hydrologic cycle via global high-resolution imaging and topographic and mineralogical data.
		Q5.5 HOW HAVE SURFACE CHARACTERISTICS AND COMPOSITIONS OF SOLID BODIES BEEN MODIFIED BY, AND RECORDED, EXTERNAL PROCESSES?	**Investigate the effects of sublimation, space weathering and interior processes on the surfaces of ice-dominated worlds (including icy satellites, active asteroids, and comets)** via high-resolution imaging, spectroscopy and topography.
			Assess processes producing lunar regolith heterogeneity by measuring the thickness variations, and vertical and lateral compositional variability of the lunar regolith, using geophysical profiling, high-resolution multi-spectral imaging, and petrologic analyses of in situ or returned samples.
		Q5.6 WHAT DRIVES ACTIVE PROCESSES OCCURRING IN THE INTERIORS AND ON THE SURFACES OF SOLID BODIES?	**Investigate the potential for active volcanism and deformation, and where and how crustal recycling is happening on Venus** with synthetic aperture radar infrared, ultraviolet, or repeat-pass interferometry measurements of the Venusian surface and atmosphere.
			Characterize present-day plate mobility and recycling on Europa, Titan, and Enceladus by visible imaging at regional scale, global, high-resolution gravity and topography and/or repeat-pass interferometry.
			Characterize the style and intensity of active tectonism occurring on rocky or icy worlds, through seismic and other geophysical measurements.

Question 6: Solid Body Atmospheres, Exospheres, Magnetospheres, and Climate Evolution What establishes the properties and dynamics of solid body atmospheres and exospheres, and what governs material loss to and gain from space and exchange between the atmosphere and the surface and interior? Why did planetary climates evolve to their current varied states?	Q6.2 WHAT PROCESSES GOVERN THE EVOLUTION OF PLANETARY ATMOSPHERES AND CLIMATES OVER GEOLOGIC TIMESCALES?	**Determine how and why Mars' climate has changed over orbital time scales** by performing radar and spectroscopic mapping of the polar layered terrain and by making in situ measurements of their structure and composition (thickness of layers, dust content, and isotope ratios) and their local meteorology (including volatile and dust fluxes).
	Q6.3 WHAT PROCESSES DRIVE THE DYNAMICS AND ENERGETICS OF ATMOSPHERES ON SOLID BODIES?	**Determine how the atmospheric circulation is driven on bodies with thin, transient atmospheres** by measuring the thermal state and winds, and distribution of surface topography, ices, and (where relevant) plumes, via remote sensing of Pluto, Triton, and Io.
	Q6.4 HOW DO PLANETARY SURFACES AND INTERIORS INFLUENCE AND INTERACT WITH THEIR HOST ATMOSPHERES?	**Investigate how and where stable water ice deposits form on Mars** by measuring their distribution through radar and spectroscopic mapping from orbit, and by measuring the ice vertical distribution, volatile fluxes, and environmental drivers at the surface.
Question 7: Giant Planet Structure and Evolution What processes influence the structure, evolution, and dynamics of giant planet interiors, atmospheres, and magnetospheres?	Q7.1 WHAT ARE GIANT PLANETS MADE OF AND HOW CAN THIS BE INFERRED FROM THEIR OBSERVABLE PROPERTIES?	**Determine the bulk compositions of Saturn, Uranus, and Neptune**, and the ice-to-rock ratios in Uranus and Neptune, from gravity field and elemental abundance measurements.
	Q7.2 WHAT DETERMINES THE STRUCTURE AND DYNAMICS DEEP INSIDE GIANT PLANETS AND HOW DOES IT AFFECT THEIR EVOLUTION?	**Determine the interior structure and composition of Uranus and Neptune** using gravity and magnetic field mapping.
		Understand the deep rotation rate and dynamics in Uranus and Neptune from time-resolved gravity and magnetic field mapping, radio occultations, planet/ring seismology measurements, and deep circulation modeling.
		Constrain the ongoing interior evolution of Saturn, Uranus, and Neptune from helium abundance, thermal balance, satellite tidal evolution, occultations, and gravity and magnetic field measurements.

Q8.1 HOW DID CIRCUMPLANETARY SYSTEMS FORM AND EVOLVE OVER TIME TO YIELD DIFFERENT PLANETARY SYSTEMS?	**Determine the differentiation state, radial interior structure, tidal response, and presence/absence of water and magma oceans and reservoirs within the moons of Jupiter, Saturn, Uranus, and Neptune** by measuring their gravity fields, shape, induced magnetic field and plasma environment, and other geophysical quantities.
	Determine the composition of rings and small moons at Uranus and Neptune in order to elucidate their origin, evolution, and present-day balance between exogenic and endogenic processes through a combination of geophysical measurements, imaging, and spectroscopic observations, including at spatial resolution sufficient to resolve regional variations and layering.
	Constrain the origin of Phobos and Deimos, including whether they arose from past Mars rings, by determining their bulk composition and interior structure with in situ geochemical and geophysical measurements.
	Characterize the spin states and orbital and rotational evolution of planetary satellites (including at Jupiter, Saturn, Uranus, and Neptune) with spacecraft and radar observations, and long temporal baseline astrometry.
	Determine the differentiation state, radial interior structure, tidal response, and presence/absence of water and magma oceans and reservoirs within the Galilean, Saturnian, and Uranian moons, as well as Triton, by measuring their gravity fields, shapes, induced magnetic fields and plasma environments, and other geophysical quantities.
	Determine if/how tides have shaped the crustal structure, tectonics, and (cryo)volcanism of the large/mid-sized Saturnian (e.g., Enceladus, Titan) and Galilean (Io, Europa, Ganymede, Callisto) satellites by characterizing the three-dimensional structure of their crusts through topography, gravity, ice-penetrating radar, and other geophysical methods.

		Q8.2 HOW DO TIDES AND OTHER ENDOGENIC PROCESSES SHAPE PLANETARY SATELLITES?	**Determine if/how tides have shaped the crustal structure of the Moon,** by characterizing the three-dimensional structure of its crust through seismology, electromagnetic sounding, heat flow, and other geophysical methods.
			Characterize the thermophysical processes of the icy shells of the large/mid-sized satellites of Jupiter and Saturn (e.g., Europa, Enceladus, and Titan), and determine their present-day activity with in situ geophysical analyses, including seismology, electromagnetic sounding, heat flow measurements, and other methods.
			Characterize tectonic and eruptive processes on Io, Europa, Enceladus, and other active bodies, and assess their relationship to tides, crustal structure, and interior processes with with high-resolution imaging over a range of illumination conditions, tidal stress conditions, and observational cadences, and long-term monitoring of activity at various temporal/spatial scales and wavelengths.
			Characterize volcanic and magmatic processes on the Moon and assess their relationship to tides, crustal structure, and interior processes with in situ geochemical and geophysical analyses (including seismology, electromagnetic sounding, and heat flow measurements), and/or returned samples from key volcanic and magmatic sites across the Moon.
			Determine the size and state of the Moon's solid inner core through seismology measurements, electromagnetic sounding, and other geophysical investigations.
			Determine the nature and origin of Ganymede's intrinsic magnetic field through magnetic field mapping over time, improved knowledge of its interior structure, and dynamo modeling.
			Determine the shape, structure, and composition of Uranus's and Neptune's rings and small moons in order to elucidate their origin, evolution, and present-day balance between exogenic and endogenic processes through a combination of geophysical measurements, imaging, and spectroscopic observations, including at high spatial resolution sufficient to resolve regional variations and layering.

		Q8.3 WHAT EXOGENIC PROCESSES MODIFY THE SURFACES OF BODIES IN CIRCUMPLANETARY SYSTEMS?	**Test the hypotheses for the origin of planetary asymmetries, including leading-trailing asymmetries on planetary satellites around Jupiter and Saturn, the nearside-farside asymmetry on the Moon, and elsewhere**, by characterizing their magnetospheric and dust environment, and by geological, geochemical, and geophysical investigations of the dichotomies themselves.
			Determine the composition of Uranus and Neptune's rings and small moons in order to elucidate their origin, evolution, and present-day balance between exogenic processes and endogenic processes through a combination of geophysical measurements, imaging, and spectroscopic observations, including at high spatial resolution sufficient to resolve regional variations and layering.
		Q8.5 HOW DO RINGS EVOLVE AND COALESCE INTO MOONS?	**Elucidate the origin of Jupiter, Saturn, Uranus and Neptune's small regular satellites and ring-moons, and their relationship and interactions with their rings**, by measuring their composition and structure.
			Constrain the origin of Phobos and Deimos, including whether they arose from past Mars rings, by determining their bulk composition and interior structure with in situ geochemical and geophysical measurements.
		Q10.1 WHAT IS "HABITABILITY"?	**Understand interior structures, tidal dissipation dynamics, and surface-interior exchange for icy shells of ocean worlds** via measurement by spacecraft, theory, and modeling to determine the magnitudes and timescales of heating and persistence of liquid water.
			Establish whether liquid water is present on Mars today in the subsurface by geochemical measurements of ices and recent hydrous minerals and geophysical measurements to probe the upper crust.